COMPRESSION OF SMART MATERIALS: SQUEEZE FLOW OF ELECTRORHEOLOGICAL AND MAGNETORHEOLOGICAL FLUIDS

by

Ernest Carl McIntyre

A dissertation submitted in partial fulfillment
of the requirements for the degree of
Doctor of Philosophy
(Macromolecular Science and Engineering)
in The University of Michigan
2008

Doctoral Committee:

Professor Frank E. Filisko, Chair
Professor Peter F. Green
Professor Ronald G. Larson
Professor Richard E. Robertson
Professor Alan S. Wineman

THANKS AND PRAISES TO GOD

YADAH *For being God*

Yours, O Lord, is the greatness, The power and the glory, The victory and the majesty; for all that is in heaven and in earth is Yours; Yours is the kingdom, O Lord, and You are exalted as head over all. Both riches and honor come from You, And You reign over all. In Your hand is power and might; in Your hand it is to make great and to give strength to all. Now therefore, our God, we *thank* You and *praise* Your glorious name. (NKJV) 1 Chronicles 29:11-13

TODAH *For staying with me throughout*

When my soul fainted within me I remembered the Lord: and my prayer came in unto thee, into thine holy temple. They that observe lying vanities forsake their own mercy. But I will sacrifice unto thee with the voice of *thanksgiving*; I will pay that that I have vowed. Salvation is of the Lord. Jonah 2:7-9

HALAL *Hallelujah for the victory!*

I will love thee, O Lord, my strength. The Lord is my rock, and my fortress, and my deliverer; my God, my strength, in whom I will trust; my buckler, and the horn of my salvation, and my high tower. I will call upon the Lord, who is worthy to be *praised*: so shall I be saved from mine enemies. Psalm 18:1-3

ZAMAR *For abundantly blessing me beyond a Ph.D.*

Behold, God is my salvation; I will trust, and not be afraid: for the Lord Jehovah is my strength and my song; he also is become my salvation. Therefore with joy shall ye draw water out of the wells of salvation. And in that day shall ye say, Praise the Lord, call upon his name, declare his doings among the people, make mention that his name is exalted. Sing unto the Lord; for he hath done excellent things: this is known in all the earth. Isaiah 12:2-5

SHABACH *For guiding me through many places*

O God, thou art my God; early will I seek thee: my soul thirsteth for thee, my flesh longeth for thee in a dry and thirsty land, where no water is; to see thy power and thy glory, so as I have seen thee in the sanctuary. Because thy lovingkindness is better than life, my lips shall *praise* thee. Psalm 63:1-3

BARAK *For allowing me to trust the Lord with my whole life*

I will bless the Lord at all times: his praise shall continually be in my mouth. My soul shall make her boast in the Lord: the humble shall hear thereof, and be glad. O magnify the Lord with me, and let us exalt his name together. I sought the Lord, and he heard me, and delivered me from all my fears. Psalm 34:1-4

TEHILLAH *For His presence both at the defense and in my life*

Thou shalt fear the Lord thy God; him shalt thou serve, and to him shalt thou cleave, and swear by his name. He is thy praise, and he is thy God, that hath done for thee these great and terrible things, which thine eyes have seen. Deuteronomy 10:20-2

2008

For
Ernest S. McIntyre
Deborah J. McIntyre
And Corina J. McIntyre

Dedicated Especially To:

Michael McIntyre
And
Isaiah McIntyre

May You Both Reach
The Limits of Your True Potential

For Kim Bradford
My Fiancé

For My Spiritual Family at CLFMI

For All My Friends In My Life
Whose Names May Go
Unmentioned But Whose Actions
Won't Go Unnoticed

Acknowledgements

First I would like to thank my advisor Professor Frank E. Filisko. Dr. Filisko has been an excellent source of support, a mentor, a great researcher through and through. Not only taking on the role of friend throughout these five years, but wise grandfather and crazy uncle when needed as well. I know someday in the distant future I'll look back and really cherish my time spent learning under him.

To every one of my committee members, I truly value all of your input. Not only for this dissertation, but also for the conversations, interactions, and even perhaps unnoticed ways each of you have affected me in this process. I want to thank Dr. Richard Robertson for his mentorship and conversations about research. I'd like to thank Dr. Peter Green both for allowing me to opportunity for a postdoctoral appointment as well as for conversations about ideas for future research. I appreciate both Dr. Wineman as well as Dr. Larson for being instrumental in helping me to understand certain aspects of the research.

I would like to also thank Professor Yonggang Meng at Tsinghua University in Beijing. By allowing me the opportunity to travel to China he not only expanded my research background, but I was able to learn about the way that research is done in another country, which has expanded both my cultural background and experience as well. I would also like to thank Professor Peter Blesak, who helped a lot with the research on magnetorheology.

I would also like to thank the Macromolecular Science and Engineering Department. Not enough can be said about Nonna, who has been a source of support for me since I've arrived in Michigan. I'd also like to thank the Macro students Anne Juggernauth and Angela Knapp for both their inputs and motivation for helping me to advance.

Outside of the University of Michigan I would first have to thank my fiancé Kim Bradford who has supported and helped me throughout this process. Without Kim I would have never succeeded this far. Also I thank all of my friends in Michigan including Dr. Sarah Kenisha Womack, Kyla Mcmullen, and Andre Taylor.

I would also like to thank my family. I thank my dad and mom, Ernest S. and Deborah J. McIntyre for supporting me through undergraduate education

and for pushing me to develop myself in as many ways as possible. I thank my sister, Corina J. McIntyre. I thank my friends at Georgia Tech including William and Alana Hardison, and April Moore. I also thank my friend Danielle LeSure for the many ways she's helped along the way.

I am also so grateful for my spiritual family here in Michigan at Christian Love Fellowship Ministries International. I thank Pastors Robert and Barbara Hill for all of the work and many things they've done to help me throughout this entire process. I also thank Pastors Roger and Denese Brown for their assistance throughout this entire process. I also would like to thank Pastor James and Kathryn Green for their assistance. I want to especially thank all of the instructors at the Berean Bible College for ensuring that my intellectual growth didn't outpace my spiritual growth. This includes Pastor Denese Brown, Pastor Roger Brown, Minister David Nelson, Minister Leverta Massey and Pastor Chris Tillman. To all others many thanks and to God be the glory.

Chapter Four has been submitted and published in the Journal of Intelligent Material Systems and Structures in December 2007.

Table of Contents

List of Figures

List of Tables

Abstract

Squeeze flow behavior was experimentally tested for Newtonian fluids. The results show that the squeezing force as a function of the gap gives force $\propto$ $gap^{-2.5}$ and gap^{-4} for constant area and constant volume respectively. These results were compared with the Stefan, perfect slip, and Rady-Laun partial slip equations and found not to match exactly, but best approximated the Stefan equation. The results also show that squeezing force as a function of squeezing speed matched predictions by Stefan, perfect slip, and Rady-Laun equations, while force as a function of viscosity for these equations overestimates the force at high viscosities.

Squeeze flow behavior of zeolite suspensions was also considered. The results matched the force vs. gap of the Newtonian fluids tested. The relative viscosities of the suspensions determined by squeeze flow matched the shear viscosity measurements at less than 15% vol concentrations. Likewise at less than 15% vol concentrations the data was shown to match the Maron-Pierce equation.

Electrorheological (ER) fluids were then examined under electric field in squeeze flow using constant volume conditions to eliminate the “sealing effect” that prevented knowing the concentration of particles in the fluid. The results show that increasing the concentration significantly increases the gap at which the fluid takes on large (>100 lbs) loads. Increasing the carrier oil viscosity decreased the steepness of the force vs. gap curves.

Filtration was assessed in squeeze flow of ER fluids using the Pe number as a predictor. Decreasing squeezing speed and viscosity were both shown to encourage filtration in electrorheological squeeze flow. Similarly increasing squeezing speed and viscosity were both shown to encourage convection in squeeze flow for ER fluids.

Squeeze flow of magnetorheological (MR) fluids showed similar behavior as ER fluids in the effects of concentration of particles. For MR the results on the effect of the viscosity of the suspending oil was done at a lower—5% vol—concentration, and showed similar behavior to the results seen for filtration in ER fluids.

Chapter 1

Introduction

Compression has many implications in material science, physics and structural engineering. For example by inducing compression, mechanical properties such as compressive strength or modulus of elasticity, can be measured. Squeeze flows are flows in which a material is compressed between two parallel plates and thus squeezed out radially (Figure 1.1). A more general definition could be “a flow in which a material is deformed between two parallel or nearly parallel boundaries approaching each other.” Squeeze flows are by nature of their changing geometry, inherently transient and inhomogeneous flows.

Figure 1.1 Constant Volume Squeeze Flow with black mass compressed between plates

Squeeze flow rheometry, which involves compressing a material in order to determine its rheological and mechanical properties has in the past two decades experienced a resurgence. At least one of the reasons for this is that squeeze tests are often utilized as a straightforward technique to determine the rheological properties of highly viscous materials such as concrete, molten polymers and ceramic pastes. In industrial uses motors, bearings, and lubrication all involve squeezing flows. Compression moulding processes of metals and polymers (filled or unfilled) are essentially squeeze flows, often further complicated with a temperature gradient. Valves and diarthroidial joints are examples of squeeze flow relevant in biology and bioengineering. Even some phenomena occuring during food intake can and has been modeled using squeeze flow. The compression of food between the tongue and the palate can be approximated as a squeeze flow.

While all of these applications are definitely of interest and much of the research developed in these applications has aided in the development of this work, the focus of this dissertation is on the compression of smart materials. The "smart" adds an element of adjustability to these compression situations. Rather than having a fixed set of mechanical properties, smart materials can adjust their behavior and properties based on external stimuli such as electric and magnetic fields. This allows for adjustments to be made by the material where in one case it can't support a single pound of force, but after adjusting to a field in that same situation it can support a load of hundreds of pounds of force. It is these

remarkable properties of smart materials that is the motivation of the research in this dissertation.

This introduction will begin with the brief history of squeeze flow, in order to point out the main difficulties experienced in the field and to lead up to the current state of the field of squeeze flow rheometry. Next it will briefly describe electrorheology and magnetorheology and describe the research that has been done in squeeze flow of ER and MR fluids. Finally this chapter will introduce the research of this dissertation and the problems that it intends to address.

History of Squeeze Flow

An early publication on squeeze flow dates back to 1874 by Josef Stefan. His classic paper actually dealt with measuring the squeezing force between two plates that were being pulled apart. Likewise his paper also used plates that were fully submerged in fluid. Nevertheless his relationships for squeeze flow remain the most dominant theories for squeeze flow. Below is the equation derived by Josef Stefan for the squeezing force between two plates for constant area(Stefan 1874) and the expression developed later by Diennes and Klemm(Diennes and

Klemm 1946) for constant volume.

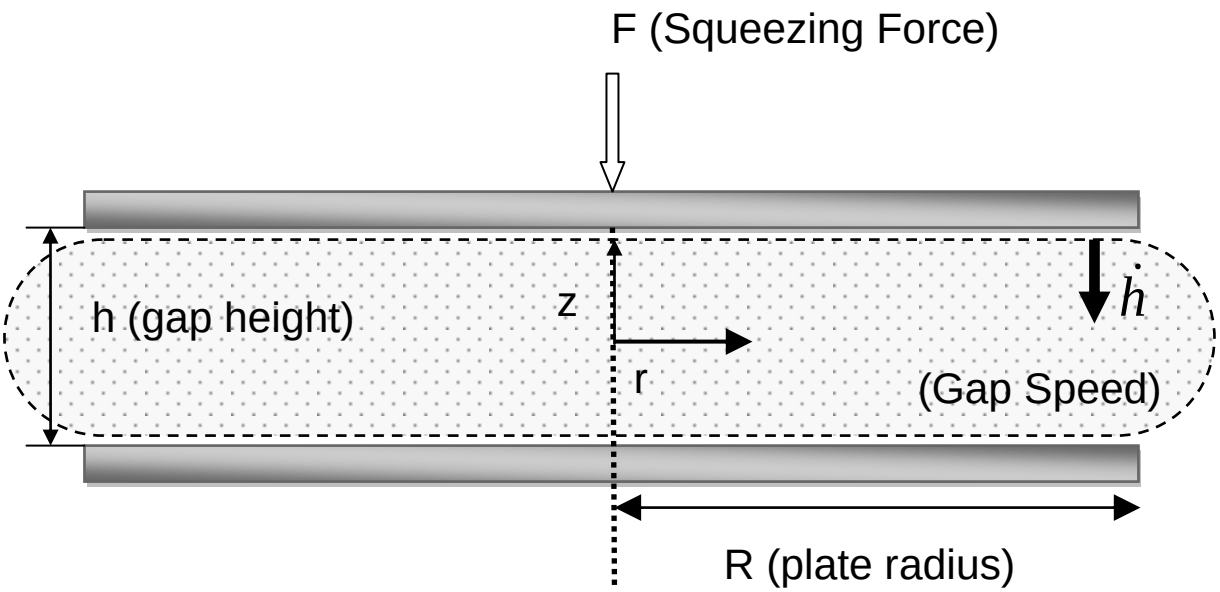

Figure 1.2 Coordinate System and Basic Dimensions Used To Describe Axisymmetric Squeeze Flows

Constant Area

$$F = \frac{3\mu_0 R^4 \dot{h}}{2\pi h^3}$$

$F - Force$

$\mu_0 - viscosity$

$R - Radius$

$h - gap$

Equation 1.1

Constant Volume

$$F = \frac{3\mu_0 V^2 \dot{h}}{2\pi h^5}$$

$F - Force$

$\mu_0 - viscosity$

$V - Volume = (\pi R^2 h)$

$h - gap$

Equation 1.2

Shortly after this popular equation for squeezing force was developed by Josef Stefan and in his paper he also verified it experimentally, Reynolds in England used the lubrication approximation to solve for the squeezing force

using the Navier-Stokes equation. Using this approximation it was found that the Navier-Stokes equation actually reduces to Stefan's Equation for the normal force in squeezing flow.

While this equation was restricted to Newtonian fluids it wasn't until 1931 that J. R. Scott extended this relationship to power law fluids(Scott 1931). In his classic paper J. R. Scott put forth the following relationship.

$$F = \left(\frac{2n+1}{n}\right)^n \left(\frac{2\pi m R^{n+3}}{n+3}\right)\left(\frac{\dot{h}^n}{h^{2n+1}}\right) \qquad \textbf{(1.3)}$$

For a power law fluid defined as

$$\tau = m\dot{\gamma}^n$$

Where m and n are power law parameters representing the preexponential consistency and the power law index respectively.

It can quickly be shown that if in the Scott equation n = 1 and m is set to equal the fluid viscosity that the equation reduces to Stefan's Law. The Stefan's Law and the Scott equation form the widely used basis for applications and for most other theories in squeeze flow(Engmann, Servais et al. 2005).

Squeeze flow rheometry prior to many advances in technology was done using constant force measurements. For these a constant load of known weight was placed on the upper plate and the gap was recorded as a function of time. For these types of measurements an inherent problem was that of inertial considerations. But for many applications during this time inertia wasn't an issue

(Wolfe 1965). One published treatment of this was by Jackson in 1962 (Jackson 1962). Dennis Kuzma developed an expression for squeeze flow that included the effects for inertia(Kuzma 1968). Below is the original expression:

$$F_s = -\frac{\pi R^4}{4}\left(\frac{6\mu\dot{h}}{h^3} + \frac{3\rho\ddot{h}}{5h} - \frac{15\rho\dot{h}^2}{14h^2}\right) \quad \textbf{(1.4)}$$

By adjusting the expression to Stefan's it's easier to see the inertial contribution to squeezing force (making some adjustments).

$$F = \frac{3\pi R^4 \mu_0 \dot{h}}{2h^3}\left[1 + \frac{5\rho h\dot{h}}{28\mu_0} + \frac{\rho h^2 \ddot{h}}{10\mu_0 \dot{h}}\right] \text{(Bird 1987)} \quad \textbf{(1.5)}$$

As squeeze flow rheometry developed and more and more confidence was placed in using squeeze flow to determine rheological parameters many non-Newtonian fluids began to be tested. Phillip Leider took several fluids and compared their properties in squeeze flow with what was expected in terms of their rheological properties. (Leider 1974; Leider and Bird 1974)

Soon after these developments in 1981 Chaetraei, Macosko, and Winter developed a parallel plastometer or squeeze flow device to measure biaxial elongation(Chatraei, Macosko et al. 1981). Here they treated the plates so that they were fully lubricated so that "full slip" could be used as a boundary condition. That is rather than assuming a no slip boundary condition for the fluid being squeezed at the surface of the plate, they were able to treat the plate as a frictionless surface.

While it was well known that in the case of squeeze flow between parallel plates there obviously were situations where slip was occurring that didn't necessarily indicate "full slippage"(Bagley, Christianson et al. 1985). It wasn't until 1999 that Hans Martin Laun developed an analytical expression to evaluate partial slip occurring at the surface of the plate(Laun, Rady et al. 1999). It should also be noted that he used an internal report at BASF written by Hassager ten years earlier in 1989 and included Hassager's work in the publication. The Laun-Rady equation for squeezing force with partial slip occurring at the surface is:

$$F = \frac{3\mu_0 \dot{h} \pi R^4}{8h^3}\left[(1-2\delta)+\frac{4h^2}{R^2}(1+2\delta)\right] \qquad \textbf{(1.6)}$$

δ = slip parameter

Since this publication many other papers have developed that include frictional models for squeeze flow(Burbridge and Servais 2004; Meeten 2004; Estelle, Lanos et al. 2006; Estelle and Lanos 2007). Some of the more recent work has been attempts of solving for the slip parameter in the squeeze flow equation, which actually is not straightforward in practice(Kalyon and Tang 2007). This is because in applications and rheometry the slip parameter is varying. This again is due to the transient nature of the squeeze flow as was stated in the beginning.

Electrorheology

Electrorheological (ER) fluids are suspensions of extremely fine non-conducting particles (up to 100 micrometres diameter) in an electrically insulating

fluid.(Larson 1999) Electrorheological fluids are fluids that solidify or become extremely viscous under an electric field. Electrorheology was first observed by Duff and Quinke over a hundred years ago(Duff 1896; Quinke 1897). It took another 50 years after this discovery for Winslow in Colorado to publish his finding that certain particle suspensions formed “fibrous mass” under an electric field. (WInslow 1949)

Unfortunately, early reports of the performance of such fluids indicate they were abrasive, chemically unstable, and liable to suffer rapid deterioration. Consequently the early promise of commercial exploitation did not materialize. It was not until 30 years after the reports of Winslow’s pioneering efforts that interest in engineering applications of ER fluids was rekindled, this time by developments in the United Kingdom. In particular Stangroom (1983) described the composition of ER fluids containing nonabrasive, micron sized polymer particles dispersed in a silicone oil carrier fluid. Commercially produced ER fluids have been and continue to be available, but despite the design, construction, and testing of numerous prototype devices, the first mass produced ER device is still awaited.

Magnetorheology

Magnetorheological suspensions are the magnetic analogs to electrorheological suspensions. It is a suspension of micrometer-sized magnetic particles in a carrier fluid, usually a type of oil. Just like ER Fluids when subjected to a magnetic field, the fluid greatly increases its apparent viscosity. It is

important to note the difference between MR fluid and ferrofluid. MR fluid particles primarily consist of micron-scale particles which are too heavy for Brownian motion to keep them suspended, and thus will settle over time due to the inherent density difference between the particle and its carrier fluid. The particles in a ferrofluids primarily consist of nanoparticles which are suspended by Brownian motion and generally will not settle under normal conditions. Additionally ferrofluids contain monodomain particles, which behave differently than MR fluids. As a result, these two fluids have very different applications.

Magnetorheological fluids were first discovered by Jacob Rabinow in 1948. Except for a flurry of interest after their initial discovery there has been hardly any information published about MR Fluids until the past 15 years. In the early 1990s, an unexpected watershed occurred in the development of smart fluids when MR fluids were ‘rediscovered’.(Stanway 2004). Consequently mass-produced devices began to appear. Some of the most significant mass-produced devices have been in the automotive industry for smart suspension damping and vibration control of vehicle seats, including the Cadillac 2002 STS.(Stanway 2004)

The difficulties that challenged ER technology and the consequent overtaking of the smart materials market demand by MR fluids has been recited throughout the literature many times(Sims, Stanway et al. 1999; Stanway 2004). These include the requirement for high voltages for electrorheological fluids — even though it should be pointed out the power consumption is less on the order of micro or nanowatts. Another problem dealt with the so-called yield strength of

ER materials in shear mode. It has been reported that MR fluids have higher yield strengths than ER fluids. It has been suggested by others that the "measured yield stresses" are a result of the slippage of the particle structures across the surface of the electrodes. If this were so the structures — both ER and MR — would be much stronger than previously thought, and more importantly the measurements of the yield strengths in shear would only be a measure of slippage or adherence to the electrode/plate.(Filisko 2007)

ER/MR Applications

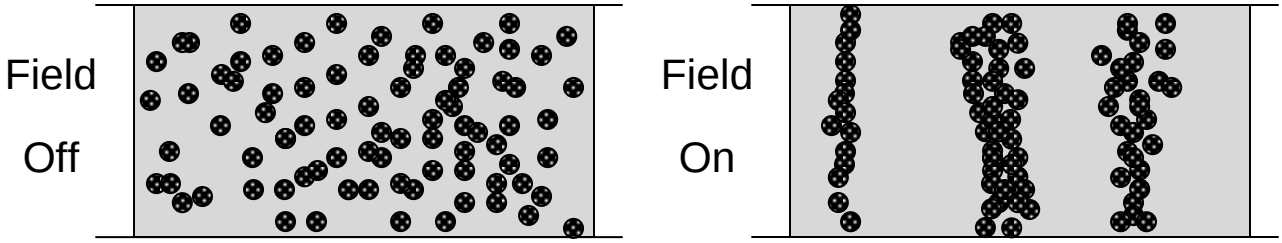

Figure 1.3 The Formation of Particle Structures in ER/MR fluids under an electric/magnetic field**.**

The cause for the change in properties for ER/MR fluids is very similar in both cases: the polarization of particles induced by either electric or magnetic fields cause the particles to form structures or particle chains which eventually bridge the electrodes. (Sims, Stanway et al. 1999) In this way the ER/MR fluids provide an elegant interface between mechanical systems and electrical/electronic control systems.

For most industrial applications and devices the use of smart materials has been divided into three modes of operation.(Jolly, Bender et al. 1999) The

first mode of operation is flow mode. Here the ER/MR fluid is contained between a pair of stationary electrodes. An example of this would be as a flow control valve. Another mode of operation is one that allows relative motion between the electrodes either in translation or in rotation. This type of relative motion causes shear in the ER/MR Fluid and is thus referred to as the shear mode. The final mode and the one of concern in this dissertation is that squeeze mode. Here the plates are free to move in a direction roughly parallel to the applied field, resulting in placing the ER/MR fluid in tension and compression. For ER it has been shown that the stresses that have been generated in these different modes follow the pattern Couette (Shear)< Pouiselle (Flow) < Squeeze Flow, which leads to the current motivation for examining smart materials in applications with squeeze mode operations (Havelka and Pialet 1996).

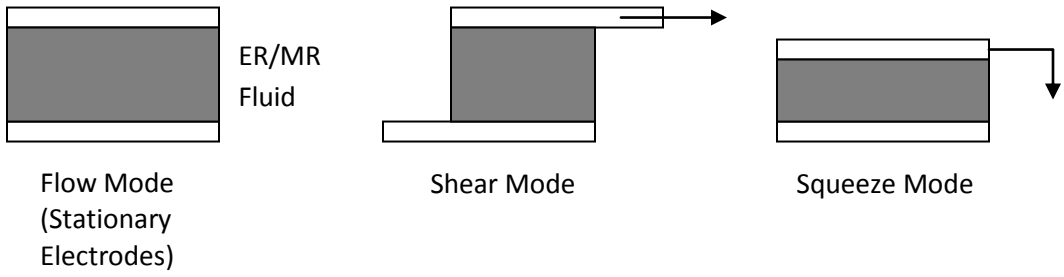

Figure 1.4 Three Modes of Smart Material ER/MR Operation

ER Squeeze Flow

The first efforts at studying ER fluids in squeeze mode were done by Stanway and Sproston et al. (Stanway, Sproston et al. 1992) They prepared an ER damper cell and tested it and measured it's transmissibility characteristics.

Some of the first experimental squeeze flow data using different ER fluids and voltages was taken by G.J. Monkman (Monkman 1995). Here Monkman measured a property that he termed the hardness of the fluids under the electric field. This was actually a plastic modulus.

During this period several models and applications were developed for industrial use of ER fluids in squeeze mode(Williams, Sproston et al. 1993; Sproston, Stanway et al. 1994). The most popular models during this time treated the ER fluids as yield stress fluids, either Bingham bodies or biviscous fluids. Williams used the biviscous model to develop some mathematical relationships that deal specifically with oscillatory squeeze flow for an engine mount.(Williams, Sproston et al. 1993)

In 2000 Chu, Lee and Ahn published a study in squeeze flow of ER fluids where for one of the first times the “sealing effect” in electrorheological squeeze flow is mentioned. This paper describes the “sealing effect” as the electric field concentrating the powder in between the plates. This paper uses the assumption that all the powder stays between the plates, but it does recognize that in the case of high concentrations and or low voltages the assumption fails. But the paper makes no mention of the effect of the carrier fluid.

In 2005 Meng and Filisko published findings that pushed the limits on the compressive stress for ER Materials.(Meng and Filisko 2005) They applied compression beyond stresses of 500 kPa. In this paper they also tested if the Williams continuum non-Newtonian equation for ER in oscillatory squeeze flow

would be able to predict the compressive stresses of the ER fluids. It was found that the Williams equation underestimated these stresses and that any attempt at modeling the behavior of these smart materials would have to include adjusting for the particle columnar structures that form between the plates during squeezing. (Williams et. al. 1993) The sealing effect was also said to be strongly influenced by the aspect ratio of the columns at the start of the test, or the initial gap size. (Meng and Filisko 2005)

In 2006 Lynch, Meng and Filisko published a study where they applied stresses of over 300 kPa on ER fluids in compression, compared with the 10 kPa applied in the previous study by Chu et. al. (Lynch, Filisko et al. 2006)This was a significant improvement over the previous experiments. In the paper the authors took notice that the ER fluids with higher viscosity oils took greater amounts of compression — strain — to reach the same stresses that the lower viscosity oils did. The authors attributed this however to the sealing effect — or the fact that for the more viscous fluids more powder was being squeezed from between the plates.

In 2007 McIntyre and Filisko proposed a technique in an article that would keep the particles in between the plates.(McIntyre and Filisko 2007) This study presented data showing that using this constant volume squeeze flow technique the effects of concentration and viscosity could be presented without having the sealing effect add uncertainty to the resulting forces that were developed.

MR Squeeze Flow

Unlike electrorheological squeeze flow, magnetorheological squeeze flow has been studied extensively and intensively by both industry and at the university level. The compressive behavior of magnetorheological (MR) fluids has been studied for industrial applications such as in dampers and as a mechanism for strengthening the materials by increasing their yield stress(Tang, Zhang et al. 2000; Tang, Zhang et al. 2001; Vieira, Ciocanel et al. 2003). The overall thrust in these studies was either towards higher yield stresses or the utilization of a commercial MR fluid that already had a high yield stress(Klingenberg, Kittipoomwong et al. 2005). Almost all studies conducted on MR fluids in squeeze mode either used about 30% by volume suspensions, usually only testing a single concentration, or used a commercially available MR fluid.

For industrial applications it has been demonstrated that MR fluids require a very high yield stress, which has been accomplished by increasing concentrations of suspensions of MR fluids to roughly 30% by volume. Recent efforts have shown that for MR fluids bidisperse suspensions with particles of two different sizes actually increases the yield strength of the fluid and decreases the off-state viscosity which leads to a greater increase in the shear stress when the field is applied. Most recently studies have shown that using microwires instead of spherical iron carbonyl particles shows a great increase in the yield stress and reduces settling at the same time.(Bell, Karli et al. 2008) Problems of settling in MR fluids have hindered their use as well. Often to solve this, proprietary thixotropic agents are typically added to MR fluid which cause the viscosities of

the suspending oils in MR fluids to remain very high. While in most studies involving MR Devices these two observations of requiring a highly concentrated suspension to allow for a high yield stress and avoiding settling through using high viscosity solutions have both been used to help optimize MR studies toward industrial applications, knowledge of the overall effects in compression for MR fluids would contribute towards researching these fundamental problems as well.

Introduction To My Research

The broad purpose of my research is to perform a comprehensive study on the compression behavior of smart materials. By examining squeeze flow of electrorheological and magnetorheological fluids this study seeks to clarify the relationships between how concentration, viscosity of the carrier oil, and other variables of interest affect the squeezing force-gap behavior. More importantly overall this research seeks to examine the overall strength of the ER/MR particle structures in compression.

Initially Chapter 2 seeks to assess the known squeeze flow theories by utilizing simple fluids (Newtonian) and seeing how well the squeeze flow data matches each of the known theories. This study required looking at single parameter partial slip equations for squeeze flow as well.

Chapter 3 involved doing a similar study, but with a more complex suspension, instead of a pure Newtonian fluid. Here squeeze flow theory was examined and the effect of concentration on squeeze flow behavior was analyzed. Also in order to further judge the rheometry these initial results were compared to some well-known suspension theories to see how well the results matched.

Chapter 4 was the first study done involving ER fluids under an electric field. In this study a new method of testing ER squeeze flow using constant volume was proposed in order to overcome the sealing effect. By doing this the

effect of concentration and viscosity were able to be examined in a situation where all the particles and fluid remained in between the plates.

Then in Chapter 5 from this insight the phenomenom of ER Squeeze flow was further examined in light of the Peclet number. Here the Peclet number was used to determine the influence that filtration had on the compressive behavior of ER fluids under an electric field. This chapter provides support that the separation and strength of the particle structures may be related to the Peclet number and the filtration that is occurring.

Finally Chapter 6 does a very similar study on magnetorheological fluids and finds that the results for MR fluids resemble closely what occurs for ER at low concentrations. This study goes on to suggest that there might be filtration occurring in MR fluids in compression under a magnetic field as well, even though it is not directly observable as it is in ER fluids in compression under an electric field.

References

Bagley, E. B., D. D. Christianson, et al. (1985). "Note: Frictional Effects in Compressional Deformation of Gelatin and Starch Gels and Comparison of Material Response in Simple Shear, Torsion, and Lubricated Uniaxial Compression." Journal of Rheology **29**(1): 103–108.

Bell, R. C., J. O. Karli, et al. (2008). "Magnetorheology of submicron diameter iron microwires dispersed in silicon oil." Smart Materials and Structures **17**: 6pp.

Bird, R. B. (1987). Dynamics of Polymeric Liquids. New York**:** 22.

Burbridge, A. S. and C. Servais (2004). "Squeeze flows of apparently lubricated thin films." Journal of Non-Newtonian Fluid Mechanics **124**: 115–127.

Chatraei, S. H., C. W. Macosko, et al. (1981). "Lubricated Squeezing Flow: A New Biaxial Extensional Rheometer." Journal of Rheology **25**(4): 433–443.

Diennes, G. J. and H. F. Klemm (1946). "Theory and Application of the Parallel Plate Plastometer." Journal of Applied Physics **17**: 458–471.

Duff, A. W. (1896). Physics Review Letters **4**: 23.

Engmann, J., C. Servais, et al. (2005). "Squeeze Flow theory and applications to rheometry: A review." Journal of Non-Newtonian Fluid Mechanics **130**: 149–175.

Estelle, P. and C. Lanos (2007). "Squeeze Flow of Bingham Fluids under slip with friction boundary conditions." Rheologica Acta **46**: 397–404.

Estelle, P., C. Lanos, et al. (2006). "Slipping Zone Location In Squeeze Flow." Rheologica Acta **45**: 444–448.

Filisko, F. E. (2007). "Alternative View for Yield Stress of ER/MR Materials." Proceedings of the 10th International Conference On Electrorheological Fluids and Magnetorheological Suspensions.

Havelka, K. O. and J. W. Pialet (1996). "Electrorheological Technology: The Future Is Now." CHEMTECH **36**: 36–45.

Jackson, J. D. (1962). "Study on Squeeze Flow." Applied Scientific Research **148**: A11.

Jolly, M. R., J. W. Bender, et al. (1999). "Properties and Applications of Commercial Magnetorheological Fluids." Journal of Intelligent Materials Systems and Structures **10**: 5–13.

Kalyon, D. M. and H. S. Tang (2007). "Inverse problem solution of squeeze flow for parameters of generalized Newtonian fluid and wall slip." Journal of Non-Newtonian Fluid Mechanics **143**: 133–140.

Klingenberg, D. J., D. Kittipoomwong, et al. (2005). "Dynamic Yield Stress Enhancement in Bidisperse Magnetorheological Fluids." Journal of Rheology **49**(6): 1521–1538.

Kuzma, D. C. (1968). "Fluid Inertia Effects In Squeeze Films." Applied Scientific Research **18**(1): 15–20.

Larson, R. (1999). The Structure and Rheology of Complex Fluids, Oxford University Press

Laun, H. M., M. Rady, et al. (1999). "Analytical solutions for squeeze flow with partial wall slip." Journal of Non-Newtonian Fluid Mechanics **81**: 1–15.

Leider, P. J. (1974). "Squeezing Flow between Parallel Disks. II. Experimental Results." Industrial & Engineering Chemistry Fundamentals **13**(4): 342–346.

Leider, P. J. and R. B. Bird (1974). "Squeezing Flow between Parallel Disks. I. Theoretical Analysis." Industrial & Engineering Chemistry Fundamentals **13**(4): 336–341.

Lynch, R., F. E. Filisko, et al. (2006). "Compression of dispersions to high stress under electric field: Effects of Concentration and Dispersing Oil." Journal of Colloid and Interface Science **297**: 322–328.

McIntyre, E. C. and F. E. Filisko (2007). "Squeeze Flow of Electrorheological Fluids Under Constant Volume." Journal of Intelligent Materials Systems and Structures **18**: 1217–1220.

Meeten, G. H. (2004). "Effects of plate roughness on squeeze flow rheometry." Journal of Non-Newtonian Fluid Mechanics **124**(1-3): 51–60.

Meng, Y. and F. E. Filisko (2005). "Unidirectional Compression of Electrorheological Fluids Under Electric Fields." JOurnal of Applied Physics **98**.

Monkman, G. J. (1995). "The electrorheological effect under compressive stress." Journal of Physics D: Applied Physics **28**(3): 588–593.

Quinke, G. (1897). Annals of Physics **62**: 1.

Scott, J. R. (1931). "Theory and Application of the Parellel-Plate Plastimeter." Transactions of the Institution of the Rubber Industry **7**(3): 169–186.

Sims, N. D., R. Stanway, et al. (1999). "Vibration Control Using Smart Fluids: A State-of-the-Art Review." The Shock and Vibration Digest **31**(3): 195–203.

Sproston, J. L., R. Stanway, et al. (1994). "The electrorheological automotive engine mount." Journal of Electrostatics **32**: 253–259.

Stanway, R. (2004). "Smart fluids: current and future developments " Materials Science and Technology **20**: 931–939.

Stanway, R., J. L. Sproston, et al. (1992). "ER fluids in the squeeze-flow mode: an application to vibration isolation." Journal of Electrostatics **28**: 89–94.

Stefan, J. (1874). "Versuche uber die scheinbare Adhasion." Sitz. Kais. Akad. Wiss Math. Nat. Wien **69**(2): 713–735.

Tang, X., X. Zhang, et al. (2001). "Enhance the Yield Shear Stress of Magnetorheological Fluids." International Journal of Modern Physics B **15**(6,7): 549–556.

Tang, X., X. Zhang, et al. (2000). "Structure enhanced yield stress of magnetorheological fluids." Journal of Applied Physics **87**(5): 2634–2638.

Vieira, S. L., C. Ciocanel, et al. (2003). "Behavior of MR Fluids in Squeeze Mode." International Journal of Vehicle Design **33**(1-3): 36–49.

Williams, E. W., J. L. Sproston, et al. (1993). "Electrorheological fluids applied to an automotive engine mount." Journal of Non-Newtonian Fluid Mechanics **47**: 221–238.

WInslow, W. M. (1949). "Induced Fibration of Suspensions." Journal of Applied Physics **20**(12): 1137–1140.

Wolfe, W. A. (1965). "Squeeze Film Pressure." Applied Scientific Research **14**(1): 77–90.

Chapter 2

An Experimental Study on Squeeze Flow of Newtonian Fluids Including Slip

Introduction

Over the past decade there's been a renewed interest in squeeze flow rheometry. Much of the interest is due to its usefulness in determining the rheological properties of highly viscous materials. These include several industrial fluids such as concrete, molten composites, food pastes, ceramic pastes, and concentrated suspensions to name a few. In squeeze flow "a material is deformed between two parallel or nearly parallel boundaries approaching each other." (Engmann, Servais et al. 2005) Assuming a rheological model, the flow parameters of the material are inferred by fitting the model with the experimental measurements. (Collomb, Chaari et al. 2004)

This paper seeks to characterize the behavior of simple (Newtonian) fluids, where shear viscosity is known throughout the test, utilizing several existing squeeze flow theories. This paper uses an experimental approach to assess the fluid behavior of the simplest case for squeeze flow, Newtonian fluids, using existing squeeze flow theory. In order to assess flow behavior for Newtonian fluids this paper utilizes two different experimental setups — constant volume and constant area squeeze flow. Stefan's equation, which is the

dominant theory used in the Newtonian squeeze flow, was taken as a starting point for analysis. The data required that effects described by recent work and current theories be utilized as well.

The experiments showed that partial slip could be used to describe the relationship between the squeezing force and the gap. The relationship between gap speed and force in the experiments matched what was predicted in all of the equations examined — Stefan's Law included. The effect of viscosity on the data agreed with Stefan's Law for low viscosity, but for the high viscosity experiments the data was unable to match Stefan's Law. By utilizing the Rady-Laun partial slip equation the power law relationship between force and gap shown by the data was able to be matched, but the magnitude of the force was better approximated using Stefan's assumptions.

Theory

The dominant theory that will be looked at is Stefan's Equation, but this study will take into account the effects described by more current theories qualitatively as well. Stefan's equation at constant area and constant volume is(Stefan 1874; Diennes and Klemm 1946):

Constant Area

$$F = \frac{3\mu_0 R^4 \dot{h}}{2\pi h^3}$$

$F - Force$

$\mu_0 - viscosity$

$R - Radius$

$h - gap$

Equation 2.1

Constant Volume

$$F = \frac{3\mu_0 V^2 \dot{h}}{2\pi h^5}$$

$V - Volume = (\pi r^2 h)$

Equation 2.2

In matching squeeze flow theories to experimental data two major problems have arisen. The first effect, which occurs in experiments is that of inertial considerations. This effect is more problematic in using constant force squeezing tests, whereas in our study utilized a constant speed apparatus instead. Inertial effects on squeezing flow has been addressed extensively in the squeeze flow literature(Kuzma 1968; Grimm 1976) Using a perturbation approach to solve for the inertial terms in the Navier-Stokes equation researchers arrived at an equation that includes the influence of inertia on the Force(Bird 1987) (*with an adjustment for h*):

$$F = \frac{3\pi R^4 \mu_0 \dot{h}}{2h^3}\left[1 + \frac{5\rho h\dot{h}}{28\mu_0} + \frac{\rho h^2 \ddot{h}}{10\mu_0 \dot{h}}\right] \qquad \textbf{(2.3)}$$

In the above equation for an experimental setup where the plates are squeezed together with a constant velocity (as is the case in this setup) the third term vanishes. The second term becomes negligible also because such slow speeds are being applied, which a quick order of analysis would reveal. (Gap and speed in the numerator are less than one, while viscosity which is in the denominator is at least three orders of magnitude greater than one.) In looking at this equation which includes inertial effects for our experiment it quickly reduces to Stefan's equation.

The second effect that occurs in squeeze flow rheometry that must be accounted for is slip at the surface of the plates. Stefan's equation assumes a no

slip boundary condition. There have been experiments where it was demonstrated that this doesn't always hold.(Chatraei, Macosko et al. 1981; Shirodkar, Bravo et al. 1982; Burbridge and Servais 2004) One attempt at resolving this is to treat the plate surfaces so that they are fully lubricated and assume a perfect slip boundary condition. The squeeze flow equation that is derived for perfect slip (*after adjusting parameters for the Newtonian fluid*) is(Raphaelides and Gioldasi 2004):

$$F = \frac{3\pi\mu_0 R^2 \dot{h}}{h} \qquad \textbf{(2.4)}$$

For a constant volume Newtonian fluid sample squeezed between two rigid plates assuming perfect slip requires a slight modification to the expression given below as stated before(Campanella and Peleg 1987):

$$F(t) = \frac{3\pi R_0^2 H_{F0} \mu V}{(H_{FO} - Vt)^2} \qquad \textbf{(2.5)}$$

R_0 – Initial Radius
H_{F0} – Initial Gap
V - Plate speed
t - Time

By converting (H_{FO}−Vt) to H(t), changing V to (dh/dt) and replacing R_0 with Volume (V equal to $\pi R_0^2 * H_{F0}$) the following equation is defined for constant volume with perfect wall slip:

$$F = \frac{3\mu_0 V \dot{h}}{h^2} \qquad \textbf{(2.6)}$$

V – Volume

The difference of a factor of 1/h in going from a constant area setup to a constant volume setup should be observed for the condition of perfect wall slip. However for our experiments the plates were not treated in order to lubricate the surface. These two equations are still important in that they express the lower limit for forces generated in the experiments. These equations also show the drastic reduction in the force when moving from a frictional (no slip) surface to a lubricated (perfect slip) surface.

Each of the two above instances represents what occurs at the limits for squeeze flow. The more important case for examining slip occurring in squeeze flow is neither perfect slip nor no slip at the surface, but partial slip occurring at the surface. The best way to look at partial slip is by examining the velocity profile at the plate surface. As expected the velocity in the z direction at the plate surface is going to be equal to the gap speed. The radial velocity at the wall gives a clear picture of what is going on in terms of slip.

For no slip the radial velocity at the plate surface is zero. For a frictionless surface the radial velocity is given below.(Chatraei, Macosko et al. 1981) For Laun's equation on partial slip the velocity at the surface of the wall takes on the linear form given below.

No Slip	**Perfect Slip**	**Partial Slip**
$v_r = 0$	$v_r = \frac{\dot{h} \cdot r}{2h}$	$v_r = \frac{v_s}{R} \cdot r$

For partial slip there is a slip parameter — v_s — which can be adjusted between no slip at a minimum ($v_s = 0$) and full slip at a maximum:

$v_{s,\max} = \frac{\dot{h} \cdot R}{2h}$. This parameter is actually nothing more than the radial velocity at the edge of the plate ($v_s = v_r(R, H)$). It can also be adjusted to include partial slip that occurs between these two extremes. Thus partial slip describes a situation when the velocity profile at the surface of the wall is not frictionless but the fluid is still moving at the surface.

There have been and continue to be several efforts in squeeze flow for quantifying partial slip into the squeeze flow equation.(Laun, Rady et al. 1999; Kalyon and Tang 2007) Laun developed such an equation(Laun, Rady et al. 1999):

$$F = \frac{3\mu_0 \dot{h} \pi R^4}{8h^3}\left[(1-2\delta) + \frac{4h^2}{R^2}(1+2\delta)\right] \qquad \textbf{(2.7)}$$

In this equation δ is a dimensionless parameter that relates a slip rate and a compression rate.

$\delta = \frac{v_s}{R\left(d\varepsilon/dt\right)}$ $\delta \rightarrow 0$ corresponds to no slip, while $\delta \rightarrow 0.5$ corresponds to perfect slip. A very similar equation has been developed by Hassager(Laun, Rady et al. 1999):

$$F = \frac{3\mu_0 \dot{h} \pi R^4}{2h^3}\left[\frac{1}{1+6(\beta\mu_0/h)} + 2\left(\frac{h}{R}\right)^2\right] \qquad \textbf{(2.8)}$$

For Hassager's equation pure equibiaxial elongation (perfect slip) occurs with $\beta \rightarrow \infty$. In this case only the second term remains. For no slip $\beta \rightarrow 0$ and we arrive at an expression that approximates Stefan's equation again. These equations deal with approximating partial slip at the surface.

Taking these partial slip equations as models some attempts have been made at solving for the slip parameters β or δ. One method of parameter identification was developed by Laun (Laun, Rady et al. 1999) that utilized a Mooney type analysis of data to arrive at the equation:

$$\dot{\gamma}_{R,N} = \frac{\tau_{R,N}}{\eta_0} + \frac{6v_s}{H} \qquad \textbf{(2.9)}$$

$$\dot{\gamma}_{R,N} = \text{nominal rim shear rate}$$

$$\tau_{R,N} = \text{nominal rim shear stress}$$

Using the above expression plotting the rim shear rate at a constant rim shear stress against 1/H should give a line with a slope of $6v_s$. Then using this, δ can be calculated from a single squeeze experiment.

Another approach at arriving at the slip parameters used by Kalyon (Kalyon and Tang 2007) involves using a least squares regression of the equation for slip. The equation that is used is

$$f = \frac{3\pi R^4 V}{2h^3} m - \frac{9\pi R^4 V}{h^4} m^2 \beta \qquad \textbf{(2.10)}$$

For the Newtonian fluid m is the viscosity,and V is the gap rate. In this approach a parameter for a least squares error is defined J:

$$J = \frac{1}{M}\sum_{i=1}^{M}\left(1-\frac{f_i}{f_i^{\,e}}\right)^2 \qquad \textbf{(2.11)}$$

$f_i = \text{analytical expression for force given above at a given gap}$

$f_i^{\,e} = \text{experimental data for force at given gap}$

Taking the above error and minimizing it by adjusting the parameters m and β one can arrive at an approximation for both m and β. The disadvantage of this approach aside from its lengthy calculation is that the estimation is only a statistical one, that yields little insight into what is happening aside from the calculation of the slip parameters. Aside from this it assumes that the data must match the equation given above to arrive at the correct parameters. (i.e. Assumes Stefan's Law always applies to no slip while ignoring other effects). Still it is a very promising method for approximating the parameters m and β in Newtonian as well as other types of fluids.

There are certainly other effects in squeeze flow other than inertial considerations and slip. For example the effects of temperature on squeeze flow, or non-Newtonian behavior are two other problems that have been and are still being investigated. For isothermal Newtonian fluid behavior the chief focus in the literature has been on inertial considerations and slip. There are other types of fluid behavior looked at in squeeze flow and an excellent review of some of this work has been published by Engmann (Engmann, Servais et al. 2005).

Materials and Methods

Three different fluids were used in these experiments. Two were viscosity standards with known viscosities. The third was silicon oil, which also had a known viscosity. The properties of these fluids are given in Table One.

Materials	Viscosity (mPa s)	Kinematic Viscosity (mm^2/s)	Density (g/cm^3)
Cannon Instrument Company Certified Viscosity Standard: S30000[1]	71,720 @25°C	*80,521*	0.8907
Cannon Instrument Company Certified Viscosity Standard: S2000[1]	4,546 @ 25°C	*5,202*	0.8739
Dow Corning FS-1265 Silicon Oil[2]	*7,874*	10,000	1.27

Table 2.1 Three Newtonian Fluids used in experiments. Calculated values are italicized.

A rheometer (RDS II, Rheometrics Inc.) was used for all three of the squeeze flow experiments. For all of these tests the recorded initial gap between the plates was 1.0 mm, but the test started at a gap of 1.2 mm to eliminate transient effects. For all of these tests a constant plate speed was used to bring the plates together by moving the upper plate while the lower plate remained stationary. The normal force developed during the test was measured by the

[1] All Certified Viscosity Standards conform to ASTM D 445/446 and have been tested and confirmed by Cannon Instrument Company according to ASTM D 2162

[2] Dow Corning FS-1265

normal force transducer connected to the upper plate, and recorded by an online computer.

Three experimental setups were used. For the constant area test two identical 25 mm plates were used. For the second one 25 mm and one 50 mm plate was used. The constant volume test used two 50 mm plates. When the same size plates were used, the fluid was allowed to pour out the sides of the plates; however when the larger bottom plate was used this eliminated the problem. The boundary conditions at the edge of the top plate in both cases were difficult to predict. While both cases had some uncertainty involved in the measurements, the apparatus with the larger plate where there was some stagnant fluid at the plate edge resembled closer to the ideal case. Therefore, the two equal diameter plates were used to test a single squeeze speed, 0.10 mm/s; while the second instrumental setup with a larger bottom plate was used to test three different squeezing speeds—0.01mm/s, 0.05 mm/s, 0.10 mm/s.

The final apparatus used constant volume test geometry. In this test two 50 mm diameter plates were used. The fluid only partially filled the gap between the upper and lower plates initially and expanded as the plates were squeezed together. For this setup all of the fluid stayed between the plates throughout the entire test. The fluid that was placed between the upper and lower plates was measured at about 0.5 mL by syringe. The three fluids were tested at three different squeezing speeds—0.01 mm/s, 0.05 mm/s, 0.10 mm/s.

Results

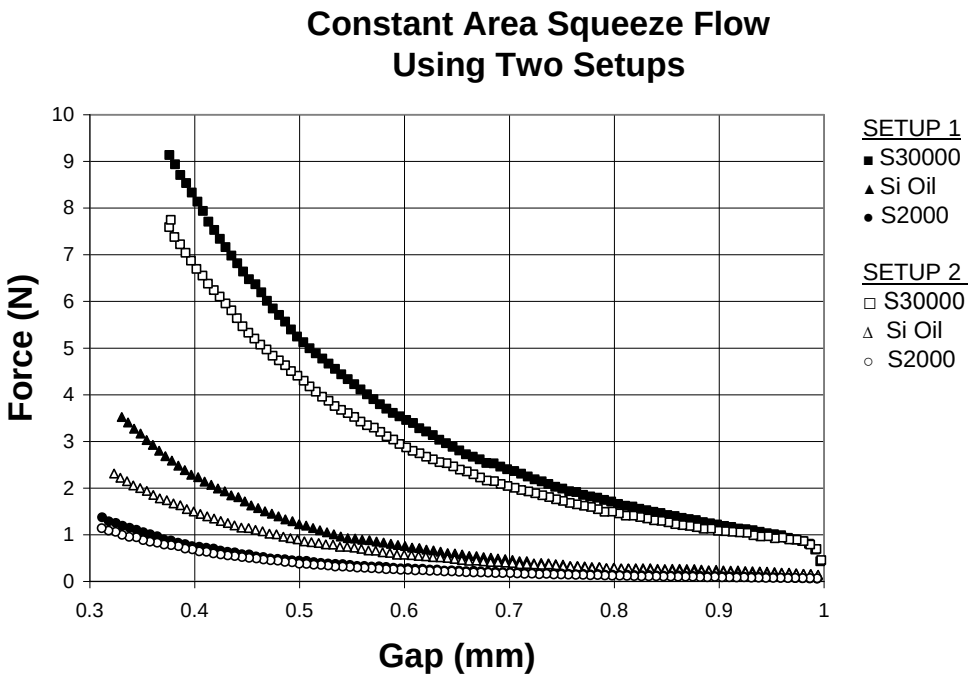

Figure 2.1 The results from the squeeze flow experiments on three different Newtonian fluids using two different constant area setups. SETUP 1 used two 25 mm plates, while SETUP 2 replaced the bottom plate with a 50 mm one. The squeezing speed of 0.10 mm/s was the samefor both setups.

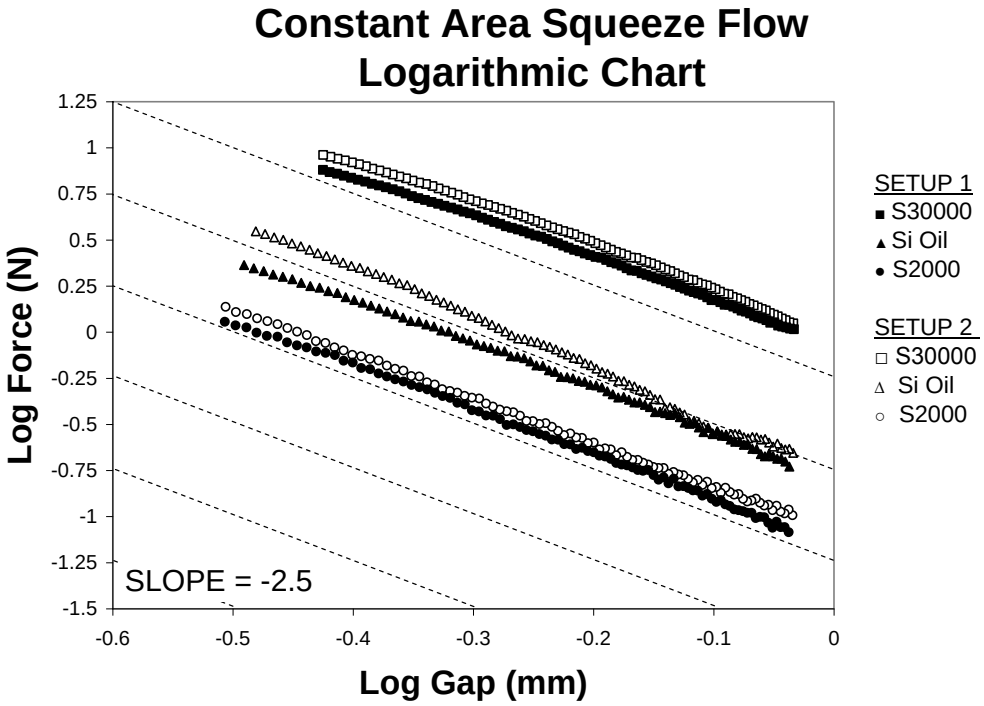

Figure 2.2 The results from both constant area squeeze flow setups at 0.1 mm/s are shown on a logarithmic scale in order to determine the relationship between the force and the gap. Lines with a slope of −2.5 are drawn to show how closely the data matches that slope regardless of which setup is used.

The results for squeeze flow experiments for three different Newtonian fluids using two different constant area experimental setups are shown in Figures 2.1 and 2.2. Figure 2.1 shows how the force increases as the fluid is squeezed out. Figure 2.2 shows the relationship between the force and gap by plotting them on a logarithmic scale. The slope of the line reveals the power dependence. The data matches approximately the slope of −2.5 which is drawn in. For the silicon oil there is a slight deviation occurred initially, but still the slope remains approximately −2.5.

Figure 2.1 shows that the squeezing force for the two different setups gave two distinctly different results. This confirms the importance of testing both

setups. Figure 2.1 also shows that the squeezing force for the second setup was greater for all three fluids. The thing to notice is that in Figure 2.2 despite these differences the slope remains approximately the same for both setups regardless of the end effects.

Qualitatively the data in Figure 2.1 shows several trends are shown. For example the squeezing force increases as the fluid viscosity gets larger. Figure 2.2 shows all the squeeze flow data show an approximate linear fit on the logarithmic scale with approximately the same slope or are roughly parallel.

Quantitatively several points can be made from Figures 2.1 and 2.2 as well. First in Figure 2.2 the data has a slope close to −2.5. Even with extensive testing varying the speed did not give a significant variation in the slope. Also the effect of viscosity can be examined in Figure 2.1. The viscosity of S30000 is at least six times greater than that of silicon oil, Stefan's Law predicts that the squeezing force should be six times greater as well. A force of 1 N crosses the curve for silicon oil in the second setup at about 0.53 mm. Going up to S30000 in the second setup it should give a value of at least 6 N at the same gap, but instead falls below 5 N. All these tests were done at the same speed 0.10 mm/s, and so the effect of speed is not shown in Figures 2.1 and 2.2.

In addition to using the constant area apparatuses this study included constant volume squeeze tests. Constant volume squeeze tests not only give an additional apparatus to compare with the constant area apparatuses, but constant volume tests give an entirely different kind of squeeze flow, that can be used to characterize the squeeze flow behavior of the liquids. For constant

volume the radius is now expanding, whereas in constant area the radius of the fluid in contact with the moving plate remained constant. The radius must therefore be replaced by the volume of the sample which remains constant. However, in order to maintain the same flow situation it must be assumed or required that the volume remains cylindrical in shape.

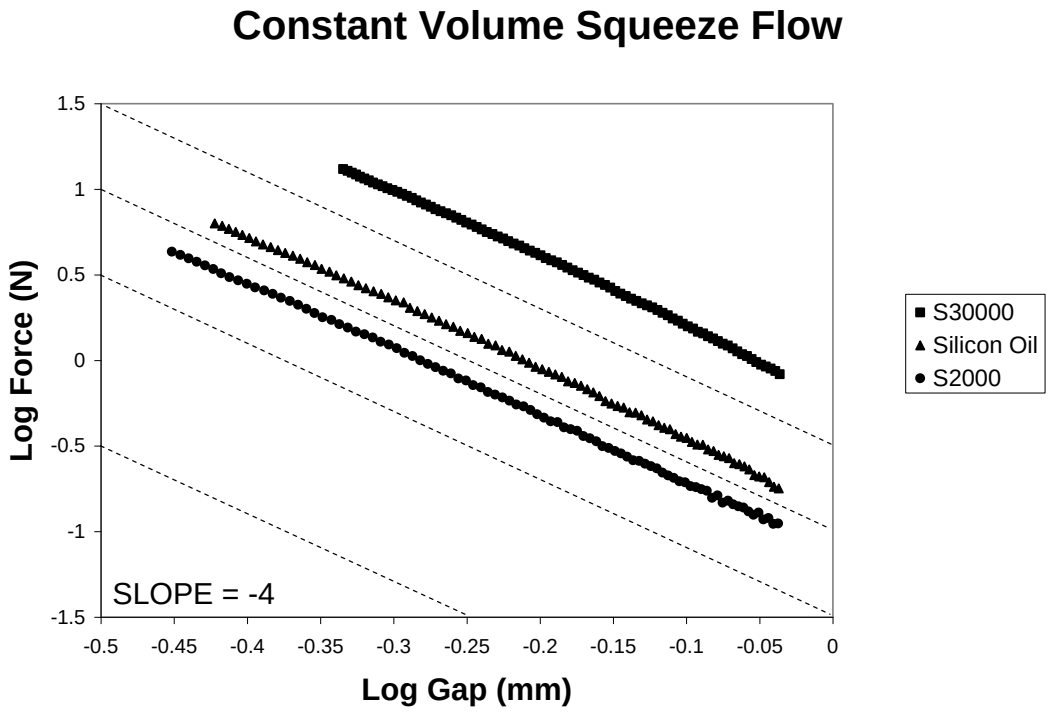

Figure 2.3 The squeeze flow result of the constant volume setup shows the relationship between the force and the gap. A line with a slope of −4 is drawn to compare with the data.

Figure 2.3 shows the squeeze flow data for the constant volume apparatus, which can then be compared with Figure 2.2. Comparing Figures 2.2 and 2.3, for constant volume the slope is closer to −4 which is greater than that for constant area which is −2.5. Qualitatively the trends exhibited in Figure 2.2 for increasing the viscosity and the fact that the curves form parallel lines are consistent in both plots.

In order to assess the effect of gap speed on each setup more experiments were performed. The effect of gap speed goes beyond its effect on the squeeze force. The gap speed can cause any number of additional effects to distort the entire flow situation.

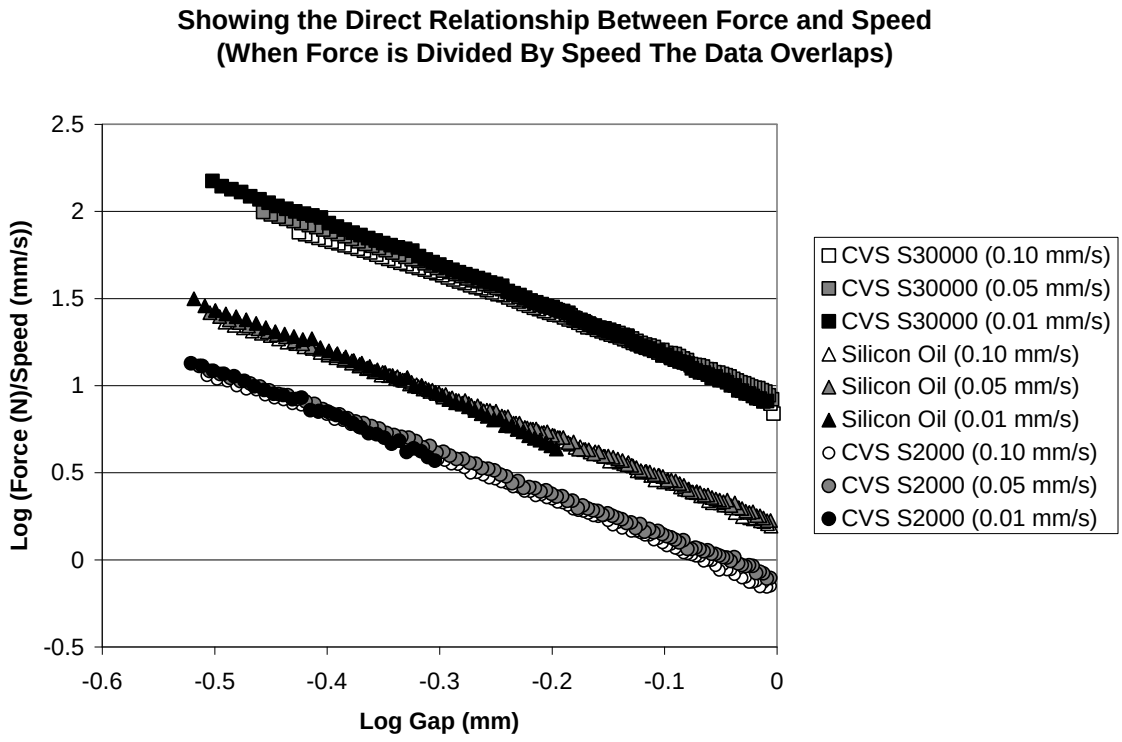

Figure 2.4 Constant area squeeze flow results using Setup 2 were done at 3 different squeeze speeds — 0.10 mm/s, 0.05 mm/s and 0.01 mm/s. For 0.01 mm/s some of the measurements fell below the sensitivity of the instrument and were excluded.

For constant area squeeze flow Stefan's Law predicts that the force is directly proportional to the gap speed. Therefore assuming Stefan's equation holds, an experiment can be done for various gap speeds using the same experimental setup with the same fluid. If the force is then divided by the gap speed the data should overlap. Figure 2.4 shows that such an experimental

curve, and the data are shown to overlap. The divergence of the curves in this figure at smaller gaps can be attributed to the compliance of the instrument. The data in Figure 2.4 therefore matches the result predicted by Stefan's Law.

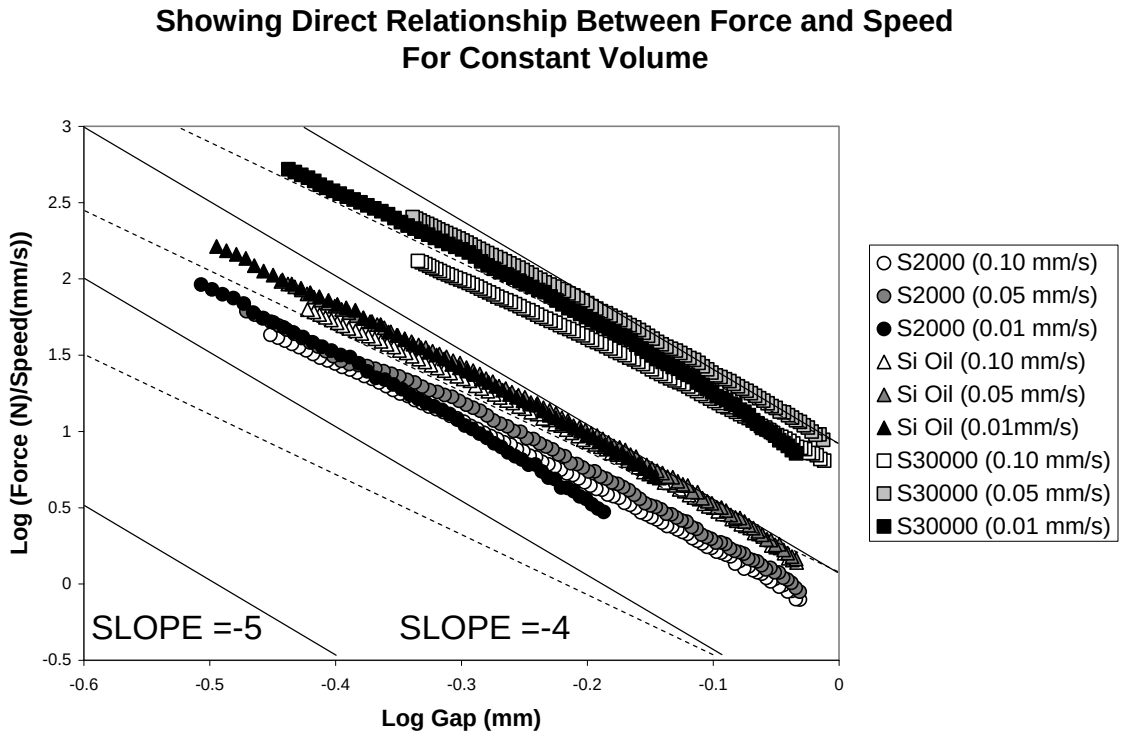

Figure 2.5 Constant volume squeeze flow results done at 3 different speeds —0.10 mm/s, 0.05 mm/s, 0.01 mm/s. Again for 0.01 mm/s some of the results fell off the sensitivity of the instrument and were excluded. Drawn on the figure are two lines for comparison of slopes −4 (dashed) and −5 (solid).

Figure 2.5 shows the results using the same material as Figure 2.4 except using a constant volume apparatus. The data nearly overlaps but not as well as that in Figure 2.4 or as obtained from the constant area apparatus. There are some similarities in the data, however worth consideration. First the slope decreases as the speed increases. The slopes for each speed show a similar

behavior. For example the data for 0.05 mm/s is always on top of the other two speeds. The curves for 0.01 mm/s have a slope that causes the curve to cross over 0.10 mm/s and then converge with 0.05 mm/s for all fluids. Finally 0.10 is usually the lowest curve. Looking very closely at Figure 2.4 these same observations could be made, but the data overlaps better and the slope doesn't change as much. This data suggests that the plate speed could have an effect on changing the slope.

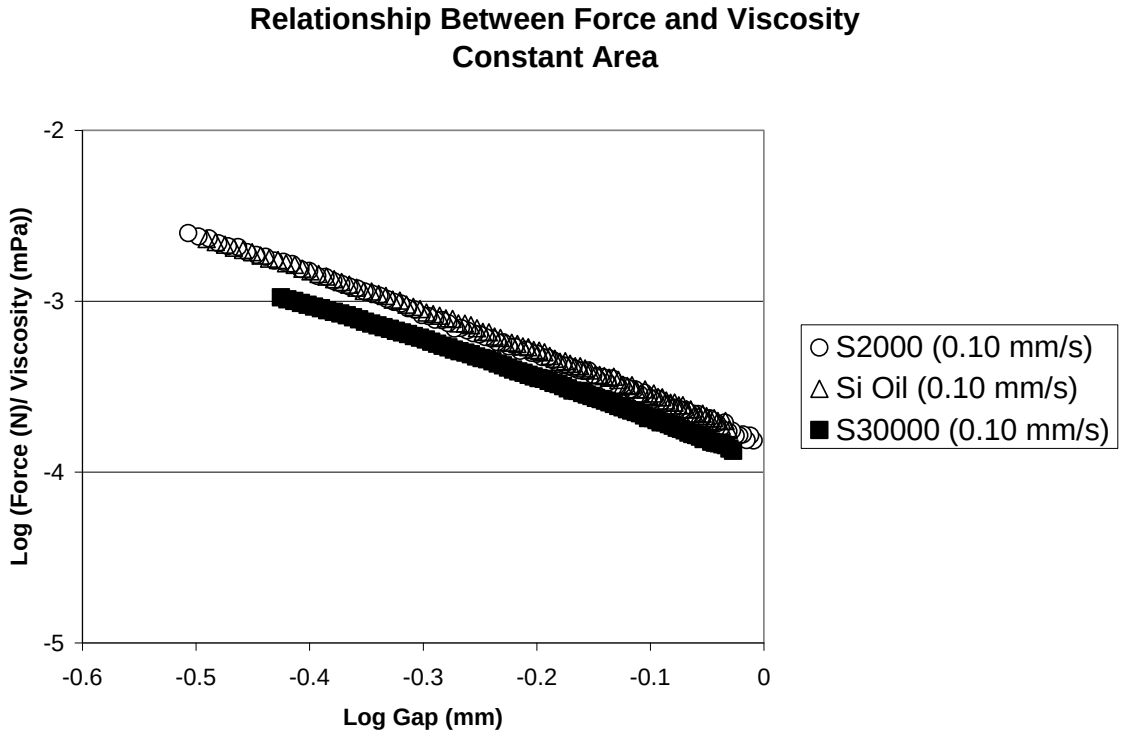

Figure 2.6 Constant Area Squeeze Results done at 0.10 mm/s showing the force divided by the viscosity. When the force is divided by the viscosity for different fluids squeezed at the same speed using the same apparatus, the data should overlap.

It has already been shown by looking at Figure 2.1 that for these experiments the squeezing force does not vary directly with the viscosity. In order

to examine the effect of viscosity further, Figure 2.6 shows a logarithmic plot of force divided by viscosity vs. gap. By dividing through by the viscosity according to Stefan's Law the data for the three fluids should overlap. Figure 2.6 shows that the S2000 and the Si Oil overlap, but the S30000 does not. Stefan's prediction for our experimental results overestimates the force for the high viscosity fluid. However, in previous work the apparent viscosity derived from Stefan's equation for high viscosity fluids has been shown to disagree with squeeze flow data as well. (Winther, Almdal et al. 1991)

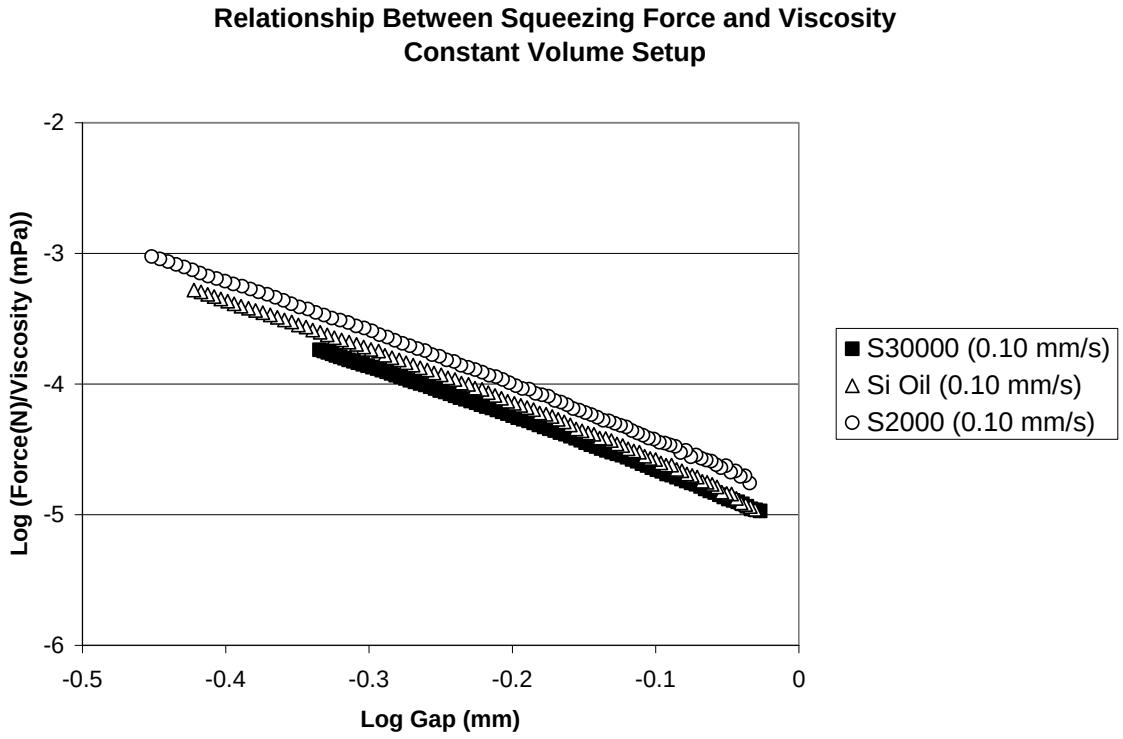

Figure 2.7 Squeeze flow results for constant volume setup showing how the force varies with the viscosity. Again the data should overlap. Also the data overlaps better for the constant area setup.

Figure 2.7 shows the results for the same materials tested at the same speed for the constant volume setup. Both Figures 2.6 and 2.7 show that in both setups the high viscosity fluid deviates from the other two fluids. The overlap for the data for Si Oil and S2000 in Figure 2.6 is better than for Figure 2.7. In conclusion Figures 2.6 and 2.7 highlight the need for an explanation for the viscosity behavior.

Another possibility that has arisen and developed significantly recently is that of partial slip in squeeze flow. If slip is occurring it can change the slope from between −3 to −1 in constant area squeeze flow setups and −5 to −2 in constant volume setups. Thus it agrees with what was observed in Figures 2.2, 2.3 and 2.4. However, the effect of viscosity on the slip parameter equation is also the same as Stefan's Law, so it could not be used to explain the effects seen for the viscosity. Below is the Laun-Rady Equation for partial slip for a Newtonian Fluid:

$$F = \frac{3}{2}\frac{(-\dot{h})\pi\eta_0 R^4}{h^3}\left[\left(1-2\delta\right)+\frac{4h^2}{R^2}\left(1+2\delta\right)\right] \text{ (Laun, Rady et al. 1999)} \qquad \textbf{(2.7)}$$

The partial slip parameter δ can range from 0 (no slip) to 0.5 (full slip).

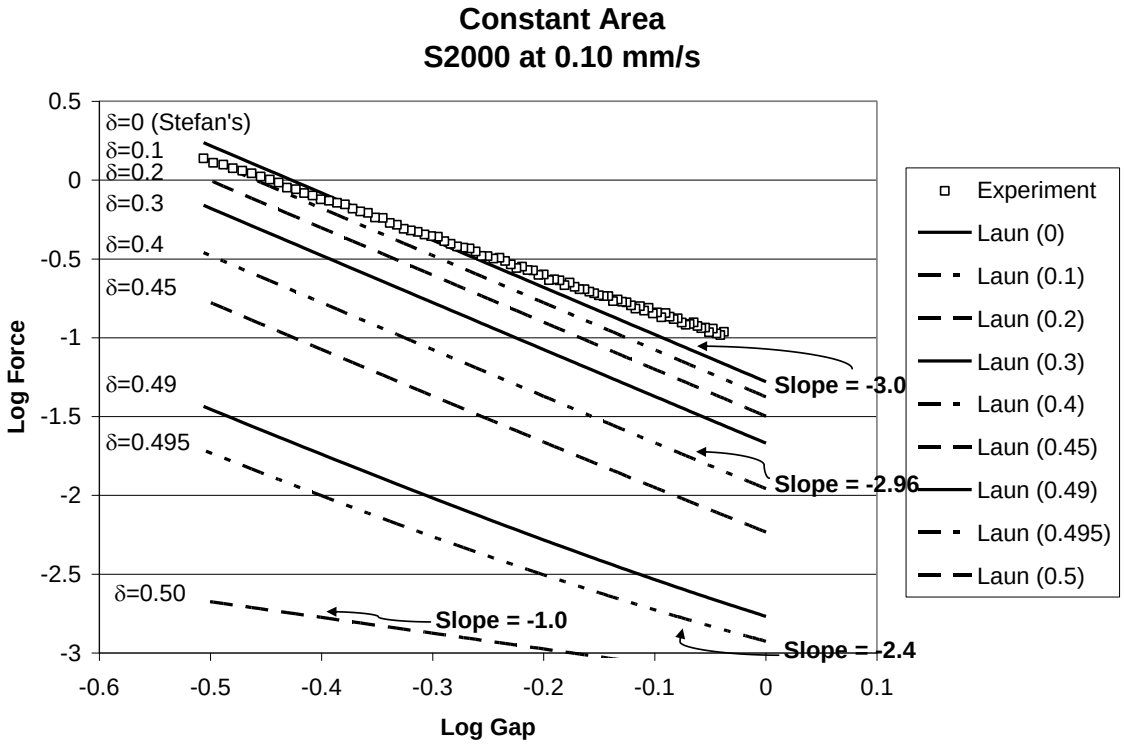

Figure 2.8 Constant Area Squeeze Flow Data for S2000 shown to compare with Laun prediction. The plot shows both how the slope varies with the slip parameter delta and how the magnitude of the force is affected by slip. Even though it is possible to arrive at a value for the slip parameter that will account for the slope the magnitude of the force doesn't match for that slip parameter.

The result in Figure 2.8 shows that for the magnitude of the force no slip matches the data the best. This is the same as Stefan's equation. However for fitting the slope of the data the best match is given by a slip parameter very close to 0.495. Figure 2.9 shows the same estimates for Laun's equation alongside the data for the highest viscosity fluid tested S30000. This fluid actually matches Stefan's equation well initially then as the gap decreases the force deviates from that ideal. This suggests that as small gaps are approached deviations from the assumptions for Stefan's Law are increased. Comparing the Figures 2.8 and 2.9 the effect of viscosity can quickly be seen as a result of the slopes of the two

curves. For S2000 notice that initially it is greater than the force predicted by the solid line (Stefan's Law), but then at smaller gaps it becomes less than the solid line. For S30000 it initially matches the solid line and fall below it at smaller gaps.

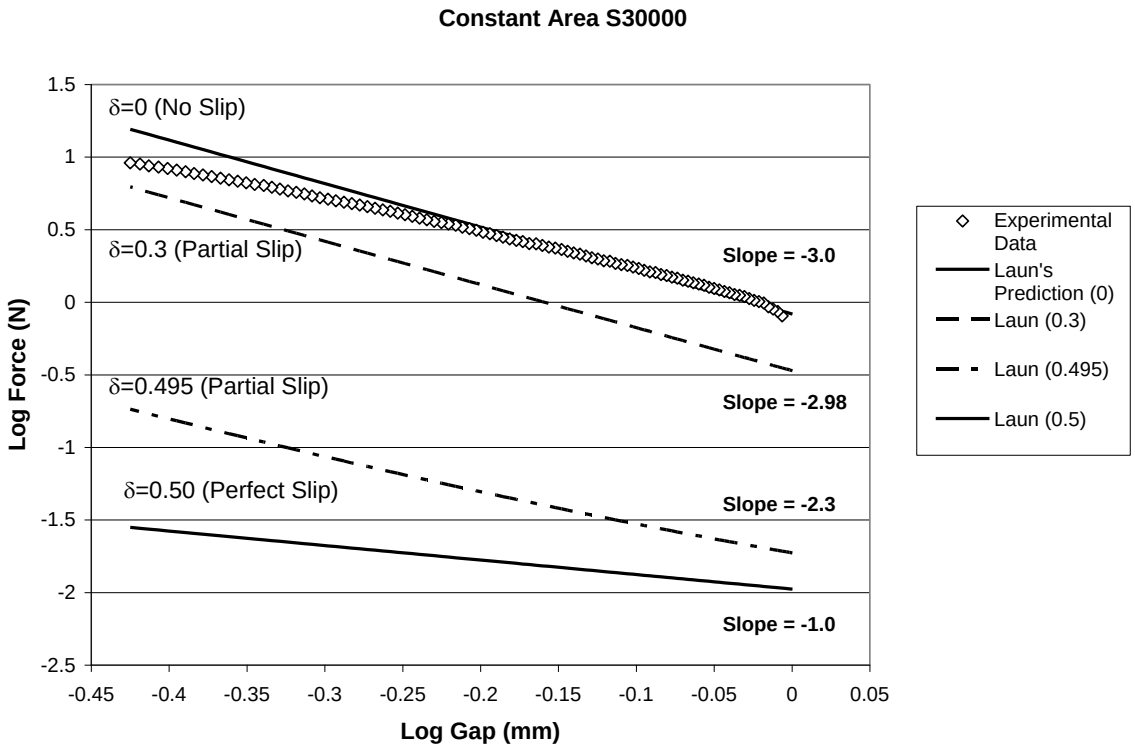

Figure 2.9 Constant Area Squeeze Flow Data for S30000 shown to compare with Laun prediction. The plot shows both how the slope varies with the slip parameter delta and how the magnitude of the force is affected by slip. Even though it is possible to arrive at a value for the slip parameter that will account for the slope the magnitude of the force doesn't match for that slip parameter for S30000 either.

Discussion

Prior to discussing how well the experiments matched the available squeeze flow theories it must be reemphasized that the purpose of this paper is to test the applicability of various squeeze flow theories using simple (Newtonian) fluids. Many of these theories are based upon assumptions that could possibly

not have held during our experiments. Any claims to be able to make suggestions about any theory requires a far more detailed analysis including much more theoretical analysis, simulation, flow visualization, and verification through experimentation as the minimum threshold.

For constant area squeeze flow Figures 2.1 and 2.2 show the differences in the squeezing force between the two constant area setups due to effects at the edge of the plates. At the edge of the upper plate in the Setup 1 is air at atmospheric pressure. Because the setup used identical size plates, the fluid sample squeezes out and falls along the sides of the bottom plate. While this setup appears ideal in matching with squeeze flow theory and simulation, experimentally, effects such as fluid pouring and gravity can affect the force due to surface tension on the sample contained between the plates, which made an additional constant area setup desirable. For the second setup the same upper disc was used, but the lower disc was replaced by one with twice the diameter of the first. At the edge of the upper disc in the second setup was more fluid, so that as the fluid squeezes out it is pushed out, but did not pour down the sides of the bottom plate.

Even though for constant area Force $\propto$ gap$^{-2.5}$ for both of the setups, the data in Figure 2.1 shows that the relationship between force and gap is different for each setup. The squeezing force is greater for Setup 2. In Setup 2 the upper plate not only has to squeeze the fluid out from between the plates, it must also force out the fluid sitting at the edge of the plate. Whereas for Setup 1 gravity removes the fluid that exits the plates, in Setup 2 the fluid must be forced out radially. Essentially this involves squeezing out more fluid than is between the two plates surface area. Therefore the contribution of the exuded material to the squeezing force is analogous to a slight extension of the plate radius. The data shows in the log-log plot that while there is a difference between the two setups for the most part the curves line up parallel, which suggests the difference in end effects does not affect the force vs. gap$^{-2.5}$ dependence. This agrees with the explanation given for a slight extension of the plate radius.

Figures 2.2 and 2.3 show the relationship between the force and the gap for each of the setups for all fluids tested. From these two figures, based on the linearity of the data, the relationship between the force and the gap in these squeeze flow experiments follows power law behavior, Force $\propto$ gap ^{a}. Figure 2.2 shows in the case of constant area squeeze flow a ≈ −2.5, and Figure 2.3 shows for constant volume a ≈ −4.

Viscosity is one of the most important fluid parameters that can be identified from rheological testing. The dependence of the viscosity on the force predicted by Stefan's Law is therefore very relevant. In order to ascertain the effect of the viscosity on the force, the viscosities of the fluids had to be determined beforehand. Because they were ASTM standards the viscosities were listed on the containers, but in order to test the fluids their viscosities were verified experimentally as well. Because Stefan's Law predicts a direct relationship between the force and the viscosity, the data in Figures 2.6 and 2.7 should fall directly on top of each other. For the highest viscosity standard however, Stefan's Law overestimates the force.

In a previous study by Winther et. al (Winther, Almdal et al. 1991) showed that measurements for viscosity do not coincide with what was expected for the apparent viscosity for Stefan's equation. Furthermore the paper concludes that for high viscosity solutions the corrected viscosity determined by squeeze flow was shown to be lower than the steady-shear viscosity. This was even after including normal stress effects. This previous work supports the observations made for the high viscosity fluid for this study.

The relationship between gap speed and the force predicted by Stefan's Law matched the data. For the same fluid tested at different squeeze speeds the log-log plots showed an overlap, converging at around a gap of 0.5 mm. The exception was the high viscosity standard, which showed increasing divergence as the gap decreased.

The slight divergence of the curves can be attributed to the compliance of the instrument. While the compliance of the instrument is accounted for in the measurements of the force, it is assumed that the speed is kept constant. As the forces become larger, due to compliance the speed actually decreased, causing the force to decrease as well.

The relationship between force and plate speed that was able to be predicted by Stefan's Law in the case of constant volume does not match the experimental data as well as for the constant area case. This is due to compliance of the instrument. As the sample area increased it increased the force causing a decrease in the gap speed.

The relationship between the squeezing force and the gap is an essential component in all squeeze flow theories and equations. Stefan's Law is an equation developed from squeeze flow theory assuming no slip at the plate surface. The relationship between force and gap for Stefan's equation is force $\propto$ gap^{-3} for constant area setups and force $\propto$ gap^{-5} for constant volume setups. Figures 2.2 and 2.3 show that the data deviate from this relationship in all the squeeze flow experiments.

In order to further explain and characterize the data other squeeze flow theories using different assumptions were tested against the squeeze flow data in this experiment. The two main objectives in looking at these other squeeze flow theories are to explain the difference in the slope for our data, and the viscosity behavior of our data. The theories examined were those that deal with Newtonian fluids, since all the fluids in this study were Newtonian. The Scott Equation is included, but only to address concerns that power law or shear thinning behavior, might be to blame for the lower slopes.

The first assumption to address is that of inertial effects. Stefan's Law ignores inertial effects in the analysis, therefore it is possible that the inertial contribution to the squeeze force creates the effects that are seen on the slope. The equation that was developed for squeeze flow to include inertial effects is given below:

$$F = \frac{3\pi R^4 \mu_0 \dot{h}}{2h^3}\left[1 + \frac{5\rho h\dot{h}}{28\mu_0} + \frac{\rho h^2 \ddot{h}}{10\mu_0 \dot{h}}\right] \text{(Bird 1987)} \qquad \textbf{(2.3)}$$

The first term is given by Stefan's Law, and the acceleration cancels out the last term with a constant squeeze speed apparatus in steady state. That only leaves the second term, which is just a fraction of the Reynold's Number for squeeze flow.

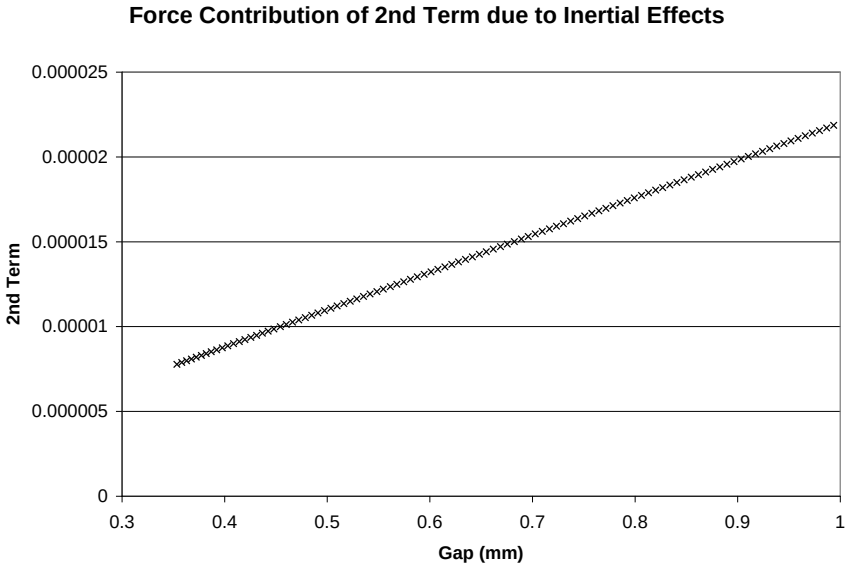

Figure 2.10 Shows the second term for the inertial equation is negligible. This was calculated for the lowest possible viscosity and the highest speed used thus maximizing the term. Still the term remained insignificant. The term should be compared to the value of 1 in the equation.

Figure 2.10 shows the 2nd term at its highest value (minimum viscosity and maximum speed and gap) falls between 7e−6 and 2.3e−5. Comparing this to 1 leads to the conclusion that the inertial contributions to the force are negligible and do not account for the experimental effects observed.

Another possible explanation is that the material is shear thinning. All fluids were tested both by manufacturer and within our lab and determined to be not only correct viscosity standards, but also Newtonian as well. However, Scott's Equation for squeezing flow of a power law fluid can quickly be broken down and examined to address this concern based on experimental evidence as well:

$$F = \left(\frac{2n+1}{n}\right)^n \left(\frac{2\pi m R^{n+3}}{n+3}\right)\left(\frac{v^n}{h^{2n+1}}\right) \text{(Scott 1931)} \qquad \textbf{(2.12)}$$

In the above equation m and n are power law parameters and v is the plate velocity. By plotting log (Fh) vs. log (v/h^2) you get n as the slope and m can be calculated from the intercept.

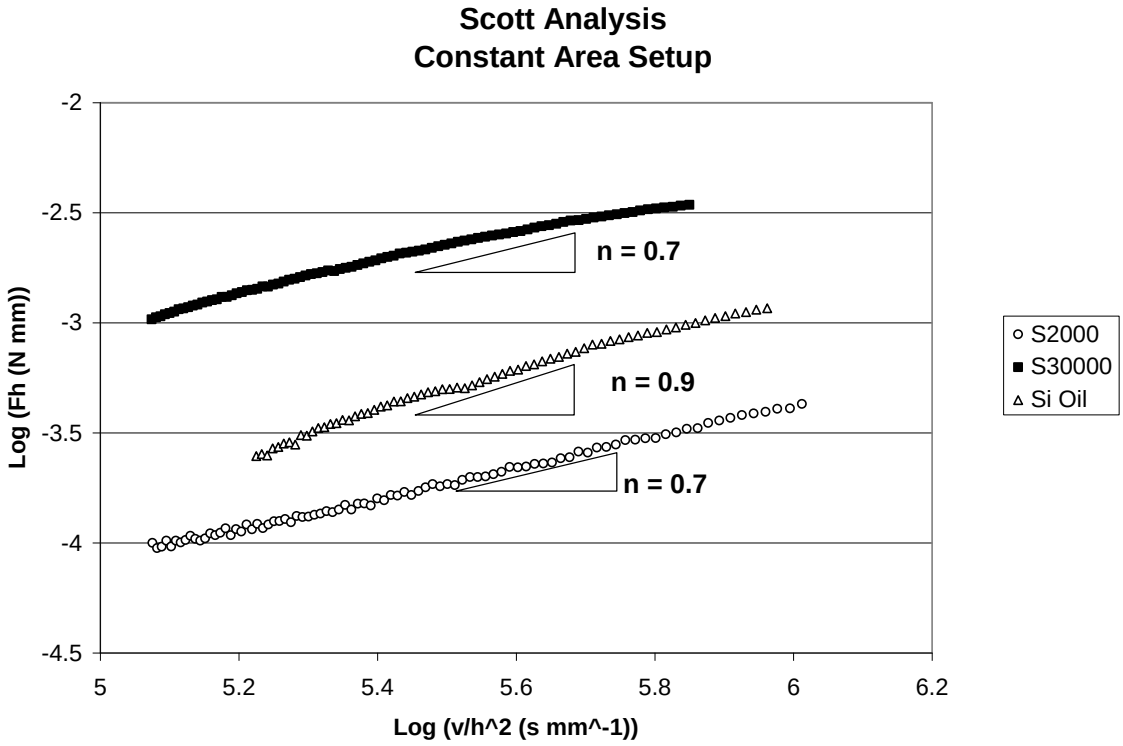

Figure 2.11 Scott Analysis gives approximate slopes to the data. The Scott Equation does not apply to these fluids because they are Newtonian.

Figure 2.11 shows that one method of matching the slope is to use the Scott Equation and just assume that the fluids are shear thinning with whatever value of power law parameters match the equation. There are two problems with this approach, the first is that the fluids were experimentally determined to be Newtonian through standard viscosity measurements done at constant shear rates. The second arises from the need to confirm experimentally that the fluid can be constitutively described by the power law parameters beyond the single experiment and analysis.

Even though using the Scott Equation allows for a slope of approximately −2.5 by adjusting the n value, and appears to provide an explanation of the slope; it must be matched with other experimental observations. First the Scott equation could be adjusted to match almost any slope within the limits of fluid behavior. For example if the slope had been −3.5 instead of −2.5 adjusting n to

1.25 would have given a correct adjustment to the slope, but may not have explained what was actually occurring. Finally the Scott equation combined with Figure 2.11 using the n-values and assuming power law squeeze flow fluid behavior for the three different fluids do not match the results shown in Figure 2.4 where the squeeze speeds overlap. Figure 2.11 shows that n ≠ 1 and actually there are 2 different values for n. This suggests that the curves in Figure 2.4 shouldn't be overlapping in any of the cases. Therefore shear thinning behavior is discounted as a potential explanation of this behavior, both from the above analysis and the experimental testing.

Another equation referred to as perfect slip or full slip which is developed from squeeze flow theory assuming full slip or a frictionless plate surface, gives a relationship between force and gap as force $\propto$ gap^{-1} for constant area and force $\propto$ gap^{-2} for constant volume. In order to achieve full slip in squeeze flow rheometry usually requires the surfaces of the plates must be treated. Because our setup used unlubricated plates, Figures 2.2–2.3 show that the data deviates from this relationship for all three setups as well. Whereas Stefan's equation with no slip gives an exponent that is too high, perfect slip gives an exponent that is too low.

The data falls in between the predictions of Stefan's Law at the upper limit and full slip at the lower limit. Because of this, an equation or relationship that utilizes partial slip would seem to be the best choice available. The Laun-Rady equation developed from squeeze flow theory gives a relationship for partial slip.

Looking at the model for partial slip at the surface developed by Laun et. al, the Rady-Laun expression for constant area is given as:

$$F = \frac{3\mu_0 \dot{h} \pi R^4}{2h^3}\left[\left(1-2\delta\right)+\frac{h^2}{R^2}\left(1+2\delta\right)\right] \qquad \textbf{(2.7)}$$

By adjusting the parameter delta a slope of −2.5 could be arrived at. For constant area R is a constant and the parameter delta could be adjusted to account for a

slope of −2.5. Because this expression is developed by assuming fluid behavior at the edge of the plate it does not easily extend to constant volume, like the other expressions were able to.

While the prediction for the above equation allows for a slope between −1 and −3 by adjusting the parameter delta, looking at the prediction for the force reveals that no slip is actually the best approximation to the magnitude of the force. The figure for the constant area experiment shows the curve that gives a slope of −3 gives a better approximation then the slope of −2.5 for the above expression. Therefore slip in the manner that it is approximated by Laun's equation does not provide an reasonable explanation to the squeeze data that was collected.

It should be noted that while the above equation provides for the progression from no slip to full slip by varying the slip parameter delta, it is unable to describe a system where slip is evolving with time as was noted by Engmann. Such a situation is more realistic in applications, but at this time could not be determined to be a factor in dealing with our experimental data.

In conclusion while the data for squeeze flow of Newtonian fluids has been examined using different squeeze flow theories, some even including the effects of inertia and slip, the best approximations for out data continue to be those put forth by Stefan's Law. Notwithstanding Stefan's Law was unable to predict a lot of the trends that were observed in our data. The other squeeze flow theories showed greater deviation from our data then Stefan's Law did. However since only one partial slip model was examined in this study, it is still very likely that another partial slip model could used to be match the data.

References

Bird, R. B. (1987). Dynamics of Polymeric Liquids. New York**:** 22.

Burbridge, A. S. and C. Servais (2004). "Squeeze flows of apparently lubricated thin films." Journal of Non-Newtonian Fluid Mechanics **124**: 115–127.

Campanella, O. H. and M. Peleg (1987). "Lubricated Squeezing Flow of a Newtonian liquid between elastic and rigid plates." Rheologica Acta **26**(4): 396–400.

Chatraei, S. H., C. W. Macosko, et al. (1981). "Lubricated Squeezing Flow: A New Biaxial Extensional Rheometer." Journal of Rheology **25**(4): 433–443.

Collomb, J., F. Chaari, et al. (2004). "Squeeze Flow of Concentrated Suspensions of Spheres in Newtonian and Shear Thinning Fluids." Journal of Rheology **48**(2): 405–416.

Diennes, G. J. and H. F. Klemm (1946). "Theory and Application of the Parallel Plate Plastometer." Journal of Applied Physics **17**: 458–471.

Engmann, J., C. Servais, et al. (2005). "Squeeze Flow theory and applications to rheometry: A review." Journal of Non-Newtonian Fluid Mechanics **130**: 149–175.

Grimm, R. J. (1976). "Squeezing Flows of Newtonian Liquid Films An Analysis Including Fluid Inertia." Applied Scientific Research **32**(2): 149–166.

Kalyon, D. M. and H. S. Tang (2007). "Inverse problem solution of squeeze flow for parameters of generalized Newtonian fluid and wall slip." Journal of Non-Newtonian Fluid Mechanics **143**: 133–140.

Kuzma, D. C. (1968). "Fluid Inertia Effects In Squeeze Films." Applied Scientific Research **18**(1): 15–20.

Laun, H. M., M. Rady, et al. (1999). "Analytical solutions for squeeze flow with partial wall slip." Journal of Non-Newtonian Fluid Mechanics **81**: 1–15.

Raphaelides, S. N. and A. Gioldasi (2004). "Elongational flow studies of set yogurt." Journal of Food Engineering **70**(4): 538–545.

Scott, J. R. (1931). "Theory and Application of the Parellel-Plate Plastimeter." Transactions of the Institution of the Rubber Industry **7**(3): 169–186.

Shirodkar, P., A. Bravo, et al. (1982). "Lubrication Flows In Viscoelastic Liquids: 2. Effect of Slip on Squeezing Flow between Approaching Parallel Rigid Plates." Chemical Engineering Communications **14**: 151–175.

Stefan, J. (1874). "Versuche uber die scheinbare Adhasion." Sitz. Kais. Akad. Wiss Math. Nat. Wien **69**(2): 713–735.

Winther, G., K. Almdal, et al. (1991). "Determination of polymer melt viscosity by squeezing flow with constant plate velocity." Journal of Non-Newtonian Fluid Mechanics **39**(2): 119–136.

Chapter 3

Squeeze Flow of Zeolite Suspensions

Introduction

Squeeze flows are found in industrial, automotive, food, biological, and engineering domains. Squeeze flow rheometry is often used as a straightforward tool to determine the flow properties of highly viscous liquids (Collomb, Chaari et al. 2004). When examining lower viscosity solutions and suspensions where particle-particle interactions can become more pronounced the technique becomes more complicated. Published reports on the squeezing flow of highly concentrated suspensions show that as the concentration of a suspension gets very large heterogeneities come into the flow profile and cause fluid behavior that is incongruous with most models.

The rheology of suspensions of particles may differ from that of pure Newtonian liquids in at least three ways. First in suspensions it is possible to reach a concentration of the suspended (solid) phase that is so high that heterogeneous flow occurs. Heterogeneous flow is flow where more than one phase is present, in the case of a concentrated suspension the suspended phase would form aggregates of solid phase in the dispersion. Already mentioned above this case has yet to be dealt with quantitatively, although several quite

useful qualitative reports have been published on this(Collomb and Chaari et al. 2005, Narumi et al. 2005, Sherwood 2002, Delhaye et al. 2000, Chaari et al. 2003). Even more significant are the particle-particle interactions between suspended particles that occur in suspensions that don't exist in pure Newtonian liquids. Finally the effect that the concentration of particles have on macro-phenomena such as viscosity becomes important as well. This paper examines experimentally the effects of some of these on the squeeze flow of zeolite suspensions and contrasts this with what is theoretically expected.

These experiments attempted to avoid the problems associated with heterogeneous flow by using low concentrations of suspensions. Even so the effects of particle-particle interactions and the effects that concentration had on the viscosity will be examined. The effects of particle-particle interactions (the ability of particles to form stable structures) were reduced in this experiment by using two relatively high viscosity fluids. Our experiments showed that these effects still could not be ignored in the analysis of the data.

In order to assess squeeze flow behavior of the suspensions this paper utilizes two different experimental setups—constant volume and constant area squeeze flow. The dominant theory which will be examined in both of these cases is Stefan's Law which assumes no slip. The purpose of this study is to examine and explain the squeeze flow behavior of suspensions based on what is known about the rheology of these suspensions and squeeze flow techniques employing Stefan's Law as a guidepost.

Increasing the concentration has been shown to increase the viscosity of the suspension in many different studies including Einstein's relationship. Particularly that increasing the volume concentration of particles increases the viscosity of the suspension. These increases in viscosity were shown to only give a partial explanation of the experimental data.

In this paper first the squeeze flow data will be compared with what's predicted by the predominant theory (Stefan's Law). Then using the theory an assessment of the suspension viscosity in squeeze flow will be made. Finally the effect that the concentration of the zeolite suspension has on the relative viscosity will be examined based on the squeeze flow behavior.

Materials and Methods

Apparatus

This experiment utilized a Rheometrics RDS-II with parallel plates setup. For the constant area test parallel plates with diameter 2.5 cm were used. For constant volume squeeze test parallel plates with 5.0 cm were used. For the constant volume test a syringe was used to squeeze 0.5 mL of the suspension or oil between the plates. All tests were done at a constant squeeze speed of 0.10 mm/s. Compliance of the instrument was included in all of the measurements. Below is a figure of the compliance

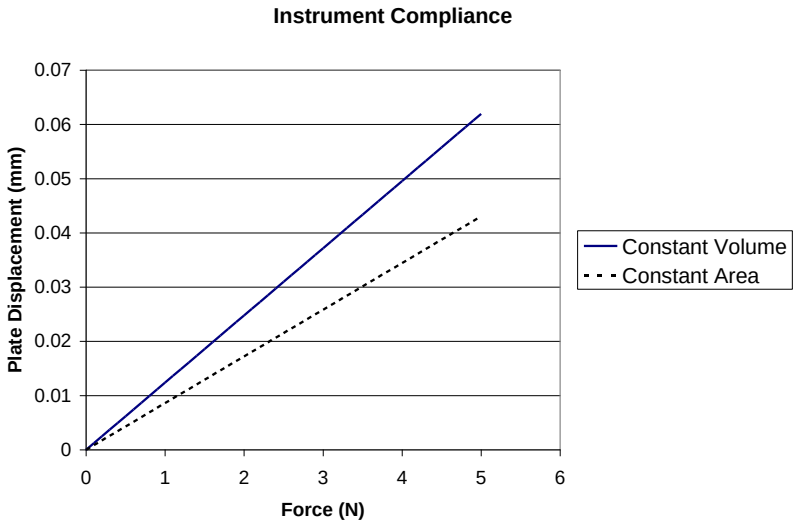

Figure 3.1 Instrument Compliance

Materials

The zeolite suspensions were prepared using aluminosilicate powder (SG 1.1 @ 25° C) the density of which was measured and determined to be 1.96 g/cm^3. This study examined both a high viscosity— 10,000 cSt (SG 1.30 @ 25° C) and a lower viscosity — 1,000 cSt (SG 1.28 @ 25° C) silicon oil. By weight 10,20 and 30% suspensions were prepared with the high viscosity oil. Similarly by weight 10, 20, 30 , and 40% solutions were prepared with the lower viscosity oil suspension.

Results

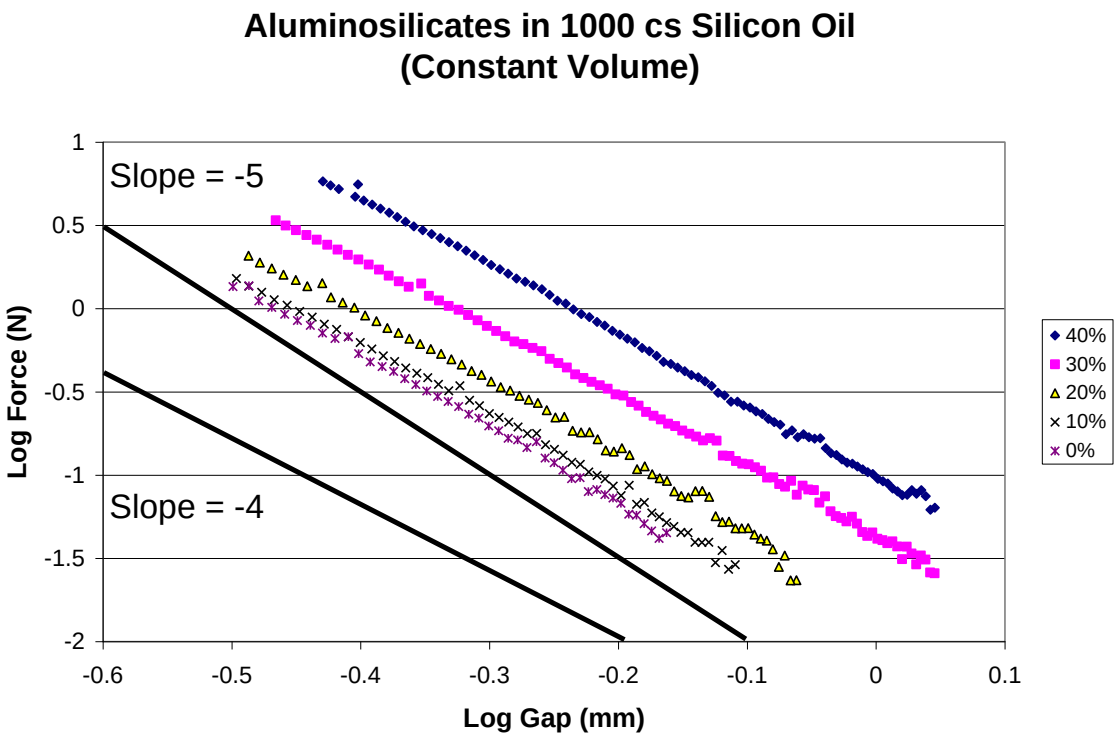

Figure 3.2 Constant Volume Squeeze Flow of Aluminosilicates in 1,000 cs Silicon Oil. Log-log Chart of Force vs. Gap shows the effect of increasing the %wt concentration of the suspension on the force. The lines represent what would be predicted by Stefan's Law for a Newtonian fluid in constant volume (Slope =−5).

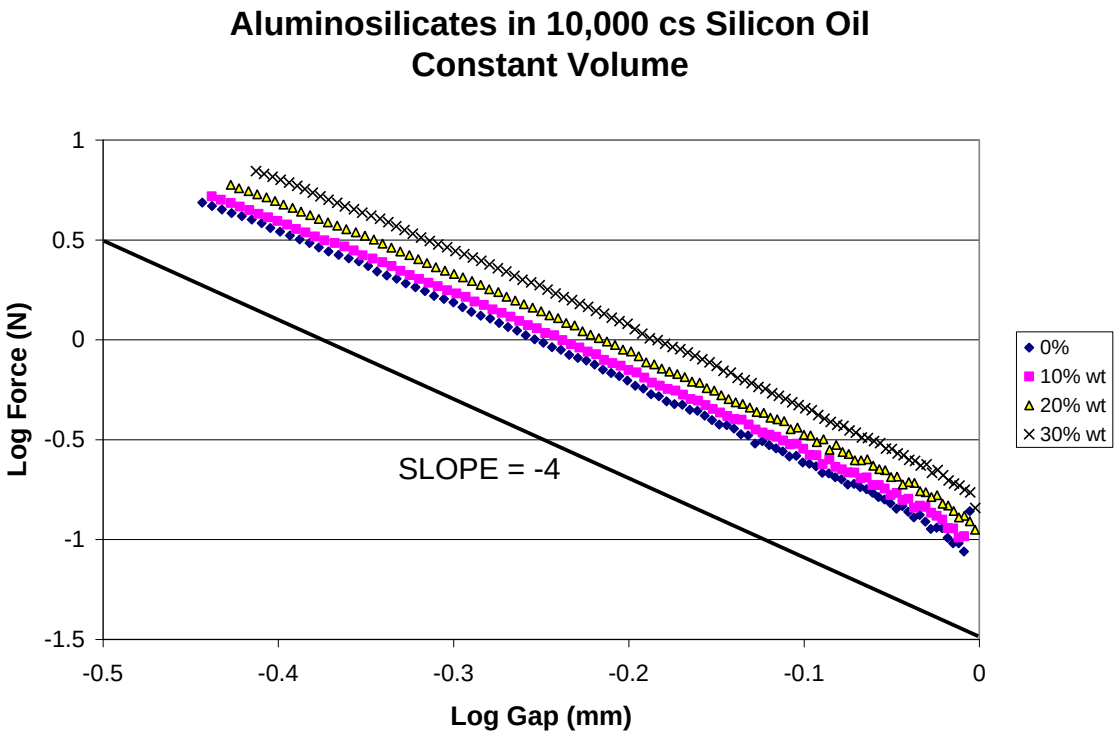

Figure 3.3 Constant Volume Squeeze Flow of Aluminosilicates in 10,000 cs Silicon Oil. Log-log Chart of Force vs. Gap shows the effect of increasing the %wt concentration of the suspension on the force. The line represents the average slope for the data.

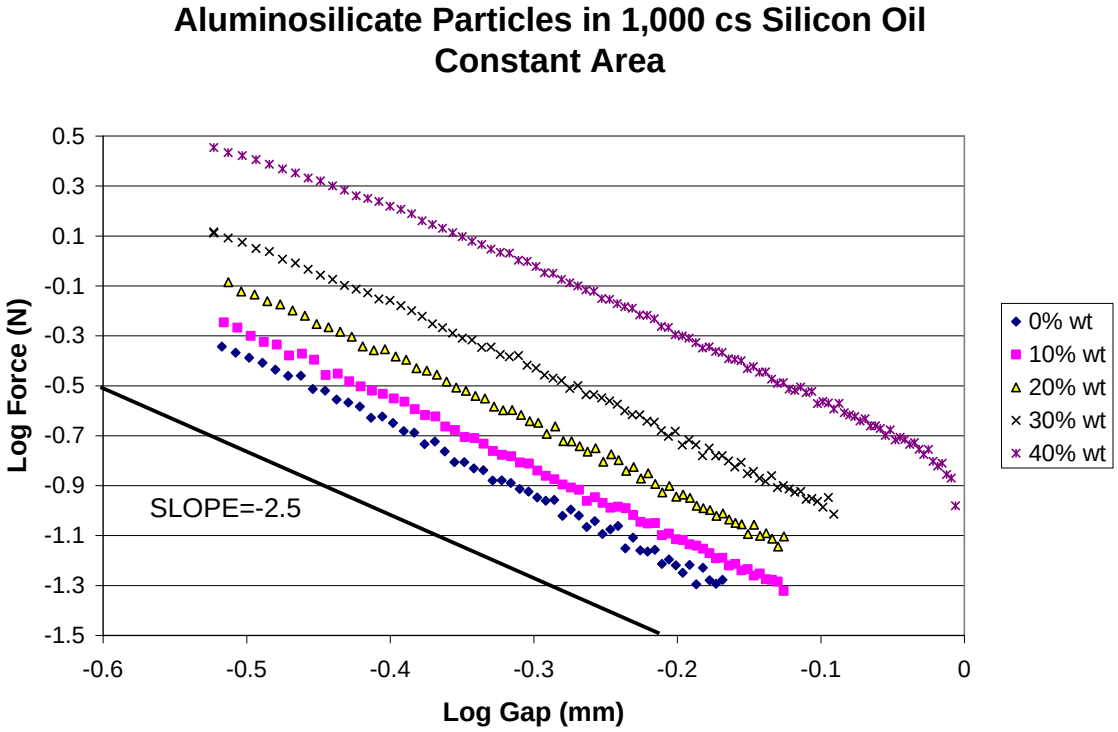

Figure 3.4 Constant Area Squeeze Flow of Aluminosilicates in 1,000 cs Silicon Oil. Log-log Chart of Force vs. Gap shows the effect of increasing the %wt concentration of the suspension on the force. The line represents the average slope for the data.

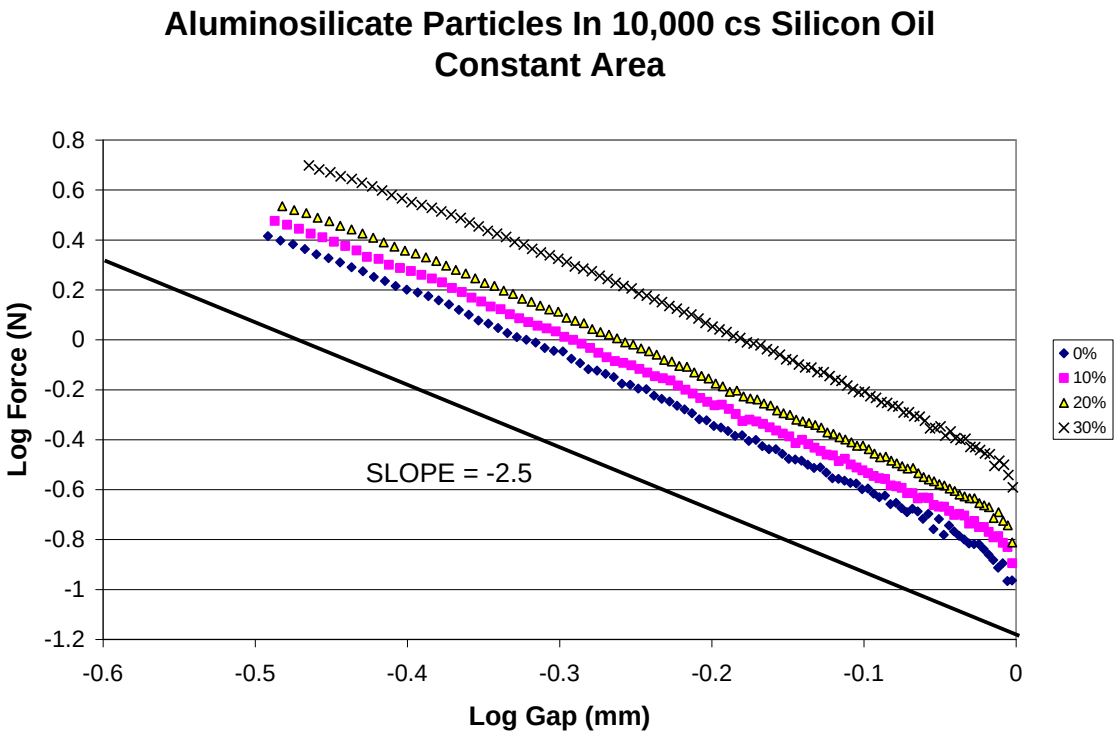

Figure 3.5 Constant Area Squeeze Flow of Aluminosilicates in 10,000 cs Silicon Oil. Log-log Chart of Force vs. Gap shows the effect of increasing the %wt concentration of the suspension on the force. The line represents the average slope for the data.

Figures 3.2–3.5 show the results of the squeeze test on the zeolite suspension. These experiments were done in order to investigate the effects of suspension concentration and suspension oil viscosity on the force vs. gap behavior in squeeze flow. The force and gap were plotted on log-log charts in order to show the linearity and slopes of the data to compare with other published squeeze flow force gap relationships. Stefan's Law is the relationship that is of primary concern to this study. Figures 3.2 and 3.4 show the results of the squeeze test on the lower viscosity zeolite suspension for constant volume

and area respectively, while Figures 3.3 and 3.5 show the same test on the higher viscosity zeolite suspension.

The results for the constant volume squeeze tests are shown in Figures 3.2 and 3.3. Both figures show that increasing the concentration of the suspension causes an increase in the force at a given gap as expected. For Figure 3.2 as the lower viscosity zeolite suspension's concentration is increased at 0.4 mm gap from 0% wt.to 10% wt. to 20% wt. to 30% wt. to 40% wt. the force goes from 0.51 N to 0.61 N to 0.93 N to 1.91 N to 4.47 N respectively. Likewise as the high viscosity zeolite suspension is increased in concentration from 0% to 10% to 20% to 30% at 0.4 mm gap the force is increased from 3.45 N to 3.85 N to 4.78 N to 6.29 N. As the concentration is increased in the log-log chart the force increases by shifting the curves up for both high and low viscosity suspensions.

The results also show that the slopes in Figure 3.2 and 3.3 actually don't match the force vs. gap relationship predicted by Stefan's Law for constant volume. This predicts a slope of −5. This relationship requires an assumption that the liquid sample volume remain cylindrical between the plates. Figure 3.2 shows the lower viscosity zeolite suspension with a slope that varies between −5 and −4. The slope actually decreases as the concentration increases. It drops from approximately −4.5 at 0% wt to about −4 for 40% wt. While it might be assumed that particle particle effects due to increasing concentration, actually the larger concentrations match more closely with the higher viscosity results. Examining Figure 3.3 for the high viscosity zeolite suspension the slope stays approximately

at −4. Recall that for high viscosity oil suspensions the particle-particle effects become smaller.

The results for the constant area squeeze tests are shown in Figures 3.4 and 3.5. Unlike constant volume, constant area doesn't require any assumptions to be made about the sample volume, but effects at the edges of the plates can affect the measurements. For this setup the increase in concentration of the suspension again resulted in an increase in the force. But the forces were smaller than those reported for the constant volume. For the low viscosity zeolite suspension increasing the concentration from 0% wt to 10% wt to 20% wt to 30% wt to 40% wt at a gap of 0.40 mm led to increases in the force of 0.22 N to 0.28 N to 0.42 N to 0.70 N. Similarly for the high viscosity zeolite suspension increasing the concentration from 0% wt to 10% wt to 20%wt to 30% wt. at a gap of 0.40 mm led to an increase in force from 1.57 N to 1.89 N to 2.25 N to 3.57 N respectively. Likewise with constant area testing the observation that the increase in concentration causes an increase in force can be seen in the shifting of the data up on the force axis as concentration increases.

Relative Viscosity

The relative viscosity or the viscosity ratio is the ratio of the viscosity of the dispersion to the viscosity of the pure dispersion oil or carrier fluid. By utilizing Stefan's relationship the squeeze data can be quickly manipulated to arrive at the

relative viscosity for the suspensions. This can be done by taking the ratio of the squeezing force at the same gap.

$$F_{dispersion} = \left(\frac{3\pi R^4 \dot{h}}{2h^3} \right) \times \eta_{dispersion} \qquad F_{oil} = \left(\frac{3\pi R^4 \dot{h}}{2h^3} \right) \times \eta_{oil}$$

For each test the plate radius (R), the plate speed ($\hat{h}$), and the gap (h) is kept the same then to get the relative viscosity of the viscosity ratio divide by the Force for the dispersion by the force for the pure oil.

$$\frac{F_{dispersion}}{\mathrm{F}_{\mathrm{pureoil}}} = \frac{\eta_{dispersion}}{\eta_{oil}} = \eta_{rel}$$

By plotting the ratio of the forces vs the gap the relative viscosity of the suspension can be determined. Because the relative viscosity of the sample doesn't change for a Newtonian suspension the data for each suspension should all fit on a single line. Additionally the viscosity should be independent of the test being used so both tests should give data very close to each other.

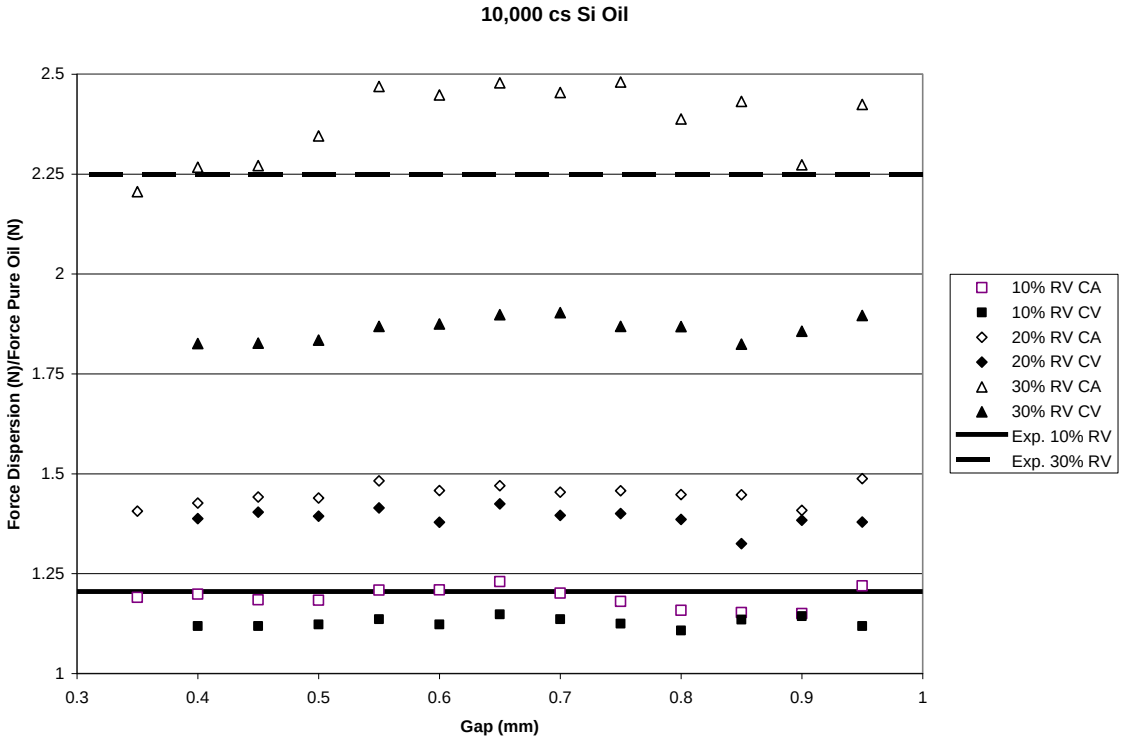

Figure 3.6 The Force Ratio of the dispersion (10,000 cs) is shown, by plotting the force ratio against the gap . The two lines represent the relative viscosity of the dispersions determined experimentally by shear**.**

Figure 3.6 shows the relative viscosity data for the suspension with the higher viscosity carrier fluid. For this suspension the data for each dispersion approximately fell on a horizontal line for the lower concentrations. For the higher concentrations (30%) the data showed less precision, but still did not significantly deviate from the average value. The two tests gave very close to the same values for at 10% and 20% wt. concentrations. At 30% wt there was significant deviation between constant area and constant volume. Finally in order to assess the accuracy of this technique, measurements of two of the dispersions viscosity were done using a parallel plate rheometer. Here the samples were placed

between two plates at a set gap and the samples were sheared instead of compressed and the viscosity was recorded. These values are given in the figure for comparison by the solid lines. The 10% dispersion concentration in shear matched with that taken using the squeeze flow data. For the 30% concentration the range between the constant area and the constant volume tests was so large as to be inconclusive as to the exact relative viscosity measurement. However, the measured shear viscosity did fall between the two determined relative viscosities.

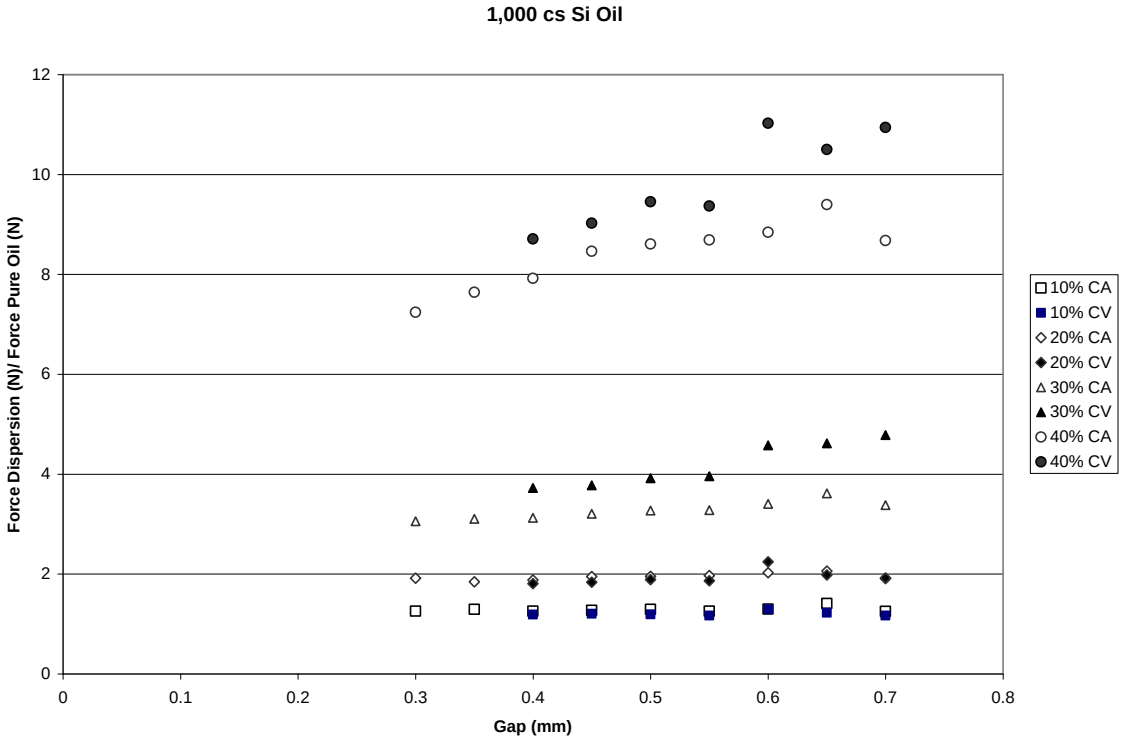

Figure 3.7 The force ratio of the dispersion (1,000 cs) is shown by plotting the force ratio against the gap.

Figure 3.7 shows the relative viscosity of the dispersion using the low viscosity carrier fluid. Again it is shown that at lower concentrations the data for constant area and constant volume fall on top of each other and the data from the two tests tend to agree. For the lower viscosity suspension an even higher concentration (40%) dispersion was able to be tested. For the viscosity ratio the data did not fall on a horizontal line, and the determined relative viscosity varied between the two tests by as much as 2.

Effect of Concentration on Viscosity

Taking the data from Figures 3.6 and 3.7, an average relative viscosity could be determined for each dispersion with each test. Those results are tabulated in Table 1.

Conc. % Wt (%Vol)	Dispersing Oil (cs)	Relative Viscosity (Constant Area)	Relative Viscosity (Constant Volume)
10 (5.1)	10,000	**1.19 ± 0.022**	**1.13 ± 0.011**
10 (5.1)	1,000	**1.26 ± 0.050**	**1.24 ± 0.083**
20 (10.2)	10,000	**1.45 ± 0.038**	**1.39 ± 0.024**
20 (10.2)	1,000	**1.93 ± 0.067**	**2.29 ± 0.193**
30 (15.3)	10,000	**2.39 ± 0.111**	**1.86 ± 0.085**
30 (15.3)	1,000	**3.24 ± 0.175**	**4.75 ± 0.868**
40 (20.4)	1,000	**8.43 ± 0.665**	**10.79 ± 1.58**

Table 3.1 The Average Relative Viscosity for Each Dispersion.

Using this data the concentration vs. viscosity curve could be determined to show how the relative viscosity varies with concentration as determined in squeeze flow. While the data may not be as precise as that determined in shear, by examining the relative viscosity vs. concentration and comparing it to different

relationships from theory certain effects could be observed that are unique to squeeze flow.

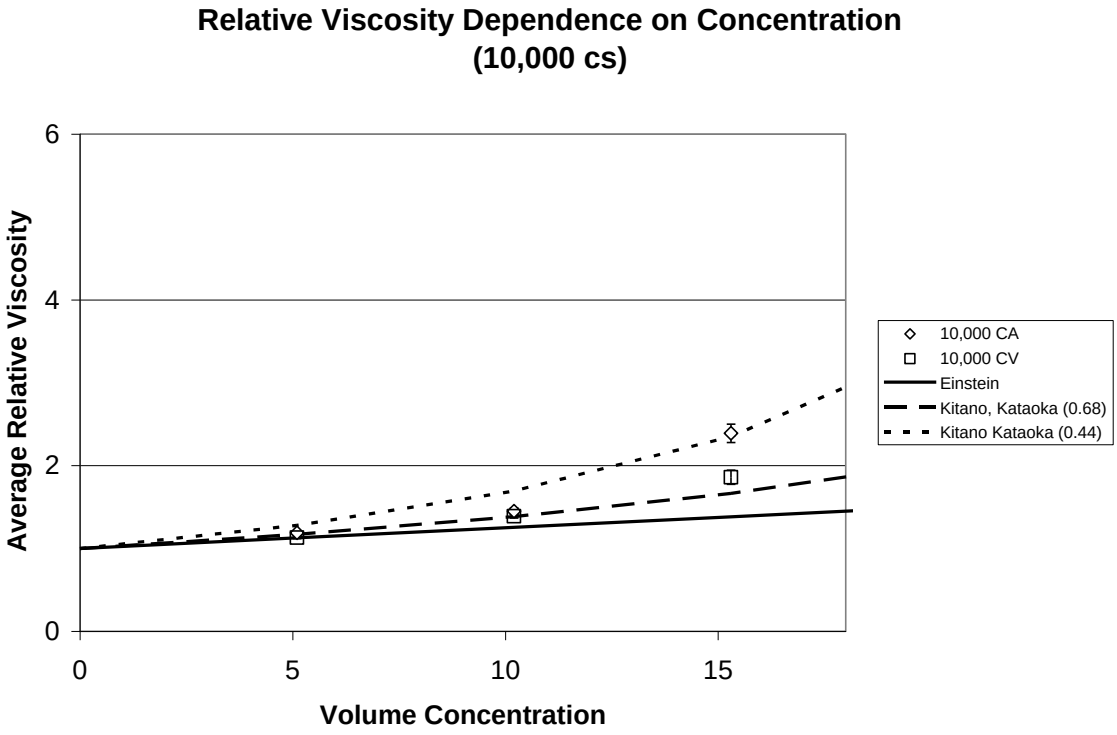

Figure 3.8 The average relative viscosity vs. concentration for (10,000 cs) suspension. It also shows the two theoretical relationships Einstein, and Maron and Pierce (Kitano, Kitaoko). for comparison.

Figure 3.8 shows the data from Table 1 plotted and compared with two relationships. Each of the relationships between concentration and viscosity is given in volume concentration so the values were converted. Probably the most well-known is that of Einstein, which gives a simple linear relationship:

$$\eta_{rel} = \frac{\eta_{dispersion}}{\eta_{oil}} = 1 + 2.5\phi \qquad \textbf{(3.1)}$$

$$\phi - Volume\ Fraction$$

This equation is only applicable within a vanishingly small range of solids concentrations. In addition the very useful empirical expression first developed by Maron and Pierce and later carefully evaluated by Kitano, Kataoka and their coworkers was also compared with the viscosity concentration data. This relationship is:

$$\eta_{rel} = \frac{\eta_{dispersion}}{\eta_{oil}} = \left[1 - (\phi / A)\right]^{-2} \qquad \textbf{(3.2)}$$

$\phi - Volume\,Fraction$

$A - Single\,Empirical\,Parameter$

Aspect Ratio	Value of A
1.0	0.68 (for smooth spheres) to 0.44 (for rough crystals)
6 to 8	0.44
18	0.32
23	0.26
27	0.18

Table 3.2 Values for the empirical parameter A

Using this expression and the table above the value of A can be varied depending on the kind of particles are in the suspension. For zeolites in a

suspension Einstein's approximation for dilute suspensions of noninteracting hard spheres isn't going to be the best formula. Figure 3.9 shows a picture of a zeolite. It is doubtful looking at Figure 3.9 that even the empirical equation for smooth spheres will can be applied. The data is Figure 3.8 shows that the actual behavior falls between the smooth spheres and the rough crystals using the empirical equation.

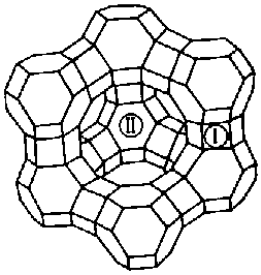

Figure 3.9 Picture of Zeolite

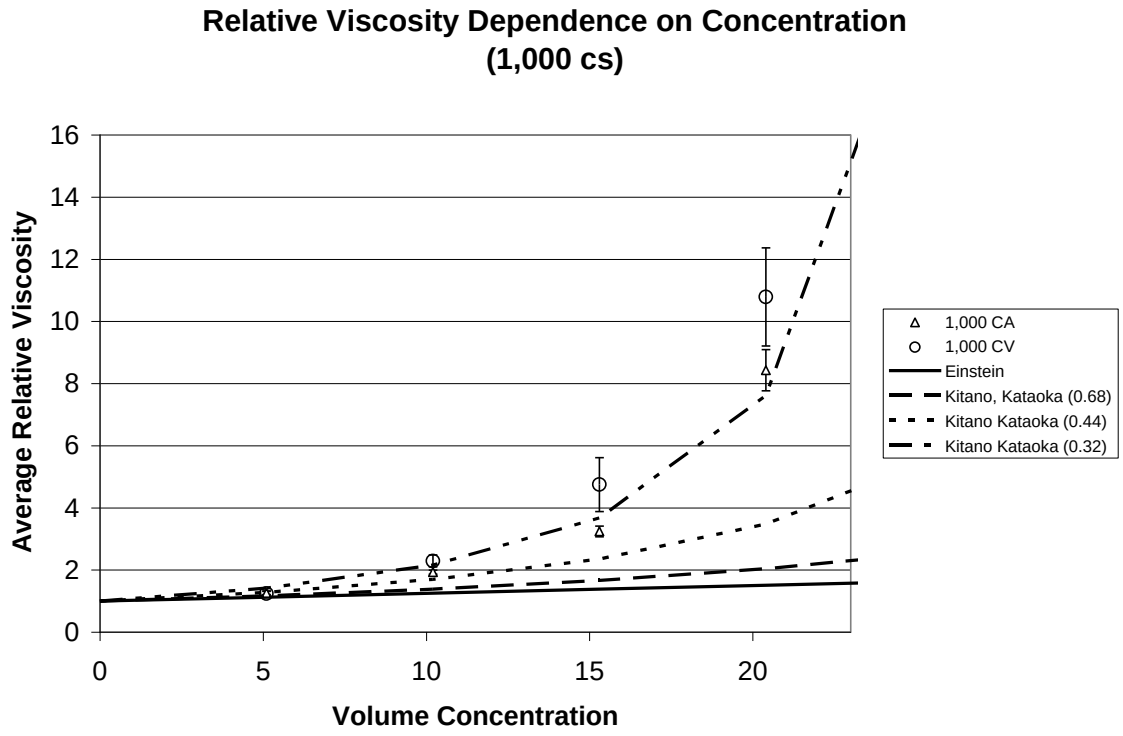

Figure 3.10 The average relative viscosity vs. concentration for (1,000 cs) the suspension. It also shows the two theoretical relationships Einstein, and Maron and Pierce (Kitano, Kitaoko). for comparison.

Figure 3.10 shows the same data for the lower viscosity suspension. The relative viscosities are higher for the lower viscosity oil suspension. In comparing the data from Table 1 to the two relationships Einstein's again doesn't match due to the reasons explained above. The empirical relationship does not match as well as it did before either. Even at an empirical constant value of 0.32 It doesn't capture the behavior of the suspension at higher concentrations.

Discussion

Although the squeeze flow data does not exactly match Stefan's Law, Figures 3.3–3.5 do reflect a consistent power-law relationship, and Figure 3.2 is only slightly inconsistent in the slope of the data. The results show in Figures 3.4 and 3.5 that instead of the predicted slope of −3 the slope actually is −2.5, and for Figures 3.2 and 3.3 instead of a slope of −5 the slope is actually approximately −4. This difference between the model and the suspensions can't be attributed to particle effects, because even the particle-free fluids show the same behavior. While slip or partial slip at the surface gives a plausible explanation for a reduction in the slope, comparing the pure fluids to partial and full slip models reveals that "no slip"— Stefan's Law — gives the best approximation for the forces generated. Therefore, while the data do not exactly fit Stefan's relationship for the slope, Stefan's relationship is the closest approximation of all models looked at for this study.

Since Stefan's model gave the best approximation for the pure Newtonian fluids, it can reasonably be assumed that Stefan's model can be used as a starting point to analyze the differences between the particle free fluids and the suspensions. By qualitatively examining Figures 3.2–3.5, every test shows that increasing the concentration of particles in the suspension increases the squeezing force. The greater the concentration of particles added to the pure fluid the greater the force is. The only fluid parameter in Stefan's Law is the viscosity. Therefore the increase in the force according to Stefan's relationship is due to an increase in the viscosity. The viscosity dependence on concentration

agrees with this conclusion. Therefore the explanation for the increase in the force as the concentration goes up in the suspension is due to an increase in the viscosity. This is not to conclude that it is only due to an increase in viscosity in all instances. But in this regime where homogenous flow dominates and particle-particle interactions are assumed at a minimum it is reasonable.

Relative Viscosity

Coming to the conclusion that the viscosity is the key parameter Stefan's Law can quickly be manipulated to arrive at an relative viscosity for the dispersions which is shown in Figures 3.6 and 3.7. Several assumptions were made to arrive at the relative viscosity. Therefore an additional test using a parallel plate rheometer shear test to determine the viscosity was done on the high viscosity sample in order to verify this method. The reason the high viscosity suspension was tested was to minimize particle-particle effects which can't be handled by Stefan's Law. Since the shear tested viscosity agreed with the results it was assumed the method worked.

Had the suspension been shear thinning it was not enough to look at Figures 3.6 and 3.7 and assume that since the viscosity didn't go down at higher shear rates (smaller gaps) that the suspension was Newtonian. Since the viscosity being determined is not absolute, but relative the fact that the relative viscosity didn't drop at higher shear rates only reveals that the non Newtonian behavior (power law exponent) was similar for both the suspension and pure silicon oil. This can further be demonstrated by looking at the Scott Equation (Scott 1931).

For high viscosity oil suspensions the viscous forces tend to dominate the particle-particle interactions. Therefore Figure 3.6 will more closely approximate the ideal conditions described by Stefan's Law. The small differences in the relative viscosity measurements can be attributed to systematic errors in measurement. For the low viscosity sample it is necessary to go back to Figure 3.2 to explain the data. The slope changes for the low viscosity test by about 0.4 for the 30% and 0.3 for 40%. The effects on the other samples are minimal. This results in an unequal method as shown below.

$$F_{dispersion} = \left(\frac{3\pi R^4 \dot{h}}{2h^{4.1}}\right) \times \eta_{dispersion} \qquad F_{oil} = \left(\frac{3\pi R^4 \dot{h}}{2h^{4.5}}\right) \times \eta_{oil}$$

$$\frac{F_{dispersion}}{F_{oil}} = \frac{\eta_{dispersion}}{\eta_{oil}} \times \frac{h^{4.5}}{h^{4.1}} = h^{0.4} \times \eta_{rel} \qquad \textbf{(3.3)}$$

This must be corrected for these two values and adjusting the chart by dividing by h^a. Below is the corrected data.

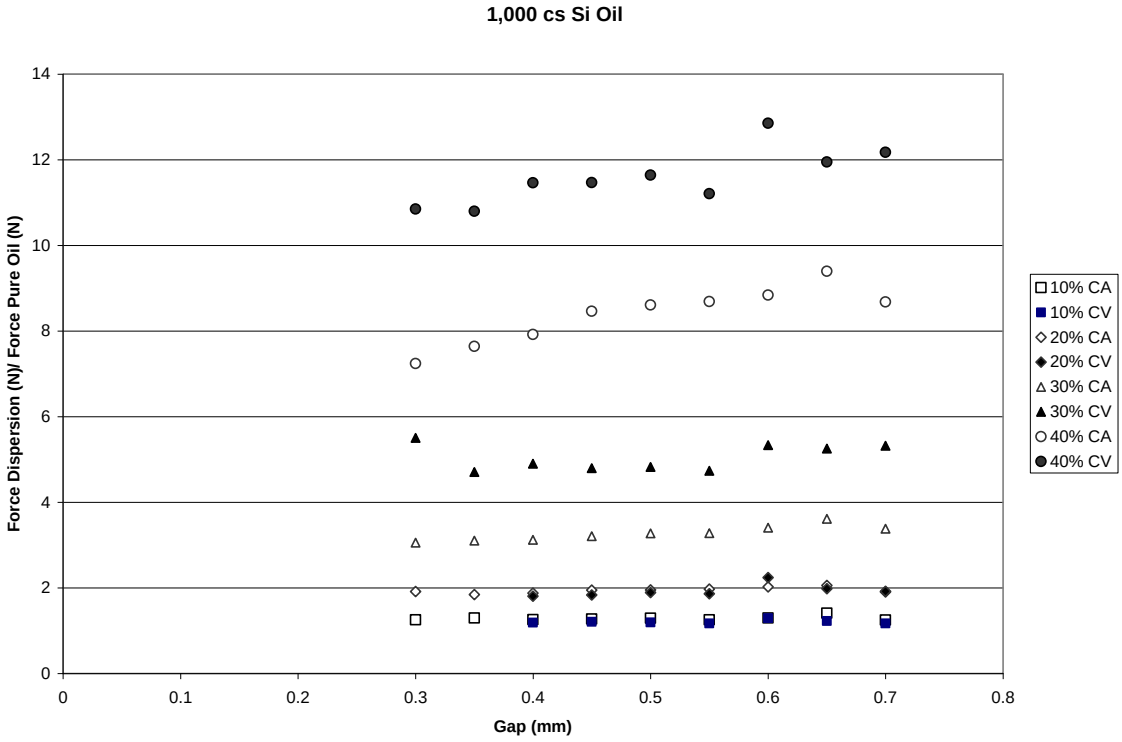

Figure 3.11 Figure showing corrections for suspensions

While this in one way corrects the data it doesn't explain the difference between the 30% and 40% constant volume and constant area measurements. This effect can be explained by particle-particle interactions. Up to this point it has been assumed that the only effects the particles had on the fluid was to increase the suspension viscosity. The zeolites agglomerating and forming particle structures in the fluid was not examined. At higher concentrations of particles with thinner fluids these effects become more significant (Metzner 1985).

The agglomeration of particles have a greater effect in squeeze flow for constant volume measurements in that the particles are not spread over the plate surface area. The concentration of particles remains the same for both tests, but the geometry of the constant volume test gives a greater height to surface area ratio. Taking this into account the fact that constant volume results in greater relative forces can be understood.

Looking back however, the high viscosity oil suspension in Figure 3.6 at 30% wt concentration has a constant area force ratio that is greater then the constant volume force ratio. The same above explanation can be used. For low viscosity suspensions the agglomerates of particles significantly increase the squeezing force, because the viscous forces are lower. For high viscosity fluids the particles that agglomerate do not significantly increase the squeezing force, because the viscous forces dominate. The agglomeration of particles reduces the concentration of particles in the bulk of solution. Therefore when phase separation occurs in a high viscosity suspension during squeeze flow the viscosity is reduced, which reduces the dominant viscous forces thereby reducing the overall squeezing force. Therefore in a high viscosity suspension the relative viscosity for constant area would be greater and for a low viscosity suspension the relative viscosity for constant volume would be greater.

Effect of Viscosity on Concentration

Having arrived at how particle-particle effects combine with the effects of suspension viscosity, the effect that particle concentration has on the relative viscosity of a suspension can be examined. Although there are numerous

theories that exist in looking at the effect of concentration on viscosity, only Einstein's relationship and an empirical equation derived by Kitano and Kataoko will be looked at (Kitano et al. 1981). Einstein's relationship is one of the simplest that exists for dispersions, and the empirical relationship derived by Kitano and Kataoko using the Maron-Pierce equation (Maron and Pierce 1956) has been shown to be one of the most broad useable relationships covering several different effects in suspensions(Metzner 1985, Cross 1975)

Einstein's correlation for a suspension of noninteracting hard spheres is given in Figure 3.8. In the figure it only matches at the lowest concentration and this agrees with other suggestions that his equation is only useful at very small volume fractions. The empirical equation requires an empirical constant A. For A = 0.68 which corresponds to spherical particles it gives a slight improvement above Einstein's equation. The equation doesn't agree with the expression because zeolites as shown in Figure 3.9 are not represented well by spheres in solution. When the empirical constant is set to 0.44 the curve agrees with the data at the highest concentration using constant area. This suggests not only that the suspension is better matched by a rough crystal than by the non interacting spheres, but further validates the relative viscosity calculations for squeeze flow.

The plot of the low viscosity sample is shown in Figure 3.10. This figure demonstrates that similar to the high viscosity suspension the spherical models don't work. However, the rough crystal model matches only at low values, but at higher values the relative viscosity values are much greater. This is due again to particle-particle interactions creating a larger overall force. Even the high aspect

ratio of 18 doesn't account for the increases in relative viscosity. Particle-particle interactions therefore offer the best explanation here.

Conclusions

From the results of the zeolite suspension squeeze flow investigation, it can be concluded that suspension concentration has at least two effects on the squeezing force. The suspension concentration increases the suspension viscosity in squeeze flow resulting in an increase in the squeeze force. Also the increasing the suspension concentration increases the likelihood that phase separation will occur, and in the case of the zeolites studied that phase separation will result in a particle-particle interactions that create a greater squeezing force for lower viscosity fluids, but a decrease in the squeezing force for high viscosity fluids.

The investigation reveals also the effects of the carrier fluid viscosity on the sample. The effect that the oil has on dependence of the concentration on the squeezing force in this test showed that this effect increased with increasing concentration. At low concentrations the suspension for high and low viscosity oils were very close to the same relative viscosities, but as the concentration increased the effect that the concentration had on viscosity for both oils diverged. The higher viscosity oils minimize particle-particle interactions for the zeolites in the suspension. The lower viscosity oils produced suspensions more prone to particle-structural effects.

Finally the investigation revealed that both effects of viscosity and concentration in a suspension for squeeze flow need to be examined not just in isolation, but synergistically. This is not just because of phase separation, but due to the nature of squeeze flow, which is transient and is strongly affected by small changes in the bulk of the material.

References

Chaari, F., et al., *Rheological behavior of sewage sludge and strain-induced dewatering.* Rheologica Acta, 2003. **42**: p. 273–279.

Collomb, J., F. Chaari, and M. Chaouche, *Squeeze Flow of Concentrated Suspensions of Spheres in Newtonian and Shear Thinning Fluids.* Journal of Rheology, 2004. **48**(2): p. 405–416.

Cross, M., *Viscosity-concentration-shear rate relationships for suspensions.* Rheologica Acta, 1975. **14**: p. 402–403.

Delhaye, N., A. Poitou, and M. Chaouche, *Squeeze Flow of highly concentrated suspensions of spheres.* Journal of Non-Newtonian Fluid Mechanics, 2000. **94**: p. 67–74.

Kitano, T., T. Kitaoka, and T. Shirota, *An empirical equation of the relative viscosity of polymer melts filled with various inorganic fillers.* Rheologica Acta, 1981. **20**: p. 207–209.

Maron, S. and P. Pierce, *Application of the Ree-Eyring Generalized Flow Theory to Suspensions of Spherical Particles* Journal of Colloid Science, 1956. **11**: p. 80–95.

Metzner, A.B., *Rheology of Suspensions in Polymeric Liquids.* Journal of Rheology, 1985. **29**(6): p. 739–775.

Narumi, T., et al., *Solid Like Behavior of Concentrated Particulate Suspensions Under Squeezing Flow.* Journal of Society of Rheology, Japan, 2005. **33**(1): p. 29–36.

Scott, J.R., *Theory and Application of the Parellel-Plate Plastimeter.* Transactions of the Institution of the Rubber Industry, 1931. **7**(3): p. 169–186.

Sherwood, J.D., *Liquid-solid relative motion during squeeze flow of pastes.* Journal of Non-Newtonian Fluid Mechanics, 2002. **104**: p. 1–32.

Chapter 4

Squeeze Flow of Electrorheological Fluids Under Constant Volume

Introduction

Compression studies of electrorheological fluids have been impeded by the "sealing effect" (Ahn et al. 2000, Monkman 1995, Vieira et al. 2001, Filisko and Meng 2005). Using a constant area parallel plate apparatus this sealing effect is responsible for squeezing out an unknown quantity of particles from between the plates while the rest are held between the plates because of the electric field. Previous studies by Ahn, Chu and Lee have dealt with this problem by assuming that all particles remain in between the plates (Ahn et al. 2000). This is an approximation that gets worse as the viscosity of the fluid is increased.

The present study avoids these restrictions by using a constant volume apparatus. In a constant volume apparatus, instead of knowing that the area of the plate in contact with the fluid is constant throughout the test, instead the area of the plates in contact with the fluid is changing throughout the test, but the volume of the fluid contained in between the plates remains constant throughout the tests. The experiment and equation developed for this type of squeeze flow was done by Diennes and Klemm (Diennes and Klemm 1946)

By using a constant volume apparatus for conducting this experiment the concentration of particles that stay in between the plates is known throughout the experiment. Because there is already a model for homogeneous Newtonian fluids in constant volume squeeze flow, the results for compression of a electrorheological fluid could be compared with this model and an analysis of both the effects of the ER fluid composition on squeeze flow and the effects of geometry and squeeze speed could be made. This study is concerned with the effects of the concentration of particles in the dispersion.

Materials and Methods

Apparatus

Figure 4.1 Experimental Apparatus and Setup

A Weissenberg rheometer with an added step motor-leadscrew loading system and an LVDT displacement sensor was used to make the measurements. For each test a syringe was used to measure a constant volume of 0.5 mL of ER fluid which was placed between the plates.Before compression, a DC voltage was imposed on the sample and was kept constant in the whole period of

compression. A PC and a laptop computer were used to record the output of the load cell and the displacement sensor.

Materials Preparation

The electrorheological fluids were prepared using dried aluminosilicate powder (SG 1.1 @ 25 °C) in silicon oil. This study examined both a high viscosity — 1,000 cSt (SG 1.27 @ 25°C) and a low viscosity — 10 cSt (SG 0.963 @ 25°C) silicon oil. By weight 10, 20, 30, and 40% solutions were prepared by weighing the aluminosilicates out and adding the silicon oil dropwise into vials. The solutions were immediately mixed and capped.

Results

Figure 4.2 shows how the compression force develops during compression of the ER fluids containing the low viscosity silicon oil without an electric field. The compression force shows that the fluid squeezes down until there is a monolayer of particles where the force increases at the very end. There isn't a large difference in the way the squeeze force increases as the concentration is increased for the ER fluid containing the low viscosity silicon oil.

Figure 4.3 shows that the compression force in squeeze flow when an electric field (E= 1,000 V) is applied. Because of the ER effect, the electric field causes an increase in the compression force for all the concentrations. The electrorheological effect is greater for larger concentrations. For example at a

gap separation of 0.1 mm the force generated by 10% and 40% ER fluid is around 0–3 N without an electric field. When the electric field is applied at 0.1 mm the force is 200 N for 10% and >>450 N for the 40% ER fluid.

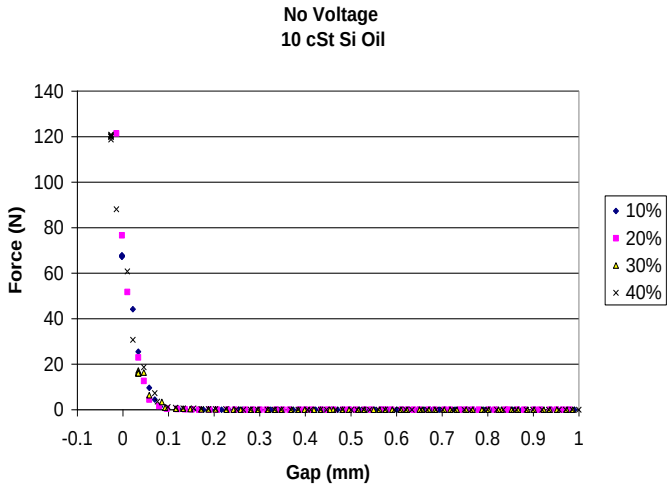

Figure 4.2. Force vs. Gap Chart using constant volume to show the effect of concentration of particles in low viscosity fluid with no electric field

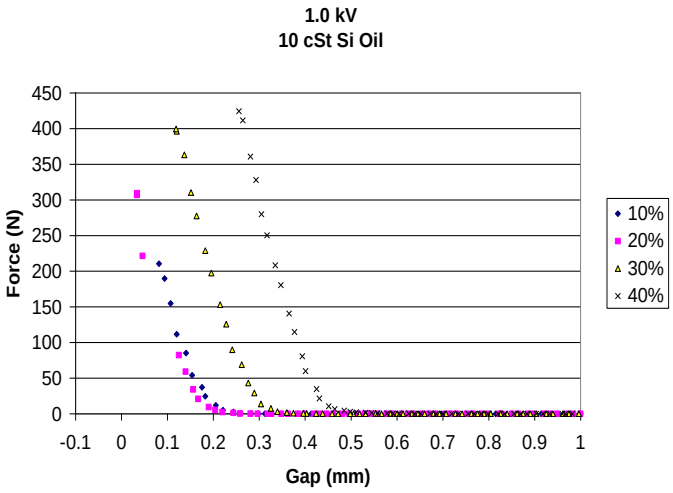

Figure 4.3. Force vs. Gap Chart using constant volume to show the effect of concentration of particles in low viscosity fluid under 1.0 kV electric field.

Figure 4.4, like Figure 4.2, shows how the compression force develops during compression of the ER fluids without an electric field, except this ER fluid contains the high viscosity silicon oil. Even though these fluids are much thicker and the forces generated by thicker fluids are larger even without an electric field, the curves still fall almost on top of each other with the exception of the most concentrated suspension 40% wt. Because this suspension had the largest concentration of particles, it is believed that compaction of those particles caused the deviation.

Figure 4.5 shows the compression force for the ER fluid with the high viscosity silicon oil under an electric field (E=1,000 V). Again the electric field causes an increase in the compression force for all the concentrations. The electrorheological effect is greater for larger concentrations. If a gap separation of 0.3 mm is taken for Figures 4.4 and 4.5, for 10% and 40% ER fluid the force generated at that gap is around 5–10 N. Under an electric field the force generated at 0.3 mm is 15 N at 10% and 200 N at 40%.

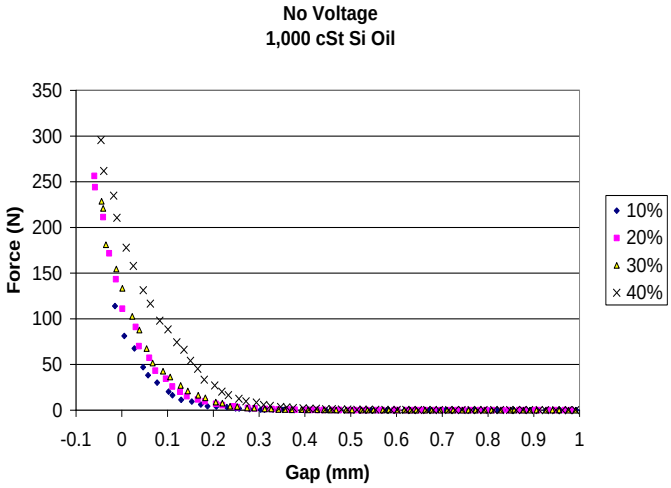

Figure 4.4. Force vs. Gap Chart using constant volume to show the effect of concentration of particles in high viscosity fluid with no electric field.

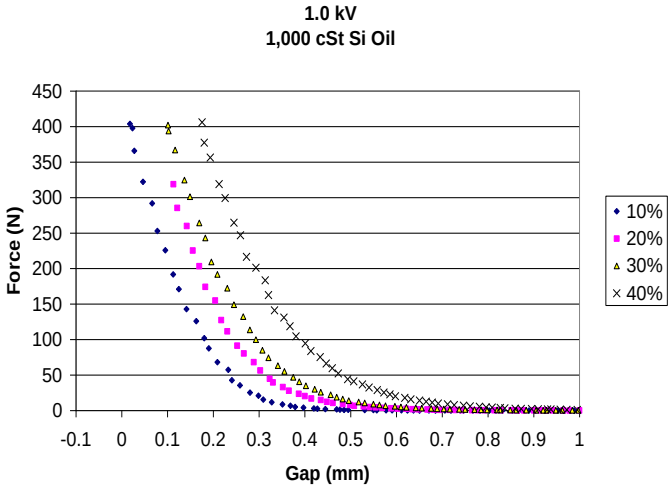

Figure 4.5. Force vs. Gap Chart using constant volume to show the effect of concentration of particles in high viscosity fluid with 1.0 kV.

Figure 4.6 gives the log-log plot data for the ER fluid containing the low viscosity silicon oil under an electric field. This figure illustrates how the results from the constant volume squeeze flow of an ER fluid matches squeeze flow theories. According to squeeze flow theories the log-log plot should produce a

line with a slope of −5. The diagonal line on the graph has a slope of −5. The data shows a dependence greater than −5. Figure 4.7 is a similar plot for the ER fluid containing the high viscosity silicon oil under an electric field. Again the slopes of the data curves are greater than −5.

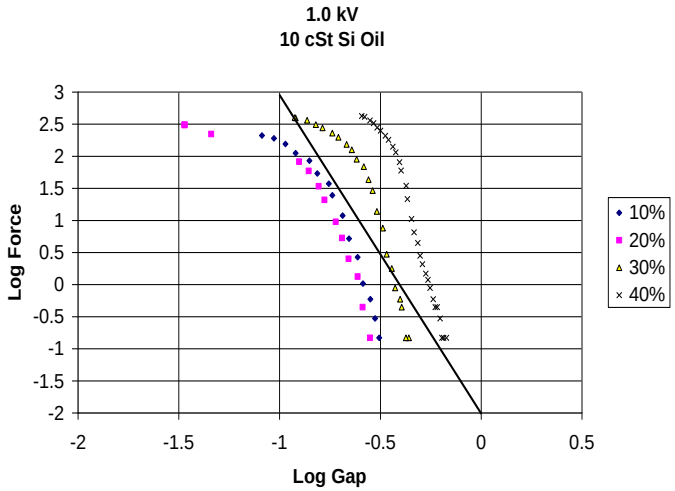

Figure 4.6. A log-log chart of Force vs. Gap for the low viscosity ER fluid at different concentrations of particles. The line represents the slope that would be predicted by Stefan's law for a constant volume Newtonian fluid.

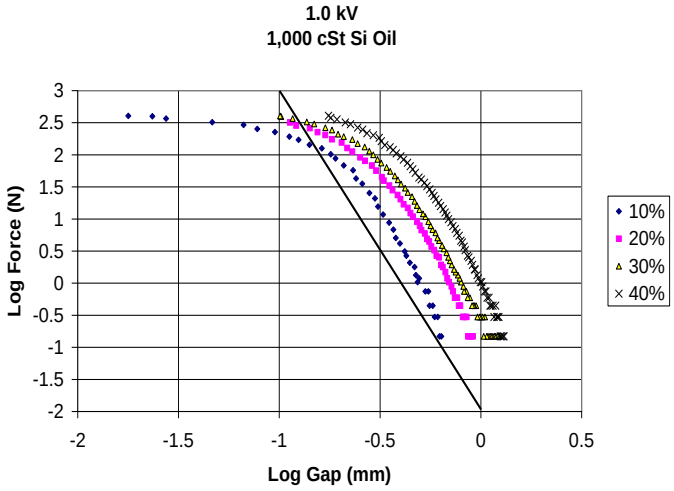

Figure 4.7. A log-log chart of Force vs. Gap for the high viscosity ER fluid at different concentrations of particles. The line represents the slope that would be predicted by Stefan's law for a constant volume Newtonian fluid.

Discussion

Figures 4.2–4.7 show that the effect of particle concentration on the force is greater under an electric field than without one. This was true for both the high and the low viscosity fluids. Because this experiment was done using a constant volume setup where the concentration of particles between the plates was known throughout the test this suggests that the concentration of particles are a strong factor in the compressive forces generated by an ER fluid. While this result was implied in similar studies done using a constant area setup this is the first experiment where the concentration of particles is known and the experimental setup is unaffected by the “sealing effect”

Comparing Figures 4.3 and 4.5 the effect of the continuous phase of the ER fluid can also be better understood. In previous studies the effect of the concentration was unable to be isolated. In fact the concentration was not even able to be accurately determined once the particles started squeezing beyond the plates. Therefore any attempt to assess the effect of the continuous phase by such studies would have been contaminated by the inability to pin down the effects of the changing concentration of the ER fluid.

One observation was made for the compression experiments about the viscosity of the continuous phase under an electric field. It was observed that in fluids containing low viscosity oils, only pure oil is exuded radially during compression. Whereas for fluids containing high viscosity oils the powder particles and oil were exuded radially during the compression.

The effect of the viscosity is best illustrated in plots 4.5 and 4.6 where the dependence of the force on the gap is shown in a log-log plot. Using the extension of Stefan's law for constant volume for a log-log plot of force vs. gap it should give a linear plot with a slope of −5. Looking at both Figures 4.6 and 4.7 the data for the ER fluids containing both the high and low viscosity oils gave slopes that were larger then −5. The ER fluid containing the high viscosity oil had a slope closer to −5 than the ER fluid containing the low viscosity. First this shows that ER fluids do not exhibit behavior described by the ideal models for squeeze flow. More importantly this suggests that the behavior deviates from the ideal model for squeeze flow systematically based on the viscosity of the dispersing oil. This has been found to be the case with other fluid systems as well (Collomb et al. 2004).

One description as stated in the observation made in the previous paragraph is that this can be the result of particles staying in the center of the fluid for the low viscosity sample. The high viscosity oil sample as noted above would push both particles and oil together resembling a homogeneous flow situation which is closer to the ideal case where the slope is equal to five for constant volume. In the low viscosity case the oil could be spreading out between the plates while the particle structures stayed close to the center, which would deviate from the ideal flow case. This description is supported by both observations for the fluid squeezing out from the plates in previous studies, as well as observations of the particles staying in the center after the plates were separated.

References

Ahn, K.H., S. Chu and S.J. Lee “An Experimental Study on the squeezing flow of electrorheological suspensions” *J. Rheol.* **44** (2000) pg. 105–120

Collomb, J., F. Chaari and M. Chaouche “Squeeze Flow of Concentrated Suspensions of Spheres in Newtonian and Shear Thinning Fluids” J. Rheol. **48** (2004) pg. 405–416

Diennes G.J. and H.F. Klemm “Theory and Application of the Parellel Plate Plastomer” *Appl. Phys.* **17** (1946) pg. 458–471

Filisko, F. and Meng Y. “Unidirectional Compression of Electrorheological Fluids in Electric Fields” J. Appl. Phys. **98** (2005)

Monkman, G.J. “Electrorheological Effect Under Compressive Stress” *J. Phys. D: Appl. Phys.* **28** (1995) pg. 588–593

Viera, S.L., M. Nakano, R. Oke, T. Nagata “Mechanical Properties of an ER fluid in Tensile, Compressive, and Oscillatory Squeeze Tests” **15** (2001) pg. 714–722

Chapter 5

Structuring Related To Peclet Number in Electrorheological Squeeze Flow

Introduction

While the separation of particles from dispersing oil under an electric field for ER fluids has been well documented in the literature, a thorough investigation on the impact of filtration on electrorheological squeeze flow has yet to be completed (Monkman 1995, Chu et al. 2000, Vieira et al. 2001, Meng and Filisko 2005, Lynch, Filisko and Meng 2006). One hindrance to such an investigation is that the concentration of particles between the plates changes due to the fluid being squeezed out from between the plates during compression. Previous work showed that by using a constant volume ER squeeze flow approach that one can account for the effects of concentration (McIntyre and Filisko 2007). However an additional complication arises due to the aggregation of particles under the electric field. This paper uses this approach to examine the effects of both squeezing speed and viscosity on filtration that occurs in ER squeeze flow. Furthermore because the Peclet number (Pe) has been speculated to measure filtration effects in ER squeeze flow (Lynch, Filisko and Meng 2006) this study examined how filtration and the Pe number can be related to electrorheological compression behavior.

One qualitative observation often made in compression studies of ER fluids with low viscosity oils (<100 mPa s) is that during compression the electric field holds most of the powder between the plates and the dispersing phase (clear oil) is squeezed out (Vieira et al. 2001, Meng and Filisko 2005, Lynch, Filisko, and Meng 2006). This is a function of the electric field and the compression rate, but at high enough fields and low compression rates, only clear oil is observed to exude from the plates. An approximation made in one article assumed that all the powder always stays in between the plates during the squeeze test, while the liquid squeezed out is 100% dispersing phase (clear oil) (Chu et al. 2000).This approximation is not adhered to strictly as the viscosity of the fluid or the squeeze rate is increased or as the electric field is decreased. This highlights the need for a better understanding of filtration in electrorheological squeeze flow.

An earlier study used Darcy's law to show that filtration (solid-liquid separation) in squeeze flow of a concentrated suspension with a Newtonian fluid and shear thinning fluid can actually be related to the dimensionless parameter Pe — the Peclet Number (Collomb et al. 2004). This parameter has previously been used in other studies to provide an explanation of ER squeeze flow (Lynch, Filisko and Meng 2006). This parameter gives a ratio of viscous or convective forces to diffusive terms.

The Peclet number is defined as (Collomb et al. 2004) :

$$Pe = \frac{\mu_w U^{1-m} h^{m+1}}{Ak} \qquad \textbf{(5.1)}$$

μ_w= Suspending Fluid Viscosity

U = squeeze velocity; dh/dt

h = gap size

k = Darcy's Permeability

A = consistency for power law fluid, pre-exponential $\tau = A\dot{\gamma}^m$

m = shear thinning index for power law fluid

The importance of this definition is that a decreasing Peclet number reflects an increasing filtration rate. The two obvious methods to enhance filtration are to greatly decrease the squeezing speed and to decrease the viscosity of the suspending fluid. Increasing the electric field will also increase the strength of the particle structures and affect the results as well.

Since fluid filtration is a diffusive phenomenon and suspension deformation is an convective one, this dimensionless parameter gives a good measure of the influence of filtration effects on squeeze flow. Another way of looking at this is that under an electric field the separation that occurs is actually a function of both the viscosity of the oil and the compression speed. This study explores this observation on ER fluids where this separation is known to occur.

In the end this study accomplished two things. First to document for the first time using a constant volume squeezing apparatus for electrorheological fluids that at low viscosities separation (filtration) occurs. The compression behavior of the ER fluid was further shown to be a strong function of the

squeezing speed for low viscosity fluids. The higher viscosity fluids where separation either didn't occur or was much less so, were shown to have a different dependence on the squeezing speed. The effect of changing the viscosity of the oil on the compression behavior was shown to be similar at both high and low squeezing speeds.

Materials and Methods

Apparatus

A modified Weissenberg rheometer with a step motor added to drive the leadscrew loading system, an LVDT displacement sensor to record the gap and a 400 N Entron quartz transducer added to the upper plate was used to make the measurements. In some instances the capacity of the transducer was pushed to 1200 N. For each test a syringe was used to measure a constant volume of 0.5 mL of ER fluid which was placed between the plates. Before compression, a DC voltage was imposed on the sample and was kept constant during the whole period of compression. Therefore the field between the plates increased as the gap decreased. A PC and a laptop computer were used to record the output of the load cell and the displacement sensor.

Materials

The electrorheological suspensions were prepared using aluminosilicate powder (SG 1.1 @ 25° C). Silicon oils were used with the following viscosities 1,000 cSt (SG 1.28 @ 25° C),40 cSt, 0.65 cSt (SG 0.765@ 25 C), 10 cSt , and 10,000 cSt. By weight 30% suspensions were prepared with the all of the oils. The solutions were immediately mixed and capped.

Results

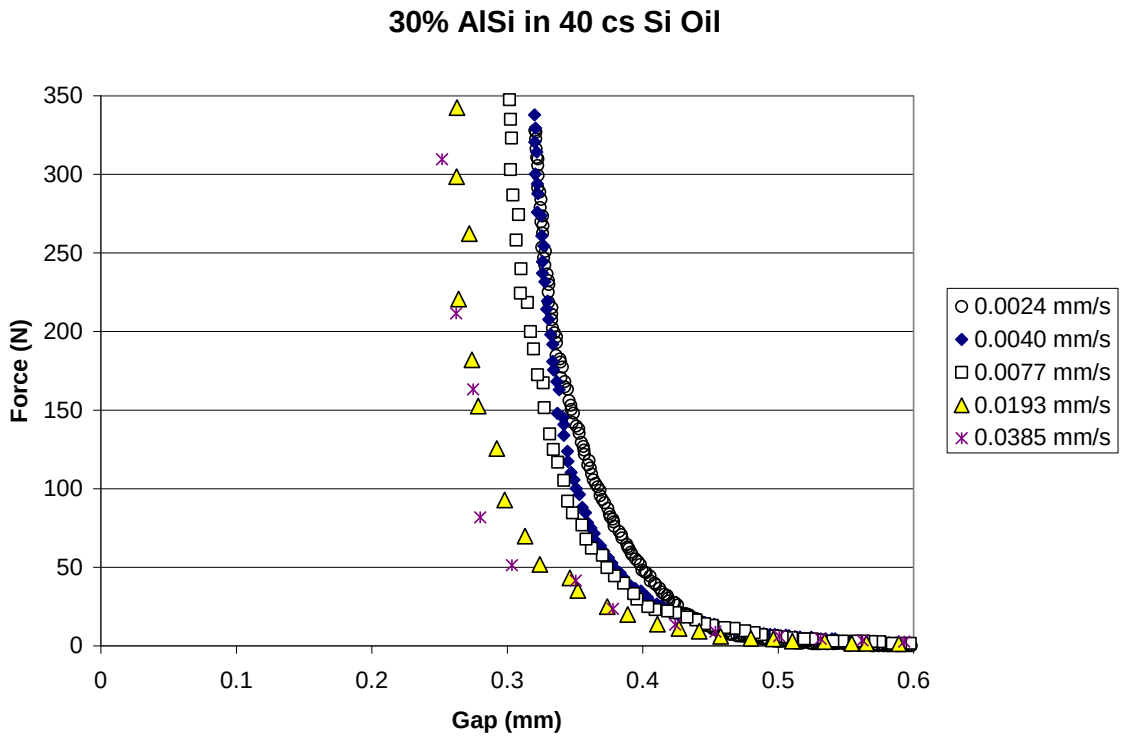

Figure 5.1 Squeeze flow data for ER Fluid using low viscosity oil under 1.0 kV Voltage. The data was taken at very low squeezing speeds in order to observe the effects of filtration flow (phase separation)

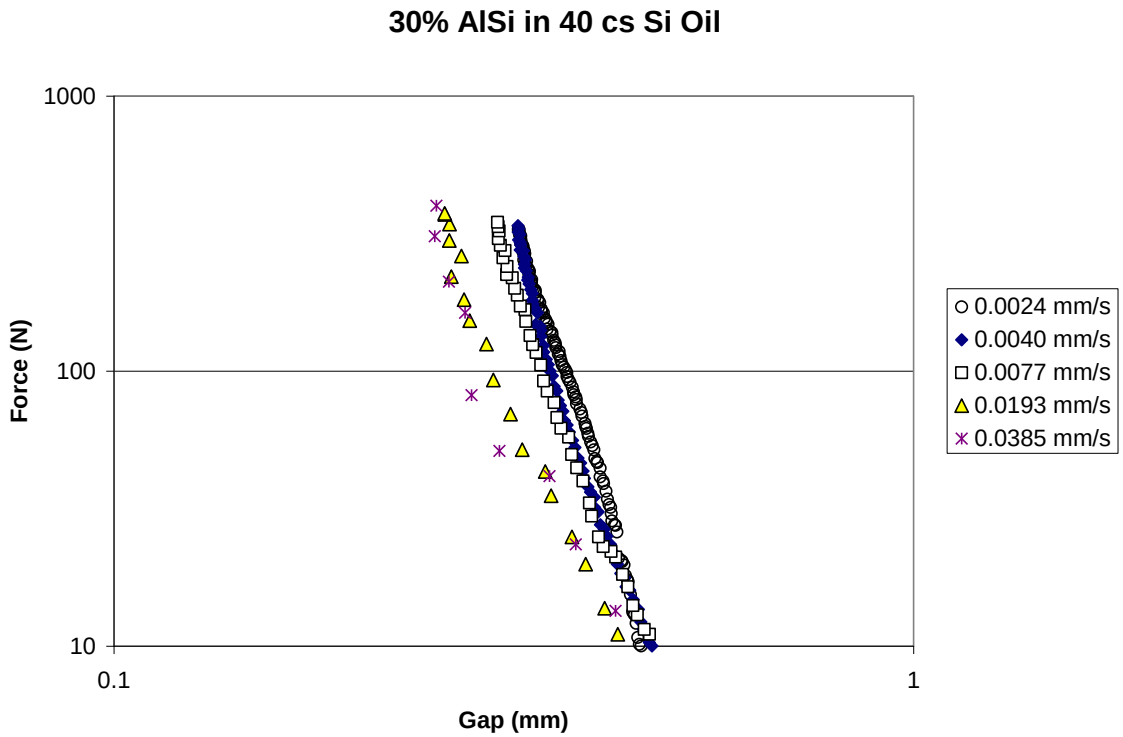

Figure 5.2 Squeeze flow data on log scale for ER Fluid using 40 cs oil under 1.0 kV Voltage.

Figure 5.1 shows compression data for an ER fluid using a constant volume setup to account for concentration and a low viscosity suspending oil. Notice that there is a trend showing the effect of squeezing speed on the ER squeeze flow behavior in this case. Under these conditions the slower gap speeds actually produce larger forces at similar gaps. This is the opposite of what is expected in squeeze flow. While it appears that there is a jump between 0.0077 mm/s and 0.0193 mm/s, the speed is actually increased by a larger factor of 2.5 in this case. From this figure there is shown to be an effect of the squeezing speed on the electrorhelogical squeeze flow behavior even at the very slow speeds.

Figure 5.2 shows similar data on a log scale. Notice that decreasing the speed not only increases the force at the same gaps as was shown in Figure 5.1, but even the slopes in the log plot become greater as the speed decreases. This further suggests the importance of speed in the compression behavior of ER fluids under an electric field.

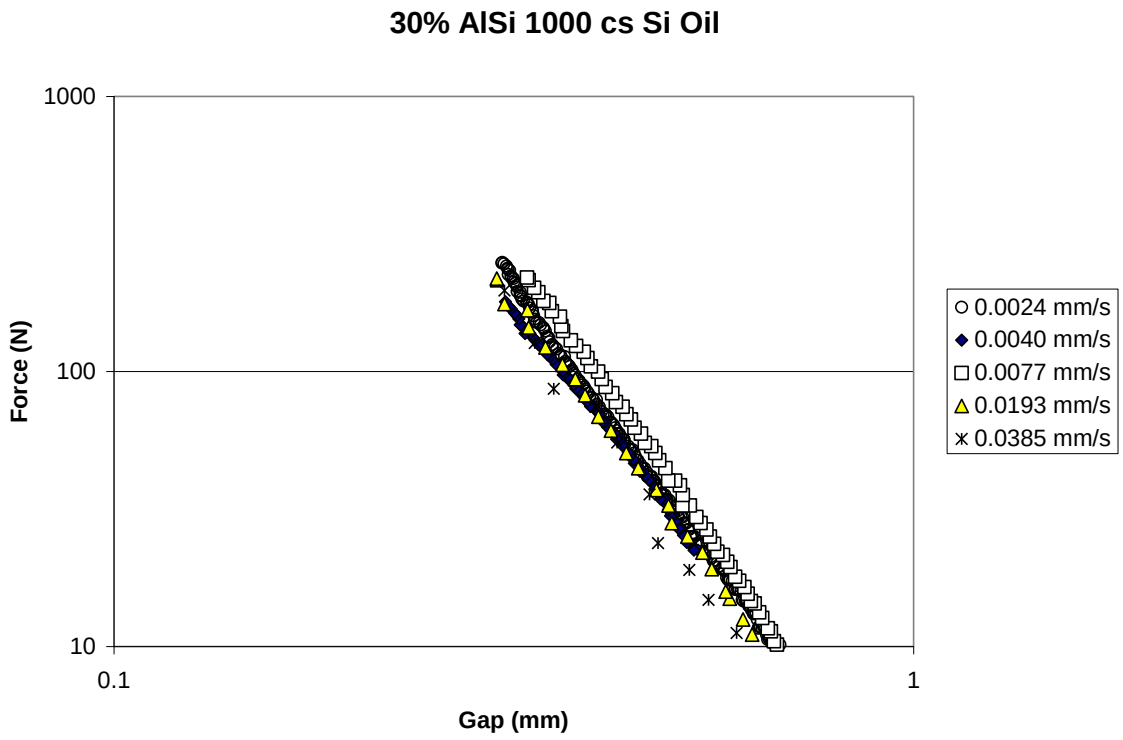

Figure 5.3 Squeeze flow data for 1000 cs viscosity oil ER Fluid under 1.0 kV Voltage.

Figure 5.3 by contrast, shows the same measurements for an oil that is over twenty times more viscous. The trend noticed in Figure 5.1and 5.2 is less pronounced in Figure 5.3 where the viscosity of the fluid is much greater. The curves approximately fall on top of each other at the different speeds. The slope also doesn't change and is lower for the 1000 cs suspension than for the 40 cs

suspension. Even though the effect of squeezing speed is not apparent from examining Figure 5.3, the electrorheological effect is still evident in Figure 5.3 for the higher viscosity suspending oil ER fluid.

In order to examine visually the separation that was occurring in Figures 5.1 and 5.2, a constant area test was done. This was done by examining the fluid squeezing out from between the plates. Figure 5.4 (A,B,C) shows that filtration rate is significant for the 40 cs ER fluid under an electric field. Likewise the Figure 5.4 (D, E, F) shows that the filtration rate was not as significant for the 1,000 cs ER fluid under an electric field. For both of these tests the squeezing speed was reduced to the slowest speed tested-0.0024 mm/s. For the 40 cs solution clear oil is seen to be squeeze out Figure 5.4 (B, C). Contrast this with what is shown for the high viscosity fluid where white suspension of powder and oil are squeezed out together under an electric field Figure 5.4 (E, F).

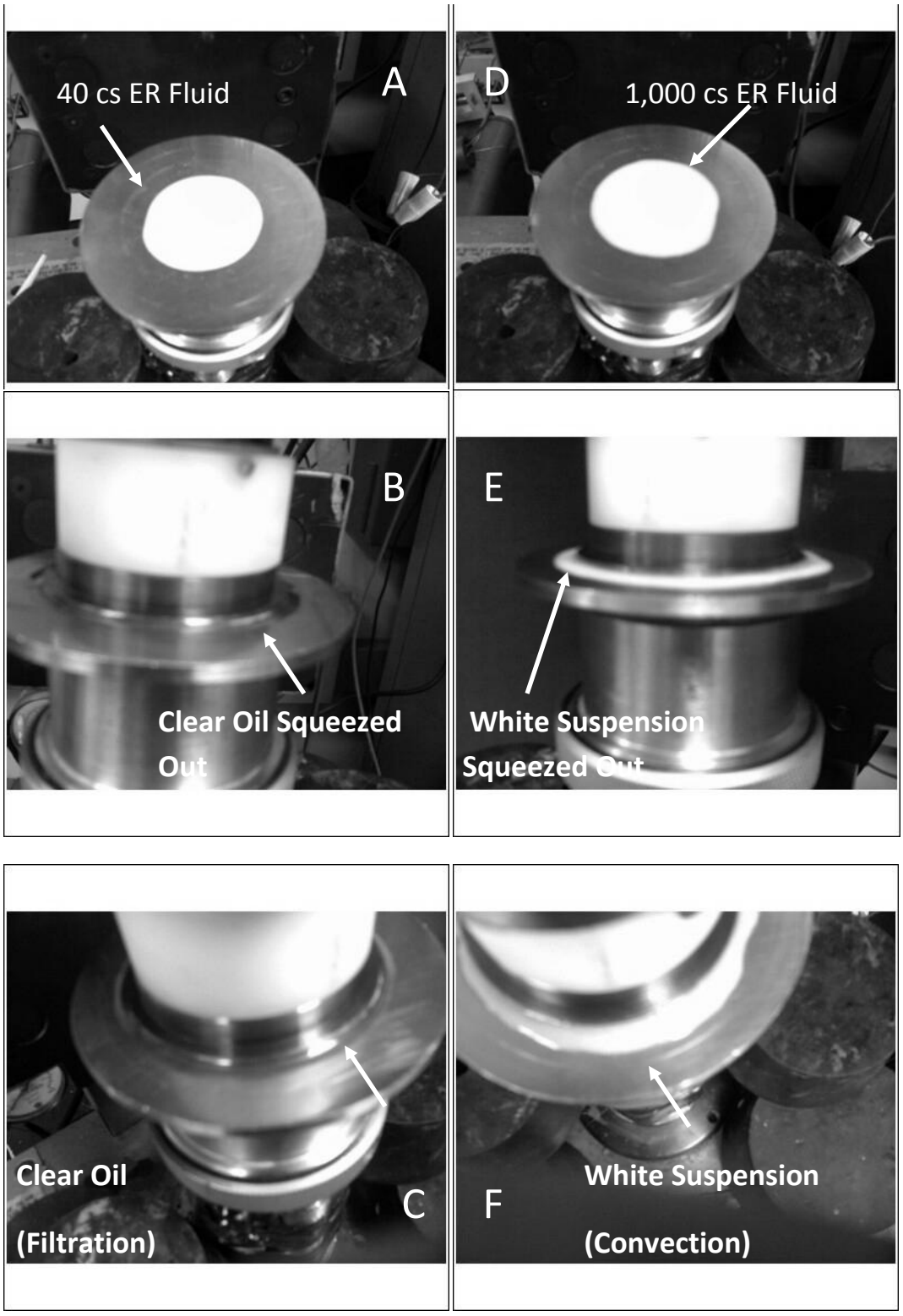

Figure 5.4 Shows 40 cs and 1000 cs ER Sample Compression Under 1.0 kV Voltage (A) 40 cs ER Sample on plate before squeezing (B) during squeezing and (C) after squeezing. (D) Shows

1,000 cs ER Sample before squeezing, (E) during squeezing and (F) after squeezing — squeezing was done at 0.0024 mm/s.

Figure 5.5 shows the comparison of the two fluids at the slowest squeezing speed. Using this figure the effect of the viscosity of the oil can be seen. The shape of the curve actually changes as the viscosity of the dispersing oil changes. Notice the 40 cs ER fluid eventually supports a greater force than the 1,000 cs fluid. This figure shows by comparing these two fluids that at higher loads a lower viscosity suspending oil supports more force at a given gap, implying that the particle structures are more intact and structurally stronger than for the 1,000 cs fluid.

Figure 5.5 also reveals the squeezing behavior of the two ER fluids. The 1,000 cs higher viscosity suspending oil ER fluid supports more of the load at a larger gap. From about 0.8 mm down the 1,000 cs ER fluid rises gradually but more rapidly than the 40 cs ER fluid. The 40 cs ER fluid doesn't begin to rise until the gap is about 0.4 mm, then it rises very rapidly ultimately crossing over the 1,000 cs data at about 0.3 mm gap and continues to rise more rapidly upon continued compression.

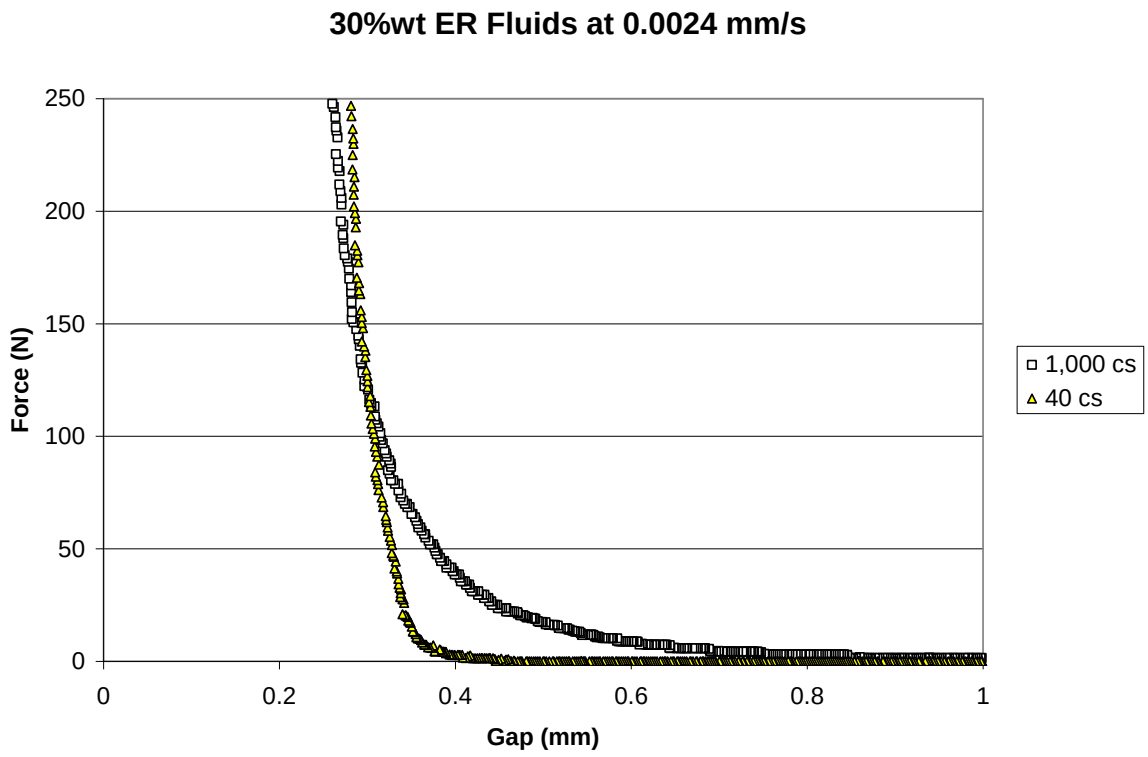

Figure 5.5 Compares the squeeze flow behavior for two ER Fluids under 1.0 kV Voltage at 0.0024 mm/s squeezing speed.

Figure 5.5 only compared two fluids and they were compared under conditions which would not be reasonable in practice — extremely slow squeeze speeds. So to test these conclusions an additional experiment was done with more ER fluids using different viscosity suspending oils at reasonable speeds. Figure 5.6 shows data for several different viscosity oils in electrorheological squeeze flow. Notice that 10 cs and 0.65 cs approximately overlap. But the curve consistently shows that as the viscosity of the oil increases the force increases at larger gaps, but at the same time as the viscosity of the oil is increased the steepness of the curve decreases. This relationship is seen in a log-log plot (Figure 5.7).

Figure 5.7 also reveals that for the highest viscosity suspending oil ER fluids the curve behaves like an ideal squeeze flow situation with a slope of −5. Stefan's Law for squeeze flow of a homogenous Newtonian fluid predicts Force $\propto$ gap^{-5}. As the viscosity is decreased the curve behaves more and more like an ideal close packed powder with a vertical ascent or a slope of infinity—assuming failure doesn't occur. These two figures show that the previous results on the effects of the viscosity from Figure 5.4 are similar at the higher and more practical squeeze speeds.

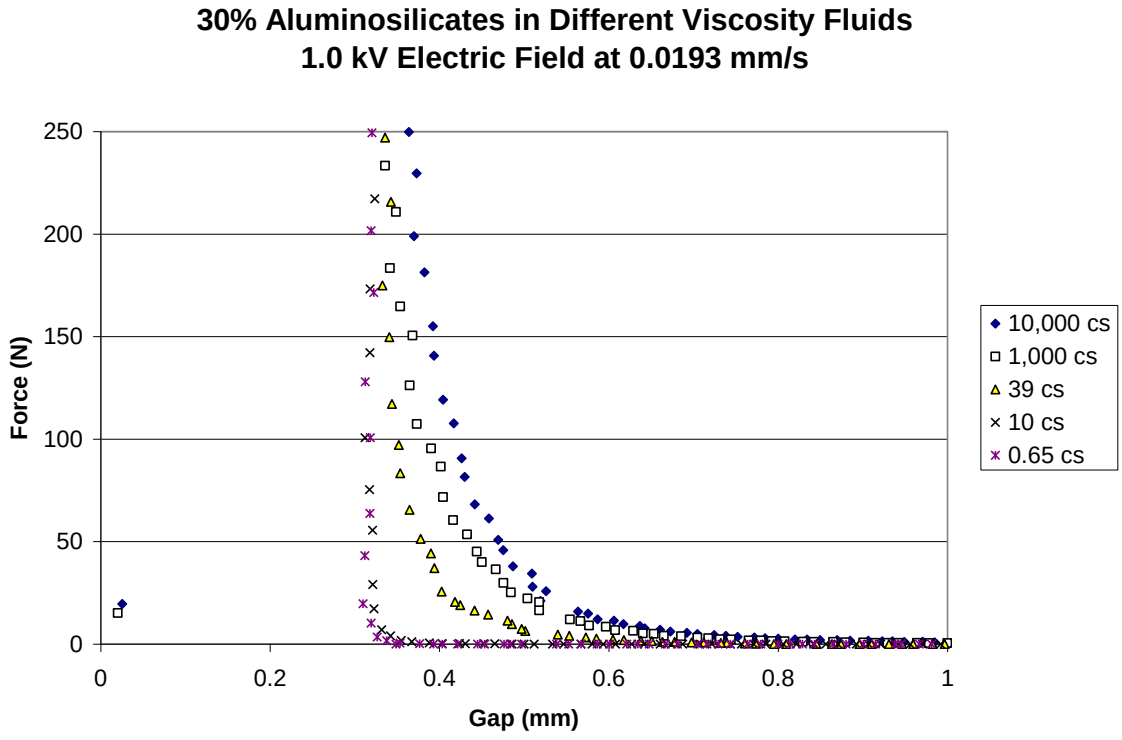

Figure 5.6 Five ER Fluids with different viscosity suspending oils tested at squeezing speed of 0.0193 mm/s

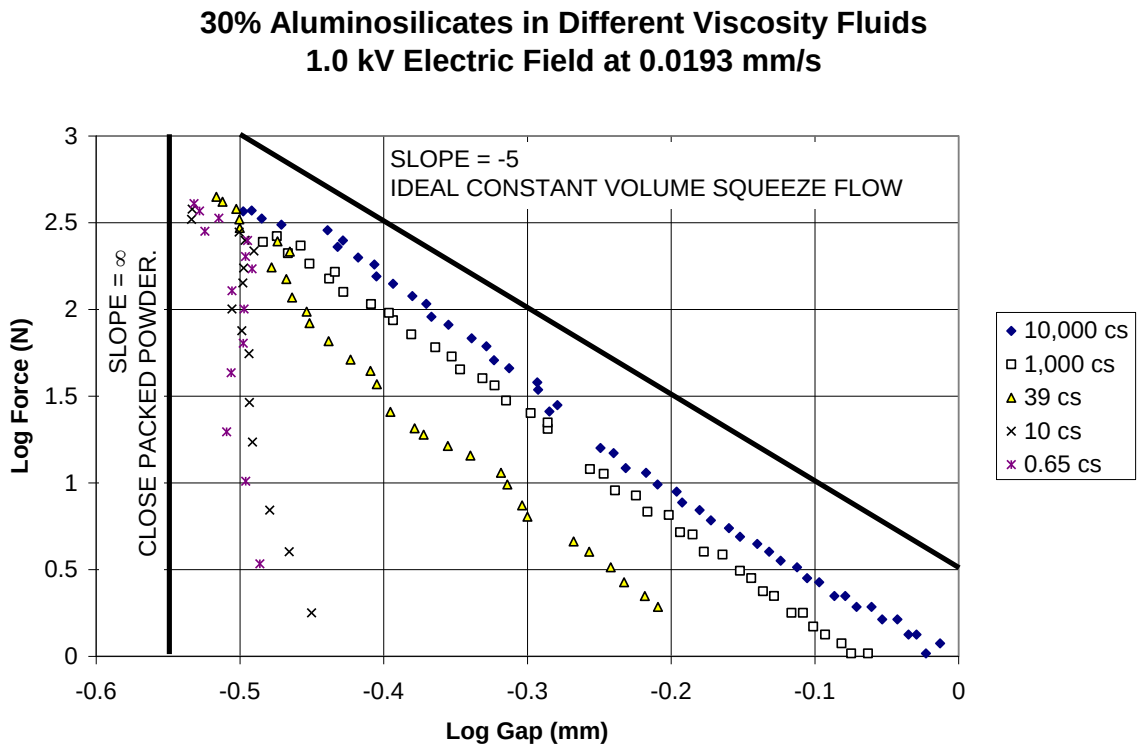

Figure 5.7 Log-log plot showing five ER fluids with five different viscosity suspending oils at 0.0193 mm/s. The figure also shows the predicted behavior for constant volume squeeze flow and close packed powder behavior.

Discussion

For high Peclet numbers the filtration rate is small, whereas for small Peclet numbers the filtration rate becomes significant. It is important to define the influence of the Peclet number in this way because for electrorheology unlike in concentrated suspensions the fluid never becomes homogenous under an electric field. There are regions where the filtration rate is significant, which suggests the structures stay intact and regions where the filtration rate is insignificant and structures are busted up or moved. Even with the very viscous

oil (10,000 cs) complete homogeneity isn't observed, because the electrorheological effect in compression shows the particle structures are still present creating a composite or heterogenous situation.

In the case of the low viscosity fluid (40 cs) compressed at different speeds, the data shows that the force increases as the squeezing speed decreases. This is not normal for homogeneous squeeze flow situations where the force normally is shown to increase with increasing squeezing speeds (Collomb et al. 2004, McIntyre and Filisko 2007) . Previously in the case of concentrated spheres in a fluid this was shown to be an effect of filtration (solid-liquid motion). In an electrorheological fluid, though, solid-liquid motion is continuously occurring due to formation and reformation of particle structures from the imposed electric field. It is therefore necessary to clarify what is meant by "filtration" in this regime.

In compression of electrorheological fluids under an electric field there are at least three different kinds of solid-liquid motion occurring, which need to be specified since filtration can occur with any of these. First there is the initial formation and reformation of the particle structures or columns due to the electric field. These structures form very quickly in low viscosity liquid after the field is turned on and continue to evolve to lamellae throughout the squeezing or shearing of fluid. In this case, the particles move through the liquid to form structures due to the imposed electric field. The destruction or the breaking up of the particle structures by the dispersing oil squeezing against them is another kind of solid-liquid motion. Here the particle structures are stationary or fixed and

the liquid is either squeezing past the structures or the liquid is busting the structures apart if the viscous forces are strong enough. Finally the diffusive flow that occurs in all concentrated suspensions previously reported for concentrated suspensions is also occurring for particles that did not form structures or came from structures that had been broken and not reformed in the ER fluid.

While dealing with these three phenomena occurring at once can seem overwhelming in terms of an overall quantitative model, many qualitative models have been put forth to describe this behavior. The unique solid-liquid motion in terms of the compressive behavior under an electric field is that which relates to the particle structures. The effects of both the strength and building of these particle structures in ER fluids in squeeze flow has been well documented. The importance of filtration and the Peclet number is that for low Pe the structures are more stable. Low Pe flows allow for ER fluid compression behavior to be observed where the particle structures are compressed and broaden but don't break whereas the oil is squeezed out, in other words where the structures are strongest,

Examining Figure 5.1 again shows that for the low viscosity oil squeezed at very slow speeds shows the trend that as the squeezing speed decreases the force increases. This agrees with data for concentrated suspensions, where at very slow speeds close packing occurs in the center. However, the speeds used in the present study are much lower than those used previously. It could be argued for Figure 5.1 that the particle structures when broken up were pushed

radially outward resulting in structures further from the center in each case as the speed increased resulting in smaller forces.

However, for this very low viscosity fluid with extremely slow squeezing speeds the viscous forces on the structures would be minimal. Another possibility is that as the plate compresses the columns of particles, the columns become shorter but thicker as some particles break away and reform on the structure. These re-formed structures are actually stronger than the original. Now the squeezing process is actually continuous it doesn't stop or slow down, the reforming of the structures while very fast is not instantaneous. So if the structures are not being broken up by the fluid the lower squeezing speeds will produce stronger structures all other conditions being equal.

For the higher viscosity oil no clear trend emerges for the force as a function of the squeezing speed. In this case the viscous forces are not only disrupting the particle structures, but also are disrupting the reformation of the particle structures. The net result is that due to the complexity of the ER squeeze flow situation the effect of speed could not be determined for the high Pe Number.

Comparing the high and low viscosity oils at the slowest squeezing speed where the viscous forces are minimized shows that viscosity of the dispersing oil has a strong effect on the behavior of the fluid. (Figure 5.5) This has been observed previously, but not at very slow speeds where the contribution of the dispersing oil due to squeezing to the force was minimal. For the high viscosity

oil, where the Pe Number is greater and the dispersing oil contribution to the force is greater, the force builds up more gradually. It can be presumed that this initial buildup is due to the fluid and not the particle structures. Once the structures are strong enough they take over the load. For the low Pe number flow the force doesn't build up gradually but once the particle structures are strong enough they take the load and quickly surpass the forces of the high viscosity oil ER fluids.

Figure 5.5 not only shows the differences of the effect of viscosity of the oil on squeeze flow, but reveals the overall impact of filtration on ER squeeze flow behavior. Here the amount of particles between the plates is the same and the speed is the same for both fluids, but the difference shown is between a case where filtration is definitely occurring and one where filtration recedes to the edges of the fluid. Looking at the upper limit where the data shows that the structures generate the highest forces where filtration is the strongest. Thus filtration is shown to contribute to the ER squeeze flow effect.

In order to validate that this didn't only occur at very slow speeds another experiment was done at a much higher speed with three other oils. Figure 5.6 shows that the effect of decreasing the viscosity is consistent with Figure 5.4 across all three oils. Figure 5.7 furthermore shows the effect of viscosity on filtration is consistent with the earlier effects on the compressive behavior of ER fluids under electric fields.

The effect of increasing the viscosity of the dispersing oil at higher speeds would be to cause both particles and fluid to be pushed out radially in a situation resembling but not the same as homogenous flow. Here filtration was decreased as can be seen by the significant increase in Pe. While this explanation was rejected in the case for lower speeds in favor of filtration, at these higher speeds this explanation still holds. This explanation matches observations made in previous studies(Lynch, Filisko, and Meng 2006, McIntyre and Filisko 2007) Interestingly though in this study unlike in others on viscosity the curves reach approximately the same point, but at different rates as is shown in Figure 5.6. This is believed to be a result of having the same amount of particles between the plates for every test, which was known due to the fact that the constant volume apparatus was used, and therefore is a consequence of eliminating the “sealing effect”. Furthermore these studies suggest that the point at which this occurs would be determined by concentration of the particles and possibly by squeeze speed, but not viscosity. (McIntyre and Filisko 2007)

References

Chu, S.-H., S.J. Lee, and K.H. Ahn, *An experimental study on squeezing flow of electrorheological suspensions.* Journal of Rheology, 2000. **44**(1): p. 105–120.

Collomb, J., F. Chaari, and M. Chaouche, *Squeeze Flow of Concentrated Suspensions of Spheres in Newtonian and Shear Thinning Fluids.* Journal of Rheology, 2004. **48**(2): p. 405–416.

Lynch, R., F.E. Filisko, and Y. Meng, *Compression of dispersions to high stress under electric fields: Effects of concentration and dispersing oil.* Journal of Colloid and Interface Science, 2006. **297**(1): p. 322–326.

McIntyre, E.C. and F.E. Filisko, *Squeeze Flow of Electrorheological Fluids Under Constant Volume.* Journal of Intelligent Materials Systems and Structures, 2007. **18**: p. 1217–1220.

Meng, Y. and F.E. Filisko, *Unidirectional compression of particle-in-oil dispersions under electric field.* Journal of Applied Physics, 2005. **98**(7): p. 074901.

Monkman, G.J., *The electrorheological effect under compressive stress.* Journal of Physics D: Applied Physics, 1995. **28**(3): p. 588–593.

Vieira, S.L., et al., *Mechanical Properties of an ER fluid in Tensile, Compressive, and Oscillatory Squeeze Tests.* International Journal of Modern Physics B, 2001. **15**(6/7): p. 714–722.

Chapter 6

Magnetorheological Fluids in Squeeze Mode at Low Concentrations

Introduction

The compressive behavior of magnetorheological (MR) fluids has been studied extensively both for industrial applications such as in dampers and as a mechanism for strengthening the materials by increasing their yield stress (Tang et al. 2001, Tang et al. 2000, Vieira 2003). The overall thrust in these studies was either towards higher yield stresses or the utilization of a commercial MR fluid that already had a high yield stress (Klingenberg 2005). Almost all studies conducted on MR fluids in squeeze mode either used 30% vol. concentrated suspensions, usually only testing a single concentration, or used a commercially available MR fluid. The scientific aim of this paper is to examine MR fluids in squeeze mode by looking at effects of concentration, viscosity of suspending oil, and magnetic field. This paper first presents the effects of changing the concentration of particles in MR fluids in squeeze mode. Then the effects of magnetic field and viscosity of suspending oil are investigated in a low concentration MR fluid. The low concentration MR fluid is used for the purposes of investigation because in very concentrated suspensions the MR effect in

compression is much stronger, possibly making other effects of the suspension more difficult to observe.

Magnetorheological fluids, a suspension consisting of magnetic particles in a carrier fluid, are able to show a dramatic increase in their apparent viscosity and the appearance of a yield stress with the application of a magnetic field. For industrial applications it has been demonstrated that MR fluids require a very high yield stress, which has been accomplished by using 30% by volume suspensions of MR fluids. Recent efforts have shown that for MR fluids bidisperse suspensions with particles of two different sizes actually increases the yield strength of the fluid and decreases the off-state viscosity, which leads to a greater increase in the shear stress when the field is applied. Most recent studies have shown that using microwires instead of spherical iron carbonyl particles gave a great increase in the yield stress and reduces settling at the same time (Bell 2008). Problems of settling in MR fluids have hindered their use as well. Often to solve this thixotropic agents are typically added to MR fluid which cause the viscosities of the suspending oils in MR fluids to remain very high. While in most studies involving MR Devices these two observations of requiring a highly concentrated suspension to allow for a high yield stress and avoiding settling through using high viscosity solutions have both been used to help optimize MR studies toward industrial applications, knowledge of the overall effects in compression for MR fluids would contribute towards researching these fundamental problems as well.

Looking at compressive behavior of MR fluids this paper examines the effect of concentration in mineral oil — a relatively low viscosity suspending oil. The concentration of the particles in MR fluids in squeeze mode affects the gap between the plates at which the force sharply increases. This paper then goes on to examine the effects of the magnetic field and the viscosity of the carrier fluid for a low concentration of MR particles—where the structures while still present, have a less significant effect. For the low concentration MR fluids the shape of the compressive curves is shown to be a strong function of both the magnetic field and the viscosity of the suspending fluid. It is proposed that this is because of the filtration flow occurring at very low viscosities of oils, whereas a situation more closely resembling homogenous flow occurs for higher viscosity oils.

Materials and Methods

Apparatus

A Weissenberg rheometer with an added step motor leadscrew loading system and an LVDT displacement sensor was used to make the measurements. Two different plates were used in this test. In testing the effect of concentration two 50 mm plates were used with an electromagnet. For all other tests 25 mm plates were used with iron cylinders attached to the sides in order to increase the magnetic field strength. Figure 6.1 below displays the setup for all the other compression tests that were done with the Weissenberg.

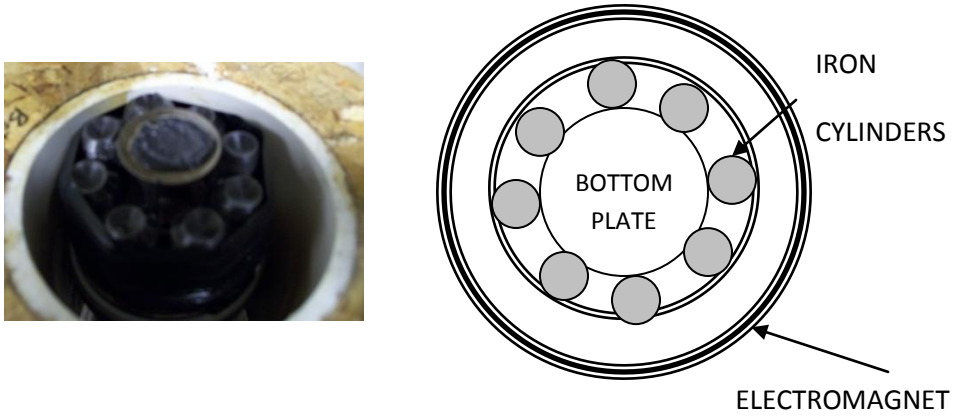

Figure 6.1 Experimental Setup #2

Materials Preparation

The MR fluids were prepared using iron carbonyl powder from BASF (density 7.18 g/cc @ 25 C) in both mineral oil (density 0.85 g/cc) and silicon oil—10,000 cSt, 1,000 cSt, 40 cSt, and 10 cSt. Small amounts of fumed silica (~⅛ Teaspoon) were added to samples (~10 mL) in order to prevent settling.

Experimental Procedure

All compression tests were done on the Weissenberg rheometer. The magnet was connected to a power supply and the fluid was placed on the bottom plate to cover the entire plate. Then the upper plate was lowered to an initial gap

of 1.0 mm. The plates were brought together at a constant speed of 1.27 mm/min.

Initially to measure the effects of concentration 50, 70, and 80% wt carbonyl iron suspensions were prepared, corresponding to approximately 10, 20, and 30% vol. For each measurement a new sample was placed between the plates. Enough sample was placed to cover the entire area of the upper plate.

For the low concentration MR fluid with different viscosity oils each was prepared and thoroughly mixed with an ultrasonic mixer immediately before being placed between the plates as settling could have become an issue with the very low viscosity fluids (e.g. 10 cSt).

Results

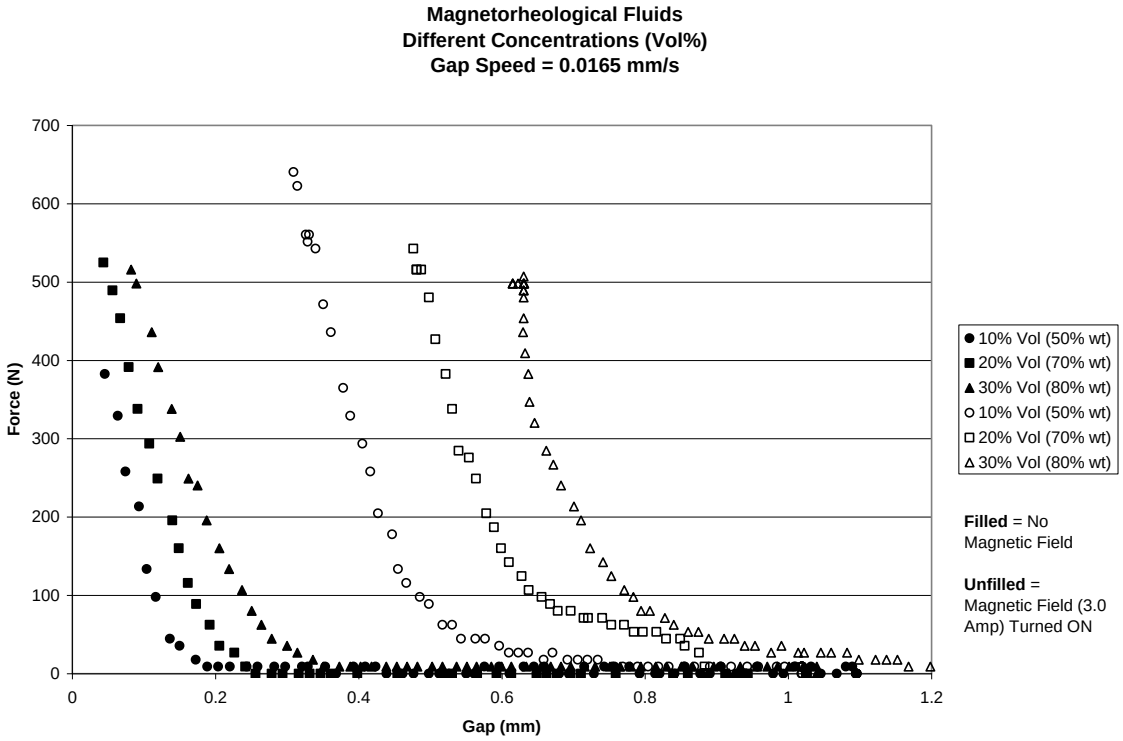

Figure 6.2 Graph showing the compression behavior for three different concentrations of magnetorheological fluid with and without magnetic fields.

Figure 6.2 shows compression behavior for three different concentrations of magnetorheological fluids both with and without a magnetic field. The magnetorheological effect can be seen in the presence of the magnetic field, because all of the fluids gave an increased force at a greater gap under a magnetic field. The effect of concentration in Figure 6.2 shows that as the concentration increased the force at a given gap increases. For example at a gap of 0.7 mm the compressive force for a 10% volume concentration is close to 30 N, but the force increases to 80 N and to 200 N for 20% and 30% volume concentrations.

Figure 6.3 shows the effect of the magnetic field on the compression behavior of a 5 % vol. MR fluid. Even at low concentrations the magnitude of the magnetic field has a strong effect on the compressive behavior of the magnetorheological fluids. Increasing the magnetic field also increases the force at a given gap in compression. This figure shows that the rate at which the force changes with respect to the gap depends on the magnetic field. However at large forces the data converge, which is something that did not occur in Figure 6.2.

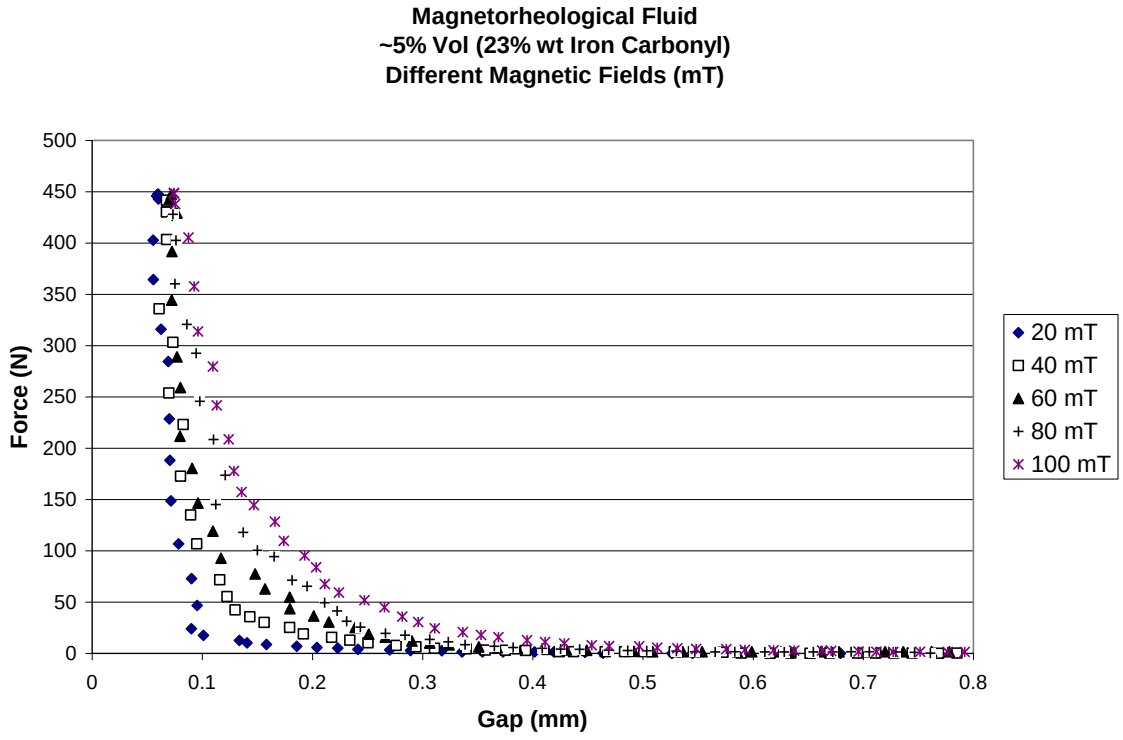

Figure 6.3 Graph showing the effect of the magnetic field on a magnetorheological fluid that has a relatively low concentration of powder.

The effects of the concentration and magnetic fields were shown to be very important in Figures 6.2 and 6.3. Figure 6.4 shows a magnetorheological fluid with the same concentration as in Figure 6.3 using different viscosity

suspending oils without a magnetic field. The two lowest oil viscosity solutions gave greater values at larger gaps than the high viscosity suspending oils without a magnetic field. This could be due to a wetting of the plate surface by these low viscosity fluids causing the particles to pile up.

Figure 6.5 shows the results of these magnetorheological fluids using four different viscosity suspending oils under a magnetic field. The magnetorheological effect of these solutions can be seen by comparing Figures 6.4 and 6.5. The effect of the viscosity can also be seen. The greater the viscosity of the oil the sooner or the larger the gap when the force began to rise. The exception to this was the 39 cSt oil. At the same time the forces of the lower viscosity suspending oils eclipsed those of the higher viscosity suspending oils at small gaps.

Also shown in Figure 6.5 are two lines where pure iron carbonyl powder was placed between the plates and compressed for comparison. The powder compression changed gave higher forces at larger gaps for the field turned on than it did without the field.

Figure 6.6 shows a log-log plot of the data for the four different viscosity oils and for the compressed powder. The rate of increase in the force is shown to increase with a decrease in the suspending oil viscosity. While the plots are not linear the linear portions of the plots reveal this to be the case.

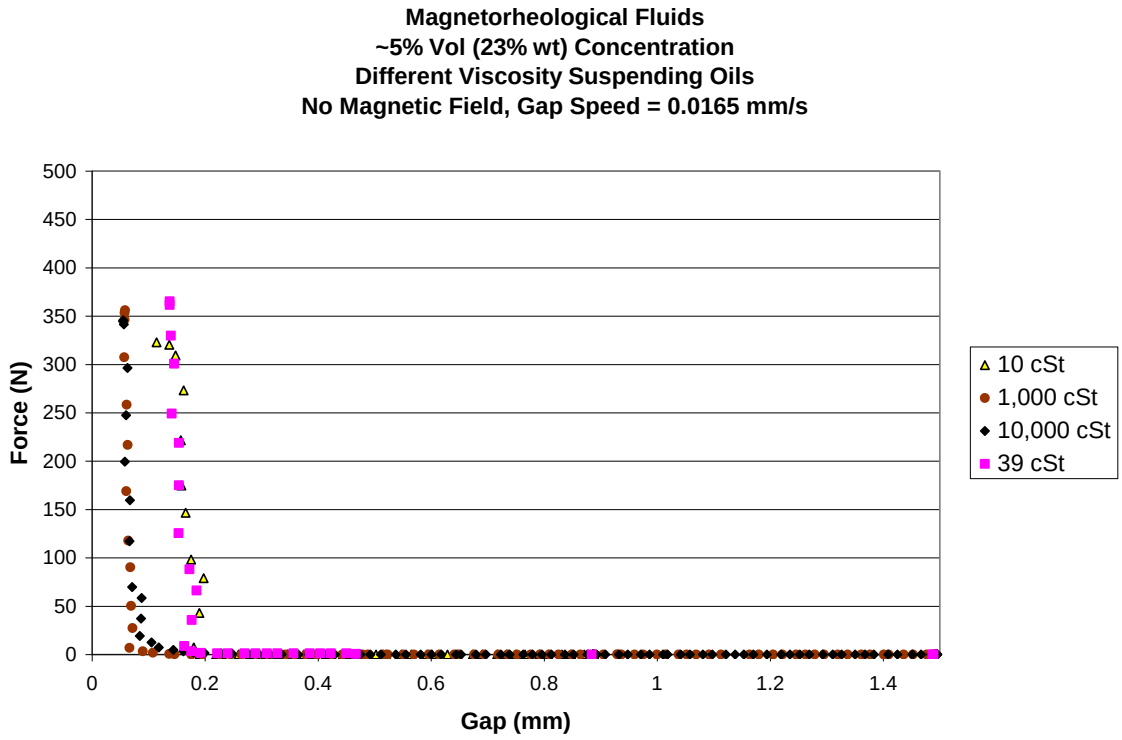

Figure 6.4 Graph showing the effect of the viscosity of the suspending oil has on the compression behavior of the magnetorheological fluid without a magnetic field.

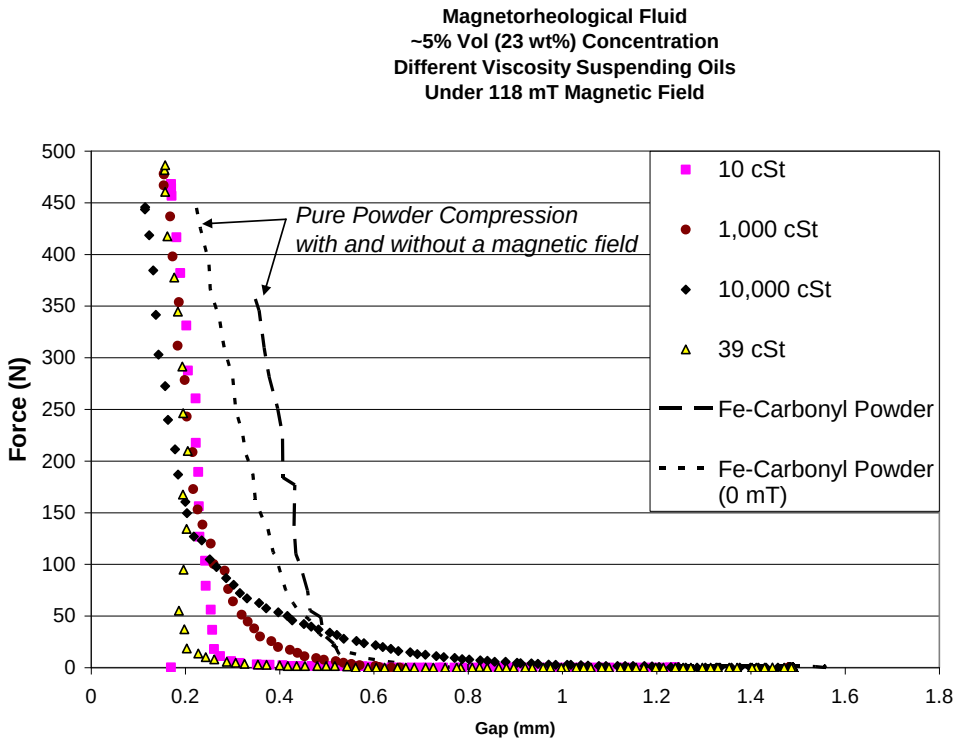

Figure 6.5 Graph showing the effect of the viscosity of the suspending oil has on the compression behavior of the magnetorheological fluid under a magnetic field**.**

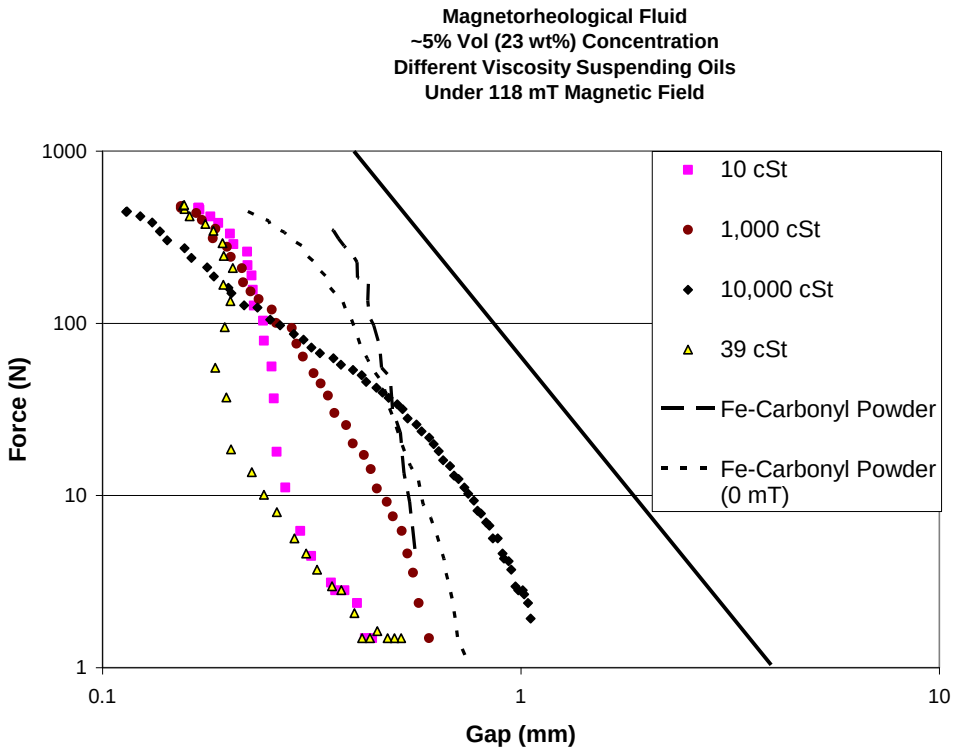

Figure 6.6 Log Plot showing the relationship between viscosity and the relationship between the force and the gap.

Discussion

The behavior of magnetorheological fluids in compression can be best understood by examining the complete picture, rather than examining each component — concentration, viscosity, magnetic field — in isolation. By gaining an overall understanding of the mechanical behavior of MR fluids the solutions for the problems facing this smart technology will become clear.

Figure 6.2 shows the effect of changing the concentration in MR fluids of the particles. As the concentration increases the data shows that the MR fluids create higher forces at larger gaps. This result agrees with what was pointed out earlier that the highly concentrated suspensions have higher strengths, which are

revealed by the greater forces at a given gap. The concentration also affects the difference between the gap for given force with no field and the gap for a given force with the magnetic field turned on. For example in Figure 6.2 at 10% concentration by volume for 100 N the difference between 0.11 mm with no field and 0.49 mm with the magnetic field gives a difference of 0.38 mm for a field vs. without a field. Using the same procedure at 100 N gives a difference of 0.50 mm and 0.54 for 20% and 30% respectively.

It has previously been shown that under a magnetic field in compression the MR particles form column-shaped structures. It has also been shown that the thickness of these structures increases as the concentration of particles increases to a limit. The data in Figure 6.2 suggest that small increases in the thickness of these column-shaped structures results in much larger contributions to the force than the viscosity increases caused by these increased concentrations.

Examining a low concentration suspension where the structures are not as thick, Figure 6.2 shows that the magnetic field still has a significant effect on the overall compressive behavior of the MR suspension. Even small changes have a noticeable effect. While this would be expected in a concentrated MR suspension this reveals even at very small concentrations the MR particles have a significant effect in compression behavior and not just with small gaps. While the fluid in this case mineral oil had a relatively low viscosity, the data in Figure 6.3 shows that the strength of the structures formed in the MR fluid depends on the magnetic field.

While the structures are therefore very important in understanding the mechanical behavior of MR fluids in compression, the contribution of the carrier fluid must also be examined to gain a more complete understanding of the MR fluid. Figures 6.4 and 6.5 reveal the effect of the viscosity of the suspending oil on the MR fluid. The effect of increasing the viscosity of the suspending oil is seen to increase the force at larger gaps for all the MR fluids.

Increasing the suspending oil viscosity causes a decrease in the rate at which the force rises under a magnetic field. This is further seen in Figure 6.6. It is possible that what is being seen in Figure 6.6 is similar to the sealing effect in ER. While no observations have been made in MR where the fluid squeezes out and the powder stays between the plates, in ER the electric field significantly drops off outside of the two plates, for the magnetic field this is not the case.

Using this explanation the MR suspension would act more like a homogenous flow exhibiting convective flow in the case of large viscosity oils or Pe numbers. Likewise it would exhibit filtration flow at very low viscosities. This is a possible explanation of the behavior in Figure 6.6. It should still be pointed out that other factors play a role in the compressive behavior as well, which can be seen from the shape of the curves.

References

Bell, R.C., et al., *Magnetorheology of submicron diameter iron microwires dispersed in silicon oil.* Smart Materials and Structures, 2008. **17**: p. 6pp.

Klingenberg, D.J., D. Kittipoomwong, and J.C. Ulicny, *Dynamic Yield Stress Enhancement in Bidisperse Magnetorheological Fluids.* Journal of Rheology, 2005. **49**(6): p. 1521–1538.

Tang, X., X. Zhang, and R. Tao, *Enhance the Yield Shear Stress of Magnetorheological Fluids.* International Journal of Modern Physics B, 2001. **15**(6,7): p. 549–556.

Tang, X., et al., *Structure enhanced yield stress of magnetorheological fluids.* Journal of Applied Physics, 2000. **87**(5): p. 2634–2638.

Vieira, S.L., et al., *Behavior of MR Fluids in Squeeze Mode.* International Journal of Vehicle Design, 2003. **33**(1–3): p. 36–49.